Variational problem of anisotropic energy and its discretization

軸丸, 芳揮

https://doi.org/10.15017/4060002

Doctoral Dissertation

Variational problem of anisotropic energy and its discretization

Yoshiki Jikumaru

Graduate School of Mathematics,
Kyushu University

Supervisor : Professor Miyuki Koiso

February 13, 2020

Contents

1 Non-uniqueness of closed embedded non-smooth hypersurfaces with constant anisotropic mean curvature 9

1.1 Introduction . . . 9
1.2 Preliminaries . . . 12
1.2.1 Piecewise-C^k weak immersion and its anisotropic energy . . . 12
1.2.2 Wulff shapes and convex functions . . . 13
1.2.3 Cahn-Hoffman map and anisotropic mean curvature . . . 14
1.3 The first variation formula of the anisotropic energy . . . 16
1.4 An example of dimension 1 . . . 18
1.5 Higher dimensional examples . . . 23
1.6 Proofs of Theorems 1.1.1, 1.1.2 . . . 26
1.7 Applications to anisotropic mean curvature flow: proofs of Theorems 1.1.4, 1.1.3 . . . 27

2 A discretization of the anisotropic energy for curves and surfaces 29

2.1 Introduction . . . 29
2.2 Preliminaries . . . 31
2.2.1 Abstract simplicial complexes . . . 31
2.2.2 Subsimplex, star and link . . . 31
2.2.3 Simplicial map . . . 32
2.2.4 Simplicial curves, simplicial surfaces . . . 32
2.2.5 Geometric simplicial complexes . . . 33
2.3 Geometry of discrete anisotropic curve energy . . . 33
2.3.1 Anisotropic curve energy and its first variation . . . 33
2.3.2 Relation with other notions of the discrete curvature . . . 37
2.3.3 Parallel curves and Steiner-type formula . . . 40
2.3.4 Critical points of the length functional . . . 44
2.3.5 Discrete constant anisotropic curvature curves . . . 47
2.3.6 Second variation of the anisotropic energy . . . 51
2.3.7 Instability of non-convex regular polygons . . . 57
2.4 Geometry of discrete anisotropic surface energy . . . 59
2.4.1 Anisotropic surface energy and its first variation . . . 59
2.4.2 Discrete constant anisotropic mean curvature surfaces . . . 63

2.4.3 Examples of discrete CAMC surfaces 66
2.4.4 Second variation of the anisotropic energy 69

Acknowledgements

Special thanks are due to the author's supervisor Professor Miyuki Koiso for her invaluable support, constant encouragement, many helpful comments and discussions. The author would like to express his gratitude to Professor Konrad Polthier to visit Freie Universität Berlin for suggesting many interesting topics about discrete surfaces supported by the Leading PhD Program in Mathematics for Key Technologies in Kyushu University. The author also thanks for Professor Manuel Ritoré for fruitful discussion about isoperimetric problems at University of Granada supported by the program "Doc-Course in Geometric Analysis". Finally, he is also grateful to the dissertation comittee: Professor Miyuki Koiso, Professor Atsushi Katsuda, Professor Yukio Otsu, Professor Hisashi Naito, and Doctor Hiroshi Ogawa for their supports.

Preface

The classical isoperimetric problem asks the minimizer of the area functional among all closed surfaces enclosing the same volume. The answer is a sphere and this gives a mathematical model of a soap bubble since its surface tension is isotropic, i.e., independent of directions. On the other hand, the shape of a small crystal is the minimizer of the total surface free energy associated to the media subject to a volume constraint condition. In order to model these objects, J. W. Gibbs (1839-1903) introduced an anisotropic surface energy which is the integral of an energy density that depends on the surface normal ([43], [44]). There exists the unique minimizer of the anisotropic energy among all hypersurfaces enclosing the same volume and the minimizer is called the Wulff shape [40]. Moreover, equilibrium hypersurfaces under a volume-constraint condition are characterized by constant anisotropic mean curvature (CAMC) hypersurfaces [24].

In Chapter 1, we prove non-uniqueness results of CAMC hypersurfaces by giving examples (Theorem 1.1.1, Theorem 1.1.2), i.e., there exists an energy such that there exists a CAMC hypersurface in $\mathbb{R}^{n+1}$ which is not the Wulff shape. Our results show that Alexandrov-type theorem and Hopf-type theorem for CAMC hypersurfaces cannot hold in general if we don't assume the convexity of the energy density function. Moreover, we will show that there exist non-trivial self-similar shrinking solutions for the anisotropic mean curvature flow as an application (Theorem 1.1.4).

In Chapter 2, we will develop a theory of discrete curves and surfaces based on the (anisotropic) isoperimetric problem. Here, we mainly focus on discrete objects themselves, not approximation or convergence problems. Such a research field called discrete differential geometry is an active research field because of the interaction among the theory, the algorithm and the visualization on the computer, e.g. [10], [21], [34], [36], [37] ,[38]. Surprisingly, a basic differential geometric treatment of discrete planar curves by using variational methods is not well understood. Therefore we first treat the planar curve case, and our basic tool here is a "discrete curvature vector" on a vertex extracted from the first variation formula. We show that this vector can be used effectively for an unifed interpretation well-known discrete curvature notions, the second variation and stability criteria. Since there is no universal definition of the discrete curvature and our main interest is CAMC curves and surfaces, we define discrete CAMC curves and surfaces without defining the curvature itself. Our definition is inspired by the definition in [37] and we visualize them on the software JavaView.

Chapter 1

Non-uniqueness of closed embedded non-smooth hypersurfaces with constant anisotropic mean curvature

Abstract

In this chapter, we will show that there exist an anisotropic energy density function such that there exist closed embedded equilibrium surfaces with genus zero in $\mathbb{R}^3$ each of which is not (any homothety and translation of) the Wulff shape. We also give nontrivial self-similar shrinking solutions of anisotropic mean curvature flow. These results are generalized to hypersurfaces in $\mathbb{R}^{n+1}$. The contents of this chapter is contained in [20].

1.1 Introduction

In this chapter, we consider the geometry of equilibrium surfaces for the isoperimetric problem with respect to the anisotropic energy. Let $\gamma : S^n \to \mathbb{R}_{>0}$ be a positive-valued continuous function on the unit sphere $S^n = \{\nu \in \mathbb{R}^{n+1} \mid \|\nu\| = 1\}$ in the $(n+1)$-dimensional Euclidean space $\mathbb{R}^{n+1}$ and this function gives an energy density. Sometimes we assume that γ is defined on an open set in S^n. When we study variational problems of such an energy, it is natural to consider not only smooth surfaces but also surfaces with edges since the energy minimizer may have some singularities as shown in the figure 1.1. And so let M be an n-dimensional oriented connected compact C^∞ manifold and $X : M = \cup_i M_i \to \mathbb{R}^{n+1}$ be a piecewise-C^2 immersion (the definition of piecewise-C^2 weak immersion will be given in the section 1.2). Let $\mathcal{S}(X)$ be the set of singularities of X and $\nu = \nu_X : M \setminus \mathcal{S}(X) \to S^n$ be the unit normal vector field along X. We define the *anisotropic energy* $\mathscr{F}_\gamma(X)$ *of* X by

$$\mathscr{F}_\gamma(X) := \sum_i \int_{M_i} \gamma(\nu)\, dA = \int_M \gamma(\nu)\, dA,$$

(a) $\gamma \equiv 1$ (b) $\gamma(\nu) = (\nu_1^8 + \nu_2^8 + \nu_3^8)^{1/8}$ (c) $\gamma(\nu) = |\nu_1| + |\nu_2| + |\nu_3|$

Figure 1.1: Figures of the energy minimizer ($n = 2$ case)

where dA is the n-dimensional volume form of M induced by X. If the integrand γ is defined on an open set $\Omega \subset S^n$, we only consider immersions that the image of the unit normal is contained in Ω. In this case, the immersion is said to be compatible with the energy density γ.

If $\gamma \equiv 1$, $\mathscr{F}_\gamma(X)$ is the usual n-dimensional volume of the hypersurface X. For any positive number $V > 0$, there exists a unique (up to translations in $\mathbb{R}^{n+1}$) minimizer $W(V)$ of the energy $\mathscr{F}_\gamma$ among all closed hypersurfaces in $\mathbb{R}^{n+1}$ enclosing the same $(n+1)$-dimensional volume V ([40]). Here a closed hypersurface means that the boundary (having tangent space almost everywhere) of a set of positive Lebesgue measure. The minimizer $W(V_0)$ for $V_0 = (n+1)^{-1} \int_{S^n} \gamma(\nu)\, dS^n$ is called the *Wulff shape* for γ and we denote it by W_γ. The Wulff shape W_γ is the boundary of the convex set

$$\bigcap_{\nu \in S^n} \{x \in \mathbb{R}^{n+1} \mid \langle x, \nu \rangle \leq \gamma(\nu)\}.$$

When $\gamma \equiv 1$, W_γ is the unit sphere.

A piecewise-C^2 weak immersion $X : M \to \mathbb{R}^{n+1}$ is a critical point of $\mathcal{F}_\gamma$ for all variations that preserve the enclosed $(n+1)$-dimensional volume (we will call such a variation a volume-preserving variation) if and only if the anisotropic mean curvature of X is constant and X has a certain condition on its singular points (cf. [24]). Here the anisotropic mean curvature Λ of X is defined at each regular point of X as $\Lambda := (1/n)(-\mathrm{div}_M D\gamma + nH\gamma)$, where $D\gamma$ is the gradient of γ on S^n and H is the mean curvature of X (cf. [39], [25], [24]). We call such X a *CAMC (constant anisotropic mean curvature) hypersurface*. When $\gamma \equiv 1$, Λ coincides with H and CAMC hypersurfaces are CMC (constant mean curvature) hypersurfaces (of C^ω class).

A natural question here is

"is any closed CAMC hypersurface X homothetic to the Wulff shape?"

The answer is not affirmative even in the case where $\gamma \equiv 1$ ([42], [22], [23]). However, it is expected that, if X satisfies one of the following additional conditions (I)-(III), the image of X is a homothety of the Wulff shape :

(I) $n = 2$ and the genus $g(M)$ of M is 0. (II) X is an embedding. (III) X is stable. If we assume that the Wulff shape W_γ is a smooth strictly convex hypersurface, any closed CAMC hypersurface X is also smooth and the above expectation is correct, which was proved by [2], [4], [18] for $\gamma \equiv 1$, and by [16], [31], [26] and [3] for general

Energy density	$n = 2$ and $g(M) = 0$	X is embedded	X is stable
(1) $\gamma \equiv 1$ (isotropic)	true ([18])	true ([2])	true ([4])
(2) $\gamma \in C^\infty$ and strictly convex	true ([26])	true ([16])	true ([31])
(3) $\gamma \in C^2$ and convex	?	?	true ([24])
(4) $\gamma \in C^2$	false ([20])	false ([20])	?

Table 1.1: Summarization of known results and our results

γ satisfying a strong convexity condition (Table 1.1 summarizes the results). Here a CAMC hypersurface is said to be stable if the second variation of the energy $\mathcal{F}_\gamma$ for any volume-preserving variation is nonnegative. If γ has less regularity or less convexity, the Wulff shape and CAMC hypersurfaces can have "edges". In the planar case, Frank Morgan [30] proved that every closed equilibrium curve for the anisotropic energy is the (possibly multiple of) Wulff shape for any continuous γ satisfying the convexity condition.

However, the situation is not the same for non-convex γ. In this chapter, we will prove the following non-uniqueness results for CAMC hypersurfaces:

Theorem 1.1.1 ([20])**.** There exists a C^∞ function $\gamma : S^n \to \mathbb{R}_{>0}$ which is not a convex integrand such that there exist closed embedded CAMC hypersurfaces in $\mathbb{R}^{n+1}$ for γ each of which is not (any homothety or translation of) the Wulff shape.

Theorem 1.1.2 ([20])**.** There exists a C^∞ function $\gamma : S^2 \to \mathbb{R}_{>0}$ which is not a convex integrand such that there exist closed embedded CAMC surfaces in $\mathbb{R}^3$ with genus zero for γ each of which is not (any homothety or translation of) the Wulff shape.

This shows that the Alexandrov-type theorem for embedded CAMC hypersurfaces and the Hopf-type theorem for genus zero surfaces cannot hold unless we assume the convexity of γ. These results are proved by giving examples (see section 1.4, 1.5, 1.6).

The same examples will be applied to the anisotropic mean curvature flow. In order to give the precise statement, we recall that the Cahn-Hoffman map ξ_γ for γ is the mapping $\xi_\gamma : S^n \to \mathbb{R}^{n+1}$ defined as

$$\xi_\gamma(\nu) = D\gamma|_\nu + \gamma(\nu)\nu, \quad \nu \in S^n,$$

here the tangent space $T_\nu(S^n)$ of S^n at $\nu \in S^n$ is naturally identified with the n-dimensional linear subspace of $\mathbb{R}^{n+1}$. Let $X_t : M \to \mathbb{R}^{n+1}$ be one-parameter family of piecewise-C^2 weak immersions with anisotropic mean curvature Λ_t. Assume that the Cahn-Hoffman field $\widetilde{\xi}_t$ along X_t is defined on M. If X_t satisfies

$$\partial X_t/\partial t = \Lambda_t \widetilde{\xi}_t,$$

it is called an *anisotropic mean curvature flow*, which diminishes the anisotropic energy if $\Lambda_t \not\equiv 0$. By a simple observation we show the following.

Theorem 1.1.3 ([20])**.** Let c be a positive constant. Set

$$X_t := \sqrt{2(c-t)}\,\xi_\gamma, \quad t \leq c.$$

Then X_t is a self-similar shrinking solution of the anisotropic mean curvature flow for γ, that is

(1) $\partial X_t/\partial t = \Lambda_t \widetilde{\xi}_t$, and

(2) X_t is homothetic to ξ_γ and it shrinks as t increases.

By using this result and by giving examples, we prove the following result (see section 1.4, 1.5, 1.7).

Theorem 1.1.4 ([20])**.** There exists a C^∞ function $\gamma : S^n \to \mathbb{R}_{>0}$ which is not a convex integrand such that there exist closed embedded self-similar shrinking solutions in $\mathbb{R}^{n+1}$ for γ each of which is homeomorphic to S^n and is not (any homothety or translation of) the Wulff shape.

In contrast with this result, the round sphere is the only closed embedded self-similar shrinking solution of mean curvature flow in $\mathbb{R}^3$ with genus zero ([7]).

Finally we give two conjetures about the uniqueness problems studied in Theorems 1.1.1, 1.1.2, and 1.1.3.

Conjecture 1. Assume that $\gamma : S^n \to \mathbb{R}_{>0}$ is of C^2. Let $X : M \to \mathbb{R}^{n+1}$ be a closed CAMC hypersurface. We assume that the j-th anisotropic mean curvature of X for γ is integrable for $j = 1, \ldots, n$. Then, if X satisfies at least one of the conditions (I), (II), (III) above, $X(M)$ is a subset of a homothety of the image $\xi_\gamma(S^n)$ of the Cahn-Hoffman map ξ_γ.

Conjecture 2. Assume that $\gamma : S^2 \to \mathbb{R}_{>0}$ is of C^2. Then any closed embedded self-similar shrinking solution of the anisotropic mean curvature flow for γ in $\mathbb{R}^3$ with genus zero is a subset of a homothety of $\xi_\gamma(S^2)$.

1.2 Preliminaries

1.2.1 Piecewise-C^k weak immersion and its anisotropic energy

First we recall the definition of a *piecewise-C^r weak immersion*, ($r \in \mathbb{N}$), defined in [24]. Let $M = \bigcup_{i=1}^k M_i$ be an n-dimensional oriented compact connected C^∞ manifold, where each M_i is an n-dimensional connected compact submanifold of M with boundary, and $M_i \cap M_j = \partial M_i \cap \partial M_j$, $(i, j \in \{1, \cdots, k\},\ i \neq j)$. We call a map $X : M \to \mathbb{R}^{n+1}$ a piecewise-C^r weak immersion (or a piecewise-C^r weakly immersed hypersurface) if X satisfies the following conditions (A1), (A2), and (A3) ($i \in \{1, \cdots, k\}$).

(A1) X is continuous, and each $X_i := X|_{M_i} : M_i \to \mathbb{R}^{n+1}$ is of C^r.

(A2) The restriction $X|_{\operatorname{Int} M_i}$ of X to the interior $\operatorname{Int} M_i$ of M_i is a C^r-immersion.

(A3) The unit normal vector field $\nu_i : \operatorname{Int} M_i \to S^n$ along $X_i|_{\operatorname{Int} M_i}$ can be extended to a C^{r-1}-mapping $\nu_i : M_i \to S^n$. Here, if $(u^1, \cdots, u^n)$ is a local coordinate system in M_i, $\{\nu_i, \partial/\partial u^1, \ldots, \partial/\partial u^n\}$ gives the canonical orientation in $\mathbb{R}^{n+1}$.

The anisotropic energy of a piecewise-C^1 weak immersion $X : M \to \mathbb{R}^{n+1}$ is defined as follows. Assume that $\gamma : S^n \to \mathbb{R}_{\geq 0}$ is a nonnegative continuous function. Let $\nu : M \setminus \mathcal{S}(X) \to S^n$ be the unit normal vector field along $X|_{M\setminus\mathcal{S}(X)}$. The anisotropic energy $\mathscr{F}_\gamma(X)$ of X is defined as

$$\mathscr{F}_\gamma(X) := \int_M \gamma(\nu)\, dA := \sum_{i=1}^{k} \int_{M_i} \gamma(\nu_i)\, dA. \tag{2.1}$$

If $\gamma \equiv 1$, $\mathscr{F}_\gamma(X)$ is the usual n-dimensional volume of the hypersurface X (that is the n-dimensional volume of M with the metric induced by X).

1.2.2 Wulff shapes and convex functions

Next we discuss about the Wulff shape and convex functions briefly (see [24] for details). As we remarked in the preface, for an energy density $\gamma : S^n \to \mathbb{R}_{>0}$ the minimizer of the anisotropic energy $\mathscr{F}_\gamma$ among all hypersurfaces in $\mathbb{R}^{n+1}$ enclosing the same volume is (up to translation and homothety) the Wulff shape W_γ for γ. Moreover the Wulff shape can be written as

$$W_\gamma := \partial \bigcap_{\nu\in S^n} \{x \in \mathbb{R}^{n+1} \mid \langle x, \nu\rangle \leq \gamma(\nu)\}.$$

Every function $\gamma : S^n \to \mathbb{R}_{>0}$ determines its Wulff shape uniquely. In addition, if we denote

$$\widehat{W}_\gamma := \bigcap_{\nu\in S^n} \{x \in \mathbb{R}^{n+1} \mid \langle x, \nu\rangle \leq \gamma(\nu)\}.$$

the set $\widehat{W}_\gamma$ is always a convex body, i.e., $\widehat{W}_\gamma$ is compact, convex and has non-empty interior $0 \in \operatorname{Int} \widehat{W}_\gamma$.

Remark . The set $\widehat{W}_\gamma$ is also called the Wulff shape for γ. In the following we will identify W_γ and $\widehat{W}_\gamma$, and use the same notation W_γ if it is clear from the context.

Conversely, for any convex body W with $0 \in \operatorname{Int} W$, we can construct a function $\gamma_W : S^n \to \mathbb{R}_{>0}$ as its support function:

$$\gamma_W(\nu) := \max_{x\in W} \langle x, \nu\rangle, \quad \nu \in S^n.$$

We can check that γ_W is continuous and the Wulff shape for γ_W coincides with W. However, such a function is NOT unique in general.

Example 1.2.1. Let $W = [-1,1] \times [-1,1] \subset \mathbb{R}^2$ be a cube. Obviously W is a convex body with $0 \in \operatorname{Int} W$ and we can show

$$\gamma_W(\nu_1, \nu_2) = |\nu_1| + |\nu_2|$$

by some calculation. However, the function $\gamma(\nu_1, \nu_2) = (|\nu_1| + |\nu_2|)^2$ also gives the same Wulff shape W. □

This problem naturally leads to the notion of the convexity for functions. Let us recall the basic facts from the convex geometry.

For an energy density $\gamma : S^n \to \mathbb{R}_{\geq 0}$ we define the homogeneous extension of γ as

$$\overline{\gamma} : \mathbb{R}^{n+1} \to \mathbb{R}_{\geq 0}, \quad \overline{\gamma}(r\nu) := r\gamma(\nu), \quad r \geq 0,\ \nu \in S^n.$$

Then we can easily check the following well-known fact:

Lemma 1.2.2. The following conditions are equivalent:

(1) $\overline{\gamma}$ is a convex function on $\mathbb{R}^{n+1}$, i.e., $\overline{\gamma}$ satisfies the triangle inequality : $\overline{\gamma}(x+y) \leq \overline{\gamma}(x) + \overline{\gamma}(y)$ for all $x, y \in \mathbb{R}^{n+1}$.

(2) The set $F_\gamma := \{x \in \mathbb{R}^{n+1} \mid \overline{\gamma}(x) \leq 1\}$ is a convex set in $\mathbb{R}^{n+1}$. F_γ is sometimes called the Frank shape or the dual Wulff shape.

We say $\gamma : S^n \to \mathbb{R}_{\geq 0}$ to be *convex* if its homogeneous extension $\overline{\gamma}$ satisfies an either condition in the lemma. The second condition in the lemma gives a visual interpretation of the convexity (see the figure)

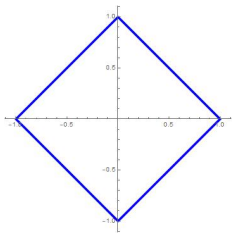

(a) Frank shape for $\gamma(\nu) = |\nu_1| + |\nu_2|$

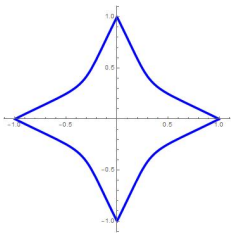

(b) Frank shape for $\gamma(\nu) = (|\nu_1| + |\nu_2|)^2$

In particular, for a convex body W with $0 \in \operatorname{Int} W$, the function γ_W is convex. Moreover, this is the unique convex function among all continuous functions $\gamma : S^n \to \mathbb{R}_{>0}$ which satisfies $W_\gamma = W$. For this reason, the function γ_W is sometimes called the *convex integrand*.

1.2.3 Cahn-Hoffman map and anisotropic mean curvature

From now on we assume that $\gamma : S^n \to \mathbb{R}_{>0}$ is a positive-valued C^2 function. We define the map which parametrizes the Wulff shape. The map defined by

$$\xi_\gamma : S^n \to \mathbb{R}^{n+1}, \quad \xi_\gamma(\nu) := D\gamma(\nu) + \gamma(\nu)\nu, \quad \nu \in S^n,$$

is called the *Cahn-Hoffman map* on S^n. Here $D\gamma$ denotes the gradient of γ on S^n and we identify it as a vector in $\mathbb{R}^{n+1}$. We put $\widetilde{W}_\gamma := \xi_\gamma(S^n)$

Remark . Let $\overline{\gamma} : \mathbb{R}^{n+1} \to \mathbb{R}_{\geq 0}$ be the homogeneous extension of γ. Then the Cahn-Hoffman map ξ_γ can be expressed as

$$\xi_\gamma(\nu) = \overline{\nabla}\overline{\gamma}|_\nu, \quad \nu \in S^n, \tag{2.2}$$

where $\overline{\nabla}$ is the gradient on $\mathbb{R}^{n+1}$. To see this, we take any $x \in \mathbb{R}^{n+1}$ and $v \in T_x\mathbb{R}^{n+1} \simeq \mathbb{R}^{n+1}$, and we have

$$\begin{aligned}\langle \overline{\nabla}\overline{\gamma}, v\rangle_{\mathbb{R}^{n+1}} &= d\overline{\gamma}(v) = \gamma \cdot d(|x|)(v) + |x| \cdot d\gamma(v) \\ &= \gamma\langle \overline{\nabla}|x|, v\rangle + |x|\langle \overline{\nabla}\gamma, v\rangle = \langle D\gamma \cdot |x| + \gamma \cdot (x/|x|), v\rangle.\end{aligned}$$

By taking $x \in S^n$ we have the desired result.

The convexity condition is also naturally appeared in this situation since we have the following fact:

Proposition 1.2.3 ([24], Theorem 4.1, (ii))**.** The image of the Cahn-Hoffman map $\widetilde{W}_\gamma$ coincides with the Wulff shape W_γ if and only if the funtion γ is the convex integrand.

Now we define the anisotropic mean curvature for piecewise-C^2 hypersurfaces.

Definition 1.2.4 ([39], [25])**.** Let $X : M = \bigcup_{i=1}^k M_i \to \mathbb{R}^{n+1}$ be a piecewise-C^2 weak immersion and $\mathcal{S}(X)$ be its singularities. For the unit normal vector field $\nu = \nu_X$ along X, we define the *anisotropic Gauss map* $\widetilde{\xi}_\gamma : M \setminus \mathcal{S}(X) \to \mathbb{R}^{n+1}$ by $\widetilde{\xi}_\gamma := \xi_\gamma \circ \nu_X$. If $\gamma \equiv 1$, this is the usual Gauss map of X.

We call the differential $-d\widetilde{\xi}_\gamma$ the *anisotropic shape operator* and the *anisotropic mean curvature* Λ *of* X is defined as

$$\Lambda = \Lambda_\gamma := \frac{1}{n} trace(-d\widetilde{\xi}_\gamma) = \frac{1}{n}(nH\gamma - \operatorname{div}_M D\gamma),$$

where H is the usual mean curvature of X.

Remark . The eigenvalues of the anisotropic shape operator $-d\widetilde{\xi}_\gamma$ are called the anisotropic principal curvatures and we denote them as $\kappa_1^\gamma, \ldots, \kappa_n^\gamma$. The j-th mean curvature H_j^γ of X is defined as

$$\binom{n}{j} H_j^\gamma := \sum_{1 \leq i_1 < \cdots < i_j \leq n} \kappa_{i_1}^\gamma \cdots \kappa_{i_j}^\gamma.$$

By using the above notation, we have $\Lambda = H_1^\gamma$.

Example 1.2.5. Let us consider the planar ($n = 1$) case. Assume that the energy density $\gamma : S^1 \to \mathbb{R}_{>0}$ is of class C^2, and denote $\gamma(\theta) := \gamma(\cos\theta, \sin\theta)$. Then, the Cahn-Hoffman map $\xi_\gamma(\theta) := \xi_\gamma(\cos\theta, \sin\theta)$ and its differential $\xi_\gamma'(\theta)$ can be represented as follows:

$$\xi_\gamma(\theta) = \gamma'(\theta)(-\sin\theta, \cos\theta) + \gamma(\theta)(\cos\theta, \sin\theta), \quad \xi_\gamma'(\theta) = (\gamma''(\theta) + \gamma(\theta))(-\sin\theta, \cos\theta)$$

For an arclength parametrized regular curve $X : I \subset \mathbb{R} \to \mathbb{R}^2$, we denote the unit normal of X as $\nu(s) = (\cos\theta(s), \sin\theta(s))$. Then the curvature of X is characterized by $\kappa = -d\theta/ds$ (note that we take the outward-pointing unit normal) and the differential $d(\xi_\gamma \circ \nu)$ can be computed as follows:

$$d\xi_\gamma \begin{pmatrix} -\sin\theta(s) \\ \cos\theta(s) \end{pmatrix} = (\gamma_{\theta\theta} + \gamma)(\theta(s)) \cdot \theta_s(s) \begin{pmatrix} -\sin\theta(s) \\ \cos\theta(s) \end{pmatrix}.$$

Therefore we have $\Lambda_\gamma(s) = (\gamma_{\theta\theta} + \gamma)(\theta(s)) \cdot \kappa(s)$. On the other hand, a basic calculation shows the curvature of the Cahn-Hoffman map $\xi_\gamma(\theta)$ is $\kappa_{\xi_\gamma}(\theta) = -1/(\gamma''(\theta) + \gamma(\theta))$ at the point satisfying $\gamma''(\theta) + \gamma(\theta) \neq 0$. Note that the image of the Cahn-Hoffman map is convex where $\gamma'' + \gamma > 0$, concave where $\gamma'' + \gamma < 0$ with respect to the outward-pointing unit normal, and the curvature diverges at the point satisfying $\gamma'' + \gamma = 0$. Therefore we have

$$\Lambda_\gamma(s) = -\kappa(s)/\kappa_{\xi_\gamma}(\theta(s)), \quad \text{where} \quad \gamma_{\theta\theta}(\theta(s)) + \gamma(\theta(s)) \neq 0.$$

In particular, the Cahn-Hoffman map ξ_γ has constant anisotropic curvature -1. Conversely, if we assume the curve X has constant anisotropic curvature $\Lambda(s) \equiv -1$, then

$$\kappa(s) = \kappa_{\xi_\gamma}(\theta(s)) \quad \text{where} \quad \gamma_{\theta\theta}(\theta(s)) + \gamma(\theta(s)) \neq 0.$$

Therefore, by the fundamental theorem for plane curves, X must be equal to a part of the Cahn-Hoffman map ξ_γ (up to translation), where $\gamma_{\theta\theta}(\theta(s)) + \gamma(\theta(s)) \neq 0$. In particular, if $\gamma'' + \gamma > 0$ on S^1, X is equal to the Wulff shape with integer multiplicity. Note that this fact holds in more general settings [30]. □

1.3 The first variation formula of the anisotropic energy

Assume that $\gamma : S^n \to \mathbb{R}_{>0}$ is of class C^2. Let M is a oriented connected compact n-dimensional C^∞ manifold with smooth boundary ∂M and $X : M \to \mathbb{R}^{n+1}$ be a C^2 mapping. We assume that following conditions:

(1) $X|_{\operatorname{Int} M}$ is a C^2-immersion.

(2) The unit normal vector field $\nu : \operatorname{Int} M \to S^n$ along $\operatorname{Int} M$ can be extended to a C^1-mapping $\nu : M \to S^n$. Here, if $(u^1, \ldots, u^n)$ is a local coordinate system in M, $\{\nu, \partial/\partial u^1, \ldots, \partial/\partial u^n\}$ gives the canonical orientation in $\mathbb{R}^{n+1}$.

We consider a C^2 variation

$$X_t : M \to \mathbb{R}^{n+1}, \quad X_t = X + t(\psi\nu + \eta) + O(t^2),$$

where $\psi\nu$, η are the normal and tangential components of the variational vector field respectively (hence these are of C^1):

$$\delta X := \frac{dX_t}{dt}_{|t=0} = \psi\nu + \eta.$$

With these notations we have the following proposition:

Proposition 1.3.1 (First variation formula of $\mathscr{F}_\gamma$, [32] for $n = 2$, [24] for general n)**.**

$$\begin{aligned}\delta\mathscr{F}_\gamma &= \int_M \psi(\operatorname{div}_M D\gamma - nH\gamma)\, dA_X + \int_{\partial M} \langle \delta X, -R(P(\xi))\rangle\, d\widetilde{s} \\ &= -n\int_M \Lambda\langle \delta X, \nu\rangle\, dA_X + \int_{\partial M} \langle \delta X, -R(P(\xi))\rangle\, d\widetilde{s}\end{aligned}$$

where N is the outer unit conormal of X along ∂M, $d\widetilde{s}$ is the $(n-1)$-dimensional volume form of ∂M induced by X and R is the $\pi/2$-rotation in (N, ν)-plane.

Remark . We will discuss about the discrete curves and surfaces and these can be considered as a special case of the piecewise weak immersions. For example, in the triangulated surface case, each piece M_i is a flat triangle and therefore we only have the boundary terms. However, if we consider these as a discrete objects, the "boundary terms" are not necessarily the boundary. Therefore the discrete differential geometry developed in the next chapter always lies in between the smooth and discrete objects, and its importance is the following viewpoint : how to extract the discrete curvature information from the "boundary terms" of the first variation formula.

Recall that $\mathcal{S}(X)$ is the set of all singular points of X. For any $p \in M_i \setminus \mathcal{S}(X)$, we may write $\widetilde{\xi}(p) := \widetilde{\xi_\gamma}(p) := \widetilde{\xi_i}(p)$.

Theorem 1.3.2 (Euler-Lagrange equations, Koiso [24]. For $n = 2$, see B. Palmer [32])**.** A piecewise-C^2 weak immersion $X : M = \bigcup_{i=1}^k M_i \to \mathbb{R}^{n+1}$ is a critical point of the anisotropic energy $\mathscr{F}_\gamma(X) = \int_M \gamma(\nu)\, dA$ for volume-preserving variations if and only if

(1) The anisotropic mean curvature Λ of X is constant on $M \setminus S(X)$, and

(2) $\widetilde{\xi_i}(\zeta) - \widetilde{\xi_j}(\zeta) \in T_\zeta M_i \cap T_\zeta M_j = T_\zeta(\partial M_i \cap \partial M_j)$ holds at any $\zeta \in \partial M_i \cap \partial M_j$, where a tangent space of a submanifold of $\mathbb{R}^{n+1}$ is naturally identified with a linear subspace of $\mathbb{R}^{n+1}$.

Example 1.3.3. Let us continue Example 1.2.5. When $n = 1$, the condition (2) in the above theorem is equivalent to $\widetilde{\xi_i}(\zeta) = \widetilde{\xi_j}(\zeta)$ at the meeting point of the curves $X(M_i)$ and $X(M_j)$. Therefore, we have the following statement:

Proposition 1.3.4. Let $\gamma : S^1 \to \mathbb{R}_{>0}$ be of class C^2 and $\gamma'' + \gamma = 0$ only on the set $\mathcal{S}_\gamma \subset S^1$, where $\mathcal{S}_\gamma = \{\theta_1, \ldots, \theta_m\}$ is a set of finite points. Then a closed piecewise C^2-smooth curve $X : I \subset \mathbb{R} \to \mathbb{R}^2$ which is a critical point of the anisotropic energy $\mathscr{F}_\gamma$ with $\Lambda = -1$ coincides with a part of the Cahn-Hoffman map ξ_γ up to translation with integer multiplicity. In particular, if $\gamma'' + \gamma > 0$ on $S^1 \setminus \mathcal{S}_\gamma$, then X coincides with the Wulff shape up to translation with integer multiplicity.

Remark . The last statement is a special case of the result of Morgan [30].

Proof. We already saw that the regular part of such a curve $X(s)$ coincides with the Cahn-Hoffman map ξ_γ except for the points satisfying $\theta(s) = \theta_j$ for some $j \in \{1, \dots, m\}$, where $\theta(s)$ is defined by the unit normal vector field $\nu(s) = (\cos\theta(s), \sin\theta(s))$. By the assumption, such points $s \in I$ are finite and must lie on the boundaries of each piece since such points correspond to the singularities of the Cahn-Hoffman map ξ_γ. By the condition of (2) in Theorem 1.3.2, each piece must glue together. □

1.4 An example of dimension 1

We give an example which will be used to prove Theorems 1.1.1, 1.1.2, and 1.1.3 in the following sections. Throughout this section $\gamma : S^1 \to \mathbb{R}_{>0}$ is the function defined by

$$\gamma(e^{i\theta}) := \cos^6\theta + \sin^6\theta, \tag{4.1}$$

where $\mathbb{R}^2$ is identified with $\mathbb{C}$.

Lemma 1.4.1. The Cahn-Hoffman map $\xi_\gamma : S^1 \to \mathbb{R}^2$ for γ is represented as follows.

$$\begin{aligned}\xi_\gamma(e^{i\theta}) = \big((\cos\theta)(\cos^6\theta + 6\cos^4\theta\sin^2\theta - 5\sin^6\theta),\\ (\sin\theta)(-5\cos^6\theta + 6\cos^4\theta\sin^2\theta + \sin^6\theta)\big)\end{aligned} \tag{4.2}$$

In other words, we have

$$\xi_\gamma(\nu) = \left(\nu_1(\nu_1^6 + 6\nu_1^4\nu_2^2 - 5\nu_2^6),\, \nu_2(-5\nu_1^6 + 6\nu_1^2\nu_2^4 + \nu_2^6)\right), \quad \nu = (\nu_1, \nu_2) \in S^1. \tag{4.3}$$

Set $\nu_2 = \pm\sqrt{1-\nu_1^2}$. Then

$$\xi_\gamma(\nu) = \left(-\nu_1(9\nu_1^4 - 15\nu_1^2 + 5), \mp\sqrt{1-\nu_1^2}(9\nu_1^4 - 3\nu_1^2 - 1)\right) \tag{4.4}$$

$$= \big(-(9\cos^4\theta - 15\cos^2\theta + 5)\cos\theta, -(9\cos^4\theta - 3\cos^2\theta - 1)\sin\theta\big) \tag{4.5}$$

holds.

Proof. We use the formula (2.2), that is

$$\xi_\gamma(\nu) = \overline{\nabla}\overline{\gamma}|_\nu, \quad \nu \in S^n.$$

where $\overline{\gamma}$ is given by

$$\overline{\gamma}(\nu_1, \nu_2) = \frac{\nu_1^6 + \nu_2^6}{(\nu_1^2 + \nu_2^2)^{5/2}}. \tag{4.6}$$

Hence, we have

$$\overline{\gamma}_{\nu_1} = \frac{\nu_1(\nu_1^6 + 6\nu_1^4\nu_2^2 - 5\nu_2^6)}{(\nu_1^2 + \nu_2^2)^{7/2}}, \tag{4.7}$$

$$\overline{\gamma}_{\nu_2} = \frac{\nu_2(-5\nu_1^6 + 6\nu_1^2\nu_2^4 + \nu_2^6)}{(\nu_1^2 + \nu_2^2)^{7/2}}. \tag{4.8}$$

(2.2) with (4.2) and (4.8) gives

$$\xi_\gamma(\nu) = \big(\nu_1(\nu_1^6 + 6\nu_1^4\nu_2^2 - 5\nu_2^6),\, \nu_2(-5\nu_1^6 + 6\nu_1^2\nu_2^4 + \nu_2^6)\big), \quad \nu = (\nu_1,\, \nu_2) \in S^1, \quad (4.9)$$

which gives the desired formulas (4.2), (4.3). Inserting $\nu_2 = \pm\sqrt{1-\nu_1^2}$ to (4.3), we obtain (4.4), (4.5). □ □

The image $\xi_\gamma(S^1)$ of the Cahn-Hoffman map ξ_γ and the Wulff shape W_γ are shown in Figure 1.4. Lemma 1.4.3 below gives rigorous explanations of these shapes. Now we

Figure 1.3: The image $\xi_\gamma(S^1)$ of the Cahn-Hoffman map (left) and the Wulff shape W_γ (right) for γ defined by (4.1). W_γ is a subset of $\xi_\gamma(S^1)$.

study the singular points of ξ_γ.

Lemma 1.4.2. (i) The the set $S(\xi_\gamma)$ of all singular points of ξ_γ is given by

$$\begin{aligned} S(\xi_\gamma) = \Bigg\{ & p_1 := \left(\frac{\sqrt{5}+1}{2\sqrt{3}}, \frac{\sqrt{5}-1}{2\sqrt{3}}\right),\ p_2 := \left(\frac{\sqrt{5}-1}{2\sqrt{3}}, \frac{\sqrt{5}+1}{2\sqrt{3}}\right), \\ & p_3 := \left(-\frac{\sqrt{5}-1}{2\sqrt{3}}, \frac{\sqrt{5}+1}{2\sqrt{3}}\right),\ p_4 := \left(-\frac{\sqrt{5}+1}{2\sqrt{3}}, \frac{\sqrt{5}-1}{2\sqrt{3}}\right), \\ & p_5 := \left(-\frac{\sqrt{5}+1}{2\sqrt{3}}, -\frac{\sqrt{5}-1}{2\sqrt{3}}\right),\ p_6 := \left(-\frac{\sqrt{5}-1}{2\sqrt{3}}, -\frac{\sqrt{5}+1}{2\sqrt{3}}\right), \\ & p_7 := \left(\frac{\sqrt{5}-1}{2\sqrt{3}}, -\frac{\sqrt{5}+1}{2\sqrt{3}}\right),\ p_8 := \left(\frac{\sqrt{5}+1}{2\sqrt{3}}, -\frac{\sqrt{5}-1}{2\sqrt{3}}\right)\Bigg\}. \end{aligned} \quad (4.10)$$

(ii) Set

$$p_j = (\cos\theta_j, \sin\theta_j), \quad j = 1, \ldots, 8,$$

where θ_1 is chosen so that $0 < \theta_1 < \pi/2$ holds. Then, by choosing suitable principal values for $\theta_1, \cdots, \theta_8$, one can write

$$\theta_2 = \pi/2 - \theta_1,\ \theta_3 = \pi/2 + \theta_1,\ \theta_4 = \pi - \theta_1,\ \theta_5 = \pi + \theta_1, \quad (4.11)$$

$$\theta_6 = 3\pi/2 - \theta_1,\ \theta_7 = 3\pi/2 + \theta_1,\ \theta_8 = -\theta_1. \quad (4.12)$$

(iii)

$$\xi_\gamma(p_8) = \xi_\gamma(p_3) = \frac{2}{\sqrt{3}}(1,1),\ \xi_\gamma(p_2) = \xi_\gamma(p_5) = \frac{2}{\sqrt{3}}(-1,1), \tag{4.13}$$

$$\xi_\gamma(p_4) = \xi_\gamma(p_7) = \frac{2}{\sqrt{3}}(-1,-1),\ \xi_\gamma(p_6) = \xi_\gamma(p_1) = \frac{2}{\sqrt{3}}(1,-1) \tag{4.14}$$

holds.

Remark . Choose the principal value for θ_1 so that $0 < \theta_1 < \pi/2$ is satisfied. Then, by computation using Mathematica ver.11.2.0.0, we get

$$\theta_1 \approx 0.1161397636\pi. \tag{4.15}$$

Proof of Lemma 1.4.2. Using (4.4), we obtain

$$\xi'_\gamma(\nu_1) = \left(-5(9\nu_1^4 - 9\nu_1^2 + 1),\ \pm\frac{5\nu_1}{\sqrt{1-\nu_1^2}}(9\nu_1^4 - 9\nu_1^2 + 1)\right). \tag{4.16}$$

Hence, $(\nu_1, \nu_2) \in S^1$ is a singular point of ξ_γ if and only if

$$9\nu_1^4 - 9\nu_1^2 + 1 = 0 \tag{4.17}$$

holds. (4.17) is equivalent to

$$\nu_1 = \frac{\sqrt{5}\pm 1}{2\sqrt{3}},\ -\frac{\sqrt{5}\pm 1}{2\sqrt{3}}, \tag{4.18}$$

which proves (i).

(ii) is a consequence of (i).

(iii) is obtained by inserting (4.10) to (4.4). □

Set

$$\xi_\gamma(\theta) = ((\xi_\gamma)_x(\theta), (\xi_\gamma)_y(\theta)) := \xi_\gamma(e^{i\theta}).$$

Lemma 1.4.3. Increase and decrease of $(\xi_\gamma)_x(\theta)$, $(\xi_\gamma)_y(\theta)$, and the sign of $A = D^2\gamma + \gamma\cdot 1$ are given by the following table.

θ	θ_8		0		θ_1		θ_2		$\pi/2$		θ_3		θ_4
$(\xi_\gamma)'_x(\theta)$	0	$-$	0	$+$	0	$-$	0	$+$	5	$+$	0	$-$	0
$(\xi_\gamma)'_y(\theta)$	0	$-$	-5	$-$	0	$+$	0	$-$	0	$+$	0	$-$	0
$(\xi_\gamma)_x(\theta)$	$2/\sqrt{3}$	$\searrow$	1	$\nearrow$	$2/\sqrt{3}$	$\searrow$	$-2/\sqrt{3}$	$\nearrow$	0	$\nearrow$	$2/\sqrt{3}$	$\searrow$	$-2/\sqrt{3}$
$(\xi_\gamma)_y(\theta)$	$2/\sqrt{3}$	$\searrow$	0	$\searrow$	$-2/\sqrt{3}$	$\nearrow$	$2/\sqrt{3}$	$\searrow$	1	$\nearrow$	$2/\sqrt{3}$	$\searrow$	$-2/\sqrt{3}$
$A = D^2\gamma + \gamma\cdot 1$	0	$-$	$-$	$-$	0	$+$	0	$-$	$-$	$-$	0	$+$	0

θ	θ_4		π		θ_5		θ_6		$3\pi/2$		θ_7		$\theta_8+2\pi$
$(\xi_\gamma)'_x(\theta)$	0	$+$	0	$-$	0	$+$	0	$-$	-5	$-$	0	$+$	0
$(\xi_\gamma)'_y(\theta)$	0	$+$	5	$+$	0	$-$	0	$+$	0	$-$	0	$+$	0
$(\xi_\gamma)_x(\theta)$	$-2/\sqrt{3}$	$\nearrow$	-1	$\searrow$	$-2/\sqrt{3}$	$\nearrow$	$2/\sqrt{3}$	$\searrow$	0	$\searrow$	$-2/\sqrt{3}$	$\nearrow$	$2/\sqrt{3}$
$(\xi_\gamma)_y(\theta)$	$-2/\sqrt{3}$	$\nearrow$	0	$\nearrow$	$2/\sqrt{3}$	$\searrow$	$-2/\sqrt{3}$	$\nearrow$	-1	$\searrow$	$-2/\sqrt{3}$	$\nearrow$	$2/\sqrt{3}$
$A=D^2\gamma+\gamma\cdot 1$	0	$-$	$-$	$-$	0	$+$	0	$-$	$-$	$-$	0	$+$	0

Proof. Using (4.5), we obtain

$$\begin{aligned}\xi'_\gamma(\theta) &= ((\xi_\gamma)'_x(\theta),\,(\xi_\gamma)'_y(\theta))\\ &= \left(5(9\cos^4\theta-9\cos^2\theta+1)\sin\theta,\,-5(9\cos^4\theta-9\cos^2\theta+1)\cos\theta\right). \qquad (4.19)\end{aligned}$$

For $\gamma(\theta):=\gamma(e^{i\theta})=\cos^6\theta+\sin^6\theta$, we compute

$$\gamma'(\theta)=-6\cos^5\theta\sin\theta+6\sin^5\theta\cos\theta,$$

$$\gamma''(\theta)=6(5\cos^2\theta\sin^2\theta-\cos^6\theta-\sin^6\theta),$$

and hence

$$A=\gamma''(\theta)+\gamma(\theta)=-5(9\cos^4\theta-9\cos^2\theta+1)=-(\xi_\gamma)'_x(\theta)\cdot(\sin\theta)^{-1} \qquad (4.20)$$

holds, here the last equality is valid only when $\sin\theta\neq 0$. These observations with Lemmas 1.4.1, 1.4.2 give the desired result. □

Using Lemma 1.4.1, by simple calculations, we obtain the following result.

Lemma 1.4.4. Let $\rho_1,\rho_2\in(0,\pi/2)$ be the solutions of

$$\cos\rho_1=\sqrt{\frac{1+\sqrt{5}}{6}},\ \cos\rho_2=\sqrt{\frac{5-\sqrt{5}}{6}}, \qquad (4.21)$$

respectively. Then

(i) The inequality

$$0<\theta_1<\rho_1<\pi/4<\rho_2<\theta_2<\pi/2 \qquad (4.22)$$

holds.

(ii) Set

$$\alpha:=\sqrt{\frac{2+2\sqrt{5}}{3}}\,(\sqrt{5}-2). \qquad (4.23)$$

The "inner self-intersection points" of ξ_γ are the following four points.

$Q_1:=(\alpha,0)=\xi_\gamma(\rho_1)=\xi_\gamma(\rho_2+3\pi/2),\ Q_2:=(0,\alpha)=\xi_\gamma(\rho_2)=\xi_\gamma(\rho_1+\pi/2),$
$Q_3:=(-\alpha,0)=\xi_\gamma(\rho_1+\pi)=\xi_\gamma(\rho_2+\pi/2),\ Q_4:=(0,-\alpha)=\xi_\gamma(\rho_2+\pi)=\xi_\gamma(\rho_1+3\pi/2).$

Q_1, Q_2, Q_3, Q_4 are the vertices of W_γ (Figure 1.4, right).

Remark . By computation using Mathematica ver.11.2.0.0, we get

$$\rho_1 \approx 0.2374632441\pi, \quad \rho_2 = \pi/2 - \rho_1 \approx 0.2625367559\pi, \quad \alpha \approx 0.3467370642. \tag{4.24}$$

By using the previous lemmas 1.4.1, 1.4.2, 1.4.3, and 1.4.4 with Fact **??** (i), we obtain the following:

Proposition 1.4.5. Let $\gamma : S^1 \to \mathbb{R}_{>0}$ be the function defined by

$$\gamma(e^{i\theta}) := \cos^6\theta + \sin^6\theta. \tag{4.25}$$

Let θ_1, θ_2 be the constants defined in Lemma 1.4.2, and let ρ_1, ρ_2 be the constants defined in Lemma1.4.4.

(i) The Cahn-Hoffman map $\xi_\gamma : S^1 \to \mathbb{R}^2$ is represented as

$$\begin{aligned}\xi_\gamma(e^{i\theta}) = \big((\cos\theta)(\cos^6\theta + 6\cos^4\theta\sin^2\theta - 5\sin^6\theta),\\ (\sin\theta)(-5\cos^6\theta + 6\cos^4\theta\sin^2\theta + \sin^6\theta)\big)\end{aligned} \tag{4.26}$$

(Figure 1.4).

(ii) The Wulff shape W_γ is given by

$$\begin{aligned}W_\gamma = \xi_\gamma\Big(&\{\rho_1 \le \theta \le \rho_2\} \cup \{\rho_1 + \pi/2 \le \theta \le \rho_2 + \pi/2\}\\ &\cup \{\rho_1 + \pi \le \theta \le \rho_2 + \pi\} \cup \{\rho_1 + 3\pi/2 \le \theta \le \rho_2 + 3\pi/2\}\Big)\end{aligned} \tag{4.27}$$

(Figure 1.4a).

(iii) The following four closed curves which are subsets of $\xi_\gamma(S^1)$ are closed piecewise-C^∞ CAMC curves (Figures 1.4b, 1.4c, 1.4d, 1.4e).

$$(C_\gamma)_1 := \xi_\gamma\left(\{\theta_2 \le \theta \le \theta_3\} \cup \{\theta_4 \le \theta \le \theta_5\} \cup \{\theta_6 \le \theta \le \theta_7\} \cup \{\theta_8 \le \theta \le \theta_1\}\right), \tag{4.28}$$

$$(C_\gamma)_2 := \xi_\gamma\left(\{\theta_1 \le \theta \le \theta_2\} \cup \{\theta_5 \le \theta \le \theta_6\}\right), \tag{4.29}$$

$$(C_\gamma)_3 := \xi_\gamma\left(\{\theta_8 \le \theta \le \theta_1\} \cup \{\theta_3 \le \theta \le \rho_2 + \pi/2\} \cup \{\rho_1 + \pi \le \theta \le \theta_6\}\right), \tag{4.30}$$

$$\begin{aligned}(C_\gamma)_4 := \xi_\gamma\Big(&\{\theta_1 \le \theta \le \rho_1\} \cup \{\rho_2 \le \theta \le \theta_2\} \cup \{\theta_3 \le \theta \le \rho_1 + \pi/2\}\\ &\cup \{\rho_2 + \pi/2 \le \theta \le \theta_4\} \cup \{\theta_5 \le \theta \le \rho_1 + \pi\} \cup \{\rho_2 + \pi \le \theta \le \theta_6\}\\ &\cup \{\theta_7 \le \theta \le \rho_1 + 3\pi/2\} \cup \{\rho_2 + 3\pi/2 \le \theta \le \theta_8 + 2\pi\}\Big).\end{aligned} \tag{4.31}$$

The anisotropic (mean) curvature for the outward-pointing normal is -1.

(iv) The following closed curve which is a subset of $\xi_\gamma(S^1)$ is a closed piecewise-C^∞ curve (Figure 1.4f).

$$(C_\gamma)_5 := \xi_\gamma\Big(\{-\rho_1 \le \theta \le \rho_1\}\Big). \tag{4.32}$$

Its anisotropic (mean) curvature is not constant, because, for the outward-pointing normal, it is -1 at each point in the solid curve:

$$\xi_\gamma\Big(\{\theta_8 \le \theta \le \theta_1\}\Big), \tag{4.33}$$

while it is 1 at each point in the dashed curves:

$$\xi_\gamma\Big(\{-\rho_1 \le \theta \le \theta_8\} \cup \{\theta_1 \le \theta \le \rho_1\}\Big). \tag{4.34}$$

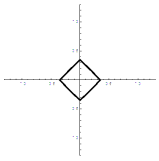

(a) Wulff shape W_γ

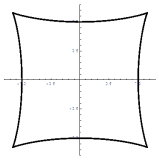

(b) CAMC curve $(C_\gamma)_1$

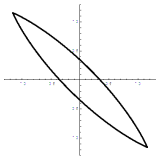

(c) CAMC curve $(C_\gamma)_2$

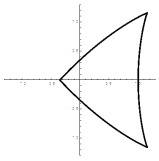

(d) CAMC curve $(C_\gamma)_3$

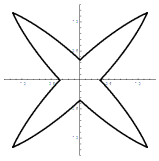

(e) CAMC curve $(C_\gamma)_4$

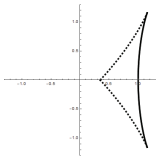

(f) curve $(C_\gamma)_5$. not CAMC

Figure 1.4: Some of the closed curves which are subsets of $\xi_\gamma(S^1)$ for γ defined by (4.1) (cf. Figure 1.4). (a), (b), (c), (d), (e) : The anisotropic (mean) curvature for the outward-pointing normal is -1. (f) : For the outward-pointing normal, the anisotropic (mean) curvature is -1 at each point in the solid curve, while it is 1 at each point in the dashed curves. Hence, this curve is not CAMC.

Remark . Proposition 1.4.5 proves Theorem 1.1.1 for $n = 1$.

Remark . In Proposition 1.4.5, we gave six closed piecewise-C^∞ curves which are subsets of $\xi_\gamma(S^1)$. Five of them were CAMC and the other one was not CAMC. We should remark that there are more piecewise-C^∞ CAMC closed curves and non-CAMC closed curves. Figure 1.5 gives all of the other closed CAMC curves included in $\xi_\gamma(S^1)$ (up to congruence in $\mathbb{R}^2$).

1.5 Higher dimensional examples

In this section we give two higher dimensional examples by rotating γ which was defined by (4.1) and studied in the section 1.4 details.

Regarding (4.6), we consider the function

$$\overline{\gamma}_1^0(\nu_1, \nu_3) = \frac{\nu_1^6 + \nu_3^6}{(\nu_1^2 + \nu_3^2)^{5/2}}$$

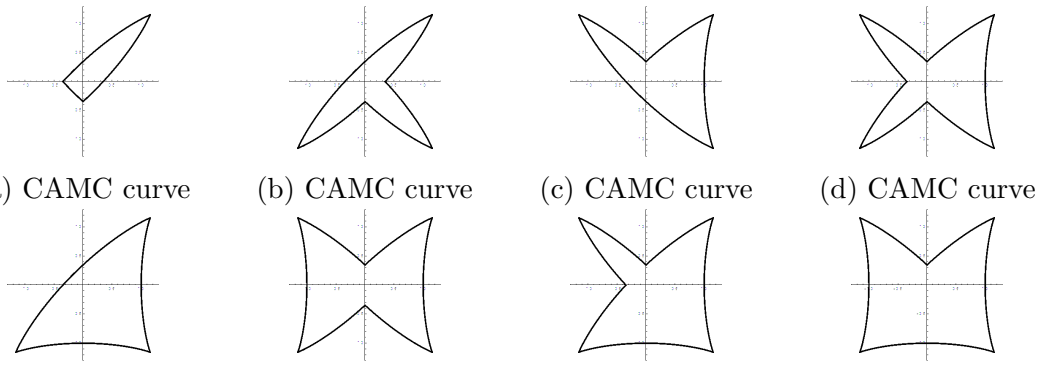

(a) CAMC curve (b) CAMC curve (c) CAMC curve (d) CAMC curve

(e) CAMC curve (f) CAMC curve (g) CAMC curve (h) CAMC curve

Figure 1.5: Closed CAMC curves which are subsets of $\xi_\gamma(S^1)$ for γ defined by (4.1) (cf. Figure 1.4). For all of these eight curves, the anisotropic (mean) curvature for the outward-pointing normal is -1. They and the five curves in Figures 1.4a, 1.4b, 1.4c, 1.4d, 1.4e give all closed CAMC curves included in $\xi_\gamma(S^1)$ (up to congruence in $\mathbb{R}^2$

defined on the (ν_1, ν_3)-plane. We denote the restriction of $\overline{\gamma}_1^0$ to S^1 by γ_1^0. Then, by Lemma 1.4.1, the Cahn-Hoffman map $\xi_{\gamma_1^0} : S^1 \to \mathbb{R}^2$ for γ_1^0 is represented as follows (Figure 1.6a).

$$\xi_{\gamma_1^0}(\nu) = \big(\nu_1(\nu_1^6 + 6\nu_1^4\nu_3^2 - 5\nu_3^6),\ \nu_3(-5\nu_1^6 + 6\nu_1^2\nu_3^4 + \nu_3^6)\big) \tag{5.1}$$

$$= \Big((\cos\theta)(\cos^6\theta + 6\cos^4\theta\sin^2\theta - 5\sin^6\theta),\\ (\sin\theta)(-5\cos^6\theta + 6\cos^4\theta\sin^2\theta + \sin^6\theta)\Big). \tag{5.2}$$

$(\nu = (\nu_1, \nu_3) = (\cos\theta, \sin\theta) \in S^1)$. The higher dimensional example obtained by rotating $\overline{\gamma}_1^0$ around the ν_3-axis is given by

$$\overline{\gamma}_1(\nu_1, \nu_2, \nu_3) = \frac{(\nu_1^2 + \nu_2^2)^3 + \nu_3^6}{(\nu_1^2 + \nu_2^2 + \nu_3^2)^{5/2}}, \quad (\nu_1, \nu_2, \nu_3) \in \mathbb{R}^3. \tag{5.3}$$

The corresponding Cahn-Hoffman map $\xi_{\gamma_1} : S^2 \to \mathbb{R}^3$ is given as follows (Figure 1.6b).

$$\xi_{\gamma_1}(\nu) = \big((\cos\theta)(\cos^6\theta + 6\cos^4\theta\sin^2\theta - 5\sin^6\theta)(\cos\rho),\\ (\cos\theta)(\cos^6\theta + 6\cos^4\theta\sin^2\theta - 5\sin^6\theta)(\sin\rho),\\ (\sin\theta)(-5\cos^6\theta + 6\cos^4\theta\sin^2\theta + \sin^6\theta)\big), \tag{5.4}$$

$(\nu = (\cos\theta\cos\rho, \cos\theta\sin\rho, \sin\theta) \in S^2)$.

By the same way as in the section 1.4, we get closed piecewise-C^∞ CAMC surfaces and closed piecewise-C^∞ non-CAMC surfaces for γ_1 which are subsets of $\xi_{\gamma_1}(S^2)$ and which are not the Wulff shape W_{γ_1} (up to homothety and translation). In fact, we have the following:

Proposition 1.5.1. Consider $\gamma_1 : S^2 \to \mathbb{R}_{>0}$ defined by

$$\gamma_1(\nu_1, \nu_2, \nu_3) = (\nu_1^2 + \nu_2^2)^3 + \nu_3^6, \quad (\nu_1, \nu_2, \nu_3) \in S^2. \tag{5.5}$$

The Wulff shape W_{γ_1} is the surface of revolution (Figure 1.7a) given by rotating $W_{\gamma_1^0}$ (Figure 1.4a) around the vertical axis. The two piecewise-C^∞ closed surfaces (Figures 1.7b, 1.7c) given by rotating the closed curves $(C_\gamma)_1$, $(C_\gamma)_4$ (Figures 1.4b, 1.4e) around the vertical axis are CAMC. The piecewise-C^∞ closed surface (Figures 1.7d) given by rotating the closed curve $(C_\gamma)_5$ (Figure 1.4f) is not CAMC.

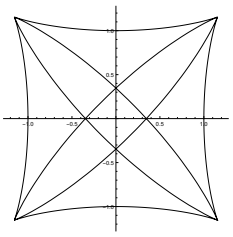

(a) The image of $\xi_{\gamma_1^0}$

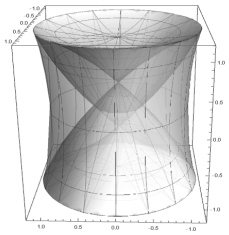

(b) The image of ξ_{γ_1}

Figure 1.6: (a): The image of the Cahn-Hoffman map $\xi_{\gamma_1^0} : S^1 \to \mathbb{R}^2$ for $\gamma_1^0 : S^1 \to \mathbb{R}_{>0}$. (b): The image of the Cahn-Hoffman map $\xi_{\gamma_1} : S^2 \to \mathbb{R}^3$ for $\gamma_1 : S^2 \to \mathbb{R}_{>0}$.

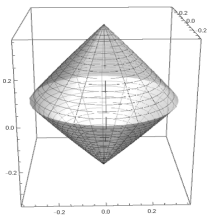

(a) Wulff shape W_{γ_1}

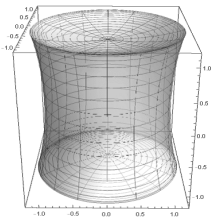

(b) CAMC surface

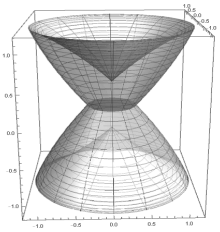

(c) CAMC surface

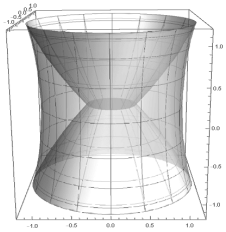

(d) not CAMC

Figure 1.7: Some of the closed surfaces which are subsets of $\xi_{\gamma_1}(S^2)$ for γ_1 defined by (5.5) (Figure 1.6b). They are surfaces given by rotating the curves W_γ, $(C_\gamma)_1$, $(C_\gamma)_4$, $(C_\gamma)_5$, respectively. (a), (b), (c): The anisotropic mean curvature for the outward-pointing normal is -1. (d) : The anisotropic mean curvature is -1 on the 'outer part', while it is 1 on the 'inner part'. Hence, this surface is not CAMC.

Let us give another example. We rotate $\overline{\gamma}_1^0$ around the origin by $\pi/4$ and obtain the following example.

$$\overline{\gamma}_2^0(\nu_1, \nu_3) = \frac{\nu_1^6 + 15\nu_1^4\nu_3^2 + 15\nu_1^2\nu_3^4 + \nu_3^6}{4(\nu_1^2 + \nu_3^2)^{5/2}} \tag{5.6}$$

defined on the (ν_1, ν_3)-plane. We denote the restriction of $\overline{\gamma}_2^0$ to S^1 by γ_2^0. The Cahn-Hoffman map $\xi_{\gamma_2^0} : S^1 \to \mathbb{R}^2$ for γ_2^0 is obtained by rotating $\xi_{\gamma_1^0}$ around the origin by

$\pi/4$, and so it is represented as follows (Figure 1.8a).

$$\xi_{\gamma_2^0}(\nu) = \frac{1}{4}\big(\nu_1(\nu_1^6 - 9\nu_1^4\nu_3^2 + 15\nu_1^2\nu_3^4 + 25\nu_3^6), \nu_3(25\nu_1^6 + 15\nu_1^4\nu_3^2 - 9\nu_1^2\nu_3^4 + \nu_3^6)\big) \quad (5.7)$$

$$= \frac{1}{4}\big((\cos\theta)(\cos^6\theta - 9\cos^4\theta\sin^2\theta + 15\cos^2\theta\sin^4\theta + 25\sin^6\theta),$$
$$(\sin\theta)(25\cos^6\theta + 15\cos^4\theta\sin^2\theta - 9\cos^2\theta\sin^4\theta + \sin^6\theta)\big). \quad (5.8)$$

($\nu = (\nu_1, \nu_3) = (\cos\theta, \sin\theta) \in S^1$). The higher dimensional example obtained by rotating $\overline{\gamma}_2^0$ around the ν_3-axis is given by

$$\overline{\gamma}_2(\nu_1, \nu_2, \nu_3) = \frac{(\nu_1^2+\nu_2^2)^3 + 15(\nu_1^2+\nu_2^2)^2\nu_3^2 + 15(\nu_1^2+\nu_2^2)\nu_3^4 + \nu_3^6}{4(\nu_1^2+\nu_2^2+\nu_3^2)^{5/2}}, \quad (\nu_1, \nu_2, \nu_3) \in \mathbb{R}^3. \quad (5.9)$$

The restriction γ_2 of $\overline{\gamma}_2 : \mathbb{R}^3 \to \mathbb{R}_{\geq 0}$ to S^2 can be written as

$$\gamma_2(\nu_1, \nu_2, \nu_3) = (\nu_1^2+\nu_2^2)^3 + 15(\nu_1^2+\nu_2^2)^2\nu_3^2 + 15(\nu_1^2+\nu_2^2)\nu_3^4 + \nu_3^6, \quad (\nu_1, \nu_2, \nu_3) \in S^2. \quad (5.10)$$

The corresponding Cahn-Hoffman map $\xi_{\gamma_2} : S^2 \to \mathbb{R}^3$ is given as follows (Figure 1.8b).

$$\xi_{\gamma_2}(\nu) = \frac{1}{4}\big((\cos\theta)(\cos^6\theta - 9\cos^4\theta\sin^2\theta + 15\cos^2\theta\sin^4\theta + 25\sin^6\theta)(\cos\rho),$$
$$(\cos\theta)(\cos^6\theta - 9\cos^4\theta\sin^2\theta + 15\cos^2\theta\sin^4\theta + 25\sin^6\theta)(\sin\rho),$$
$$(\sin\theta)(25\cos^6\theta + 15\cos^4\theta\sin^2\theta - 9\cos^2\theta\sin^4\theta + \sin^6\theta)\big), \quad (5.11)$$

($\nu = (\cos\theta\cos\rho, \cos\theta\sin\rho, \sin\theta) \in S^2$).

By the same way as above, we get closed piecewise-C^∞ CAMC surfaces (Figure 1.9) and closed piecewise-C^∞ non-CAMC surfaces for γ_2 which are subsets of $\xi_{\gamma_2}(S^2)$ and which are not the Wulff shape W_{γ_2} (up to homothety and translation).

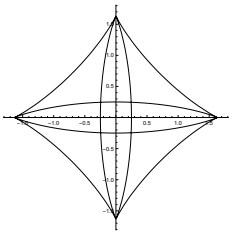

(a) The image of $\xi_{\gamma_2^0}$

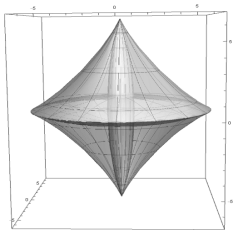

(b) The image of ξ_{γ_2}

Figure 1.8: (a): The image of the Cahn-Hoffman map $\xi_{\gamma_2^0} : S^1 \to \mathbb{R}^2$ for $\gamma_2^0 : S^1 \to \mathbb{R}_{>0}$. (b): The image of the Cahn-Hoffman map $\xi_{\gamma_2} : S^2 \to \mathbb{R}^3$ for $\gamma_2 : S^2 \to \mathbb{R}_{>0}$.

1.6 Proofs of Theorems 1.1.1, 1.1.2

The functions $\gamma_1^0 : S^1 \to \mathbb{R}_{>0}$, $\gamma_2^0 : S^1 \to \mathbb{R}_{>0}$ and their rotations around the vertical axis give examples which prove Theorems 1.1.1, 1.1.2. In fact, Propositions 1.4.5, 1.5.1

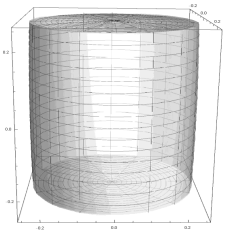

(a) Wulff shape W_{γ_2}

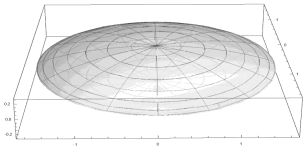

(b) CAMC surface for γ_2

(c) CAMC surface for γ_2

Figure 1.9: Some of the closed surfaces which are subsets of $\xi_{\gamma_2}(S^2)$ for γ_2 defined by (5.10) (Figure 1.8b). The anisotropic mean curvature for the outward-pointing normal is -1.

give suitable examples for $n = 1, 2$, respectively. Also, higher dimensional examples are obtained by the method given in the section 1.5.

1.7 Applications to anisotropic mean curvature flow: proofs of Theorems 1.1.4, 1.1.3

Let $\gamma : S^n \to \mathbb{R}_{>0}$ be of C^2 with Cahn-Hoffman map ξ_γ. Let $X_t : M \to \mathbb{R}^{n+1}$ be one-parameter family of embedded piecewise-C^2 hypersurfaces with anisotropic mean curvature Λ_t. Assume that the Cahn-Hoffman field $\tilde{\xi}_t$ along X_t is defined on M. If X_t satisfies $\partial X_t/\partial t = \Lambda_t \tilde{\xi}_t$, it is called an anisotropic mean curvature flow, which diminishes the anisotropic energy if $\Lambda_t \not\equiv 0$. In fact,

$$\begin{aligned}\frac{d\mathcal{F}_\gamma(X_t)}{dt} &= -\int_M n\Lambda_t \left\langle \frac{\partial X_t}{\partial t}, \nu_t \right\rangle dA_t = -\int_M n\Lambda_t^2 \langle D\gamma + \gamma(\nu_t)\nu_t, \nu_t\rangle \, dA_t \\ &= -\int_M n\Lambda_t^2 \gamma(\nu_t)\, dA_t < 0 \end{aligned} \tag{7.1}$$

holds.

Proof of Theorem 1.1.4. Since the anisotropic mean curvature of ξ_γ is -1, $\Lambda_t = -1/\sqrt{2(c-t)}$ holds. On the other hand, $\widetilde{\xi}_t = \xi_\gamma$ holds. These two facts imply that (i) and (ii) hold. □

Proof of Theorem 1.1.3. Examples stated in Propositions 1.4.5, 1.5.1 give the desired result. □

Chapter 2

A discretization of the anisotropic energy for curves and surfaces

Abstract

In this chapter, we study discrete curves and surfaces from the variational problem for the anisotropic energy. For the planar curve case, by extracting a notion of discrete curvature vector, we show that this vector can be used effectively for an unified interpretation of various discrete curvature notions, Steiner-type formula and the stability problem of critical points of the length functional. Moreover, we formulate discrete CAMC curves and give an application. For the surface case, we derive a generalization of the cotangent formula obtained in [34] and formulate discrete CAMC surfaces. We also visualize some examples and derive a stability problem which is a generalization of the result in [37].

2.1 Introduction

Discrete differential geometry is an active research field because of the interaction among the theory, the algorithm and the visualization on the computer. In this chapter, we mainly focus on discrete objects themselves, not approximation problems of smooth objects or convergence problems. In this field, from the theoretical point of view, one approach is based on the variational methods and the other focus on the integrability of equations. We take the former approach in this chapter and try to develop a theory of discrete curves and simplicial surfaces based on the variational problem for the anisotropic energy as we discussed in Chapter 1. One of the benefit of this approach is that we can consider not only a surface itself but also vector fields on the surface, thus it has many applications (see e.g. [35], [21], [36], [38]). Moreover, this approach with the anisotropic energy gives an unified formulation of discrete CMC surfaces in the Euclidean space, the Lorentz-Minkowski space and the isotropic space (see Appendix). On the other hand, a discrete surface theory using the integrable systems is originated

from [6]. The study of the relation between the integrable system approach and the variational approach has just begun recently, see e.g. [27].

In §2.2, we recall some basic notions from the (combinatorial) simplicial complexes and its geometric realization [35]. By a discrete curve or surface we mean a geometric realization of a combinatorial simplicial curve or surface, respectively. We first derive the first variation formula for the anisotropic energy and extract the vector from the formula which should be called "discrete curvature vector" in §2.3.1. In §2.3.2, by using this curvature vector, we show an unifed interpretation which derive various kinds of discrete curvature notions defined in [19], [15]. The important viewpoint here is that there is no natural notion of the line element on the vertices. In §2.3.3, we derive the Steiner-type formula for parallel curves by using the "vertex normal" constructed from the curvature vector derived in §2.3.1. Since there is no universal definition of the discrete curvature and our main interest is CAMC curves and surfaces, we will define discrete CAMC curves and surfaces without defining the curvature itself. Our definitions of discrete CAMC curves and surfaces are inspired by discrete CMC surfaces defined in [37]. In §2.3.4, we characterize closed discrete constant curvature curves as regular polygons which are possibly non-convex. In §2.3.5, we formulate discrete CAMC curves and derive the conservation law for the Euler-Lagrange equation defining the discrete CAMC curve. Then, as an application of the conservation law, we give another proof for the Chakerian-Lange theorem [8]. In §2.3.6, we will consider the stability problem of the discrete CAMC curves. For the isotropic case, we derive the second variation formula similar to the smooth case by decomposing the variation vectors into the vertex normal directions introduced in §2.3.3 and "tangential" directions. Moreover we show the instability for the non-convex regular polygons in §2.3.7 by using the normal variation and discrete Wirtinger's inequality [12].

Then, as one interpretation of this conservation law, we give another proof for the Chakerian-Lange theorem [8]. Moreover, we will give a "non-uniqueness example" for the discrete CAMC curves as in the Chapter 1. In §2.3.6, we will consider the stability problem of the discrete CAMC curves. We derive a simple criteria for the instability for the discrete CAMC curves and visualize its energy descent deformation for some cases. In the isotropic case, we can derive the second variation formula similar to the smooth case by decomposing the variation vector field to the "normal" and "tangential" directions derived in the section. Moreover, we show the instability for the non-convex regular polygons by using the second variation formula for "normal" variations and discrete Wirtinger's inequality [12] in §2.3.7.

From §2.4, we treat the surface case. We first derive the first variation formula of the anisotropic energy for simplicial surfaces (Theorem 2.4.1) which generalizes the cotangent formula obtained in [34]. Then we define the discrete CAMC surfaces as in the curve case. In §2.4.3, we give many examples of discrete CAMC surfaces from various point of view. In §2.4.4, we derive the second variation formula for the anisotropic energy and prove the stability of the very small part of the discrete CAMC surfaces if the energy density is of class C^2 and convex (Corollary 2.4.16). This result is a generalization of the result obtained in [37].

2.2 Preliminaries

We will develop a discretization theory for the anisotropic energy by using simplicial complexes. To do so, we need to recall basic notions from simplicial complexes (cf. [35]).

2.2.1 Abstract simplicial complexes

Definition 2.2.1 (abstract simplex)**.** Let $V = \{v_0, \ldots, v_m\}$ be a set, where v_j are not necessarily in the Euclidean space. Then we call the ordered set $[v_0, \ldots, v_m]$ be an *abstract m-simplex* or simply *abstract simplex*. The number m is called the dimension of the abstract simplex. For the completeness, we admit the empty set $\emptyset$.

Remark . An abstract simplex is defined just as a set. For example, we consider a triangle $T = (p, q, r)$ in $\mathbb{R}^2$. This is the convex hull of 3 vertices $\{p, q, r\}$, and the edges and faces can be reconstructed from the vertices, i.e., these can be considered as an element of the powered set of vertices. For example, the edge $\overline{pq}$ corresponds to a set $\{p, q\} \subset \{p, q, r\}$.

Definition 2.2.2 (face)**.** Let $\sigma = [v_0, \ldots, v_m]$ be an abstract m-simplex. Then we call the subsimplex consists of $(k+1)$ points $[v_{i_0}, \ldots, v_{l_k}]$ the *k-face* of σ. An $(m-1)$-face of σ is called *proper*. For completeness, we consider the empty set $\emptyset = []$ and the simplex itself as a face of σ.

Remark . Every abstract m-simplex has 2^{m+1} faces up to the order.

Example 2.2.3 (triangle (2-simplex))**.** An 2-simplex $[v_0, v_1, v_2]$ has 8 faces, that is, three 0-simplices (vertices) $[v_0]$, $[v_1]$, $[v_2]$, three 1-simplices (edges) $[v_0, v_1]$, $[v_1, v_2]$, $[v_2, v_0]$, the empty set [] and the triangle itself $[v_0, v_1, v_2]$.

Definition 2.2.4 ((abstract) simplicial complex)**.** Let $V = \{v_1, v_2, \ldots\}$ be an abstract point set. *An (abstract) simplicial complex* $K = K(V) = \{\sigma, \tau, \ldots\}$ is a set of simplices formed by finite subset of V and satisfies the following condition : if $\sigma \in K$ is a simplex, then any face τ of σ is also an element of K.

If two simplices in K share a common non-empty face, then they are called *neighbors*. The *boundary* of K is formed by any proper face that belongs to only one simplex, and its faes. The boundary is also an abstract simplicial complex.

Example 2.2.5. Let us consider the simplest case. Let $V = \{v_0, v_1\}$ be a set. Then $K_1 := \{[v_0], [v_0, v_1]\}$ is not a simplicial complex since the face $[v_1] \subset [v_0, v_1]$ does not belong to K_1. If we consider $K := K_1 \cup \{[v_1]\}$, we have a simplicial complex.

2.2.2 Subsimplex, star and link

Definition 2.2.6 (subsimplex)**.** Let K be a simplicial complex. Then a subset $L \subset K$ is called the *subcomplex* of K if L itself is a simplicial complex.

Definition 2.2.7 (p-skelton)**.** We denote the set of all p-dimensional simplices by $K^{(p)}$ and call the *p-skelton of K*.

Example 2.2.8. For a simplicial complex K, $K^{(0)}$ is the set of vertices and $K^{(2)}$ is the set of triangles.

Definition 2.2.9 (star, link)**.** Let K be an simplicial complex and $\sigma \in K$ be a simplex. Then the *star of σ* and the *link of σ* is defined as follows:

$$\begin{aligned} \text{star}\,(\sigma) &:= \{\eta \in K \mid \sigma \textit{ includes } \eta \textit{ and every face of } \eta\}, \\ \text{link}(\sigma) &:= \{\eta \in \text{star}\,(\sigma) \mid \eta \cap \sigma = \emptyset\}. \end{aligned}$$

2.2.3 Simplicial map

Definition 2.2.10 (simplicial map)**.** Let K, L be simplicial complexes. Then a map $\varphi : K \to L$ is said to be the *simplicial map* if φ satisfies the following conditions:

(1) $\varphi|_{K^0} : K^{(0)} \to L^{(0)}$, i.e, each vertex of K is mapped to a vertex of L.

(2) For any simplex $\sigma = [v_0, \ldots, v_k] \in K$, the image $\varphi(\sigma) = [\varphi(v_0), \ldots, \varphi(v_k)]$, which can be degenerate, is a simplex in L.

A simplicial map $\varphi : K \to L$ is said to be *simplicial isomorphism* if the map $\varphi|_{K^{(p)}} : K^{(p)} \to L^{(p)}$ is bijective for every p. In this case K and L are called *simplicially isomorphic*.

2.2.4 Simplicial curves, simplicial surfaces

Definition 2.2.11 (path, closed curve)**.** Let n be a non-negative integer. A *standard n-path* is a simplicial complex formed by

(1) $(n+1)$ abstract points : $V = \{v_0, \ldots, v_n\}$.

(2) the set of n edges $e_k = [v_k, v_{k+1}]$, $k = 0, \ldots, n-1$.

A *standard n-circle* is the union of a standard n-path and the "final" edge $e_n = [v_n, v_0]$. We sometimes call a standard n-path (or standad n-circle) a *simplicial curve* and denote it by G. Similarly we sometimes consider $\mathbb{N}$ or $\mathbb{Z}$ as a standard path (non-compact case).

Definition 2.2.12 (abstract m-path)**.** Let K be a simplicial complex and δ be a standard n-path. Then a simplicial map $\varphi : \delta \to \varphi(\delta) \subset K$ (or its image $\varphi(\delta)$) is called the *abstract n-path*. We define the *abstract n-circle* similarly. An abstract n-circle is called *simple* if the map φ is injective.

Definition 2.2.13 (closed simplicial surface)**.** A *closed simplicial surface* Σ is an abstract simplicial complex formed by finite number of triangles and satisfying the following conditions:

(1) Any point $p \in \Sigma$ belongs to at least one triangle $T \in \Sigma$.

(2) For any point $p \in \Sigma$, the link $\text{link}(p)$ is an abstract circle.

2.2.5 Geometric simplicial complexes

Our main object is defined by a geometric realization of an abstract simplicial complex. First we give a "parameter domain" of abstract simplices.

Definition 2.2.14 (standard simplex)**.** A *standard simplex* $\Delta^m \subset \mathbb{R}^{m+1}$ is the convex hull of the end points of the canonical basis $\{e_0, \ldots, e_m\} \subset \mathbb{R}^{m+1}$. Formally Δ^m is defined by

$$\Delta^m = \left\{ \sum_{i=0}^{m} \lambda_i e_i \mid 0 \leq \lambda_i \leq 1, \sum_{i=0}^{m} \lambda_i = 1 \right\}.$$

Here the coefficient $(\lambda_0, \ldots, \lambda_m)$ is called the *barycentric coordinates*.

Definition 2.2.15 (geometric simplicial complex)**.** A *geometric simplicial complex* $(P, K(V))$ consists of the following three objects:

(1) (Combinatorial structure) A simplicial complex $K(V)$ over a set of abstract points $V = \{v_0, v_1, \ldots\}$.

(2) (Geometric realization) A set of geometric vertices $P = \{p_0, p_1, \ldots\} \subset \mathbb{R}^n$ and a bijection $\Phi : V \to P$, $\Phi(v_i) = p_i$.

(3) (Local parametrization) For each k-simplex $\sigma = [v_{i_0}, \ldots, v_{i_k}]$ there exists a simplicial map
$$\varphi_\sigma : \Delta^k \to \sigma, \quad \varphi_\sigma(e_j) = p_{i_j}.$$

The set of affine maps $\{\varphi_\sigma\}_{\sigma \in K}$ gives a piecewise affine structure on the geometric simplicial complex K. This induced from the bijection Φ we don't denote explicitly in the pair $(P, K(V))$.

In the following sections we use the word "a simplicial curve (a discrete curve)" and "a simplicial surface (a discrete surface, a triangulated surface)" as a geometric realization of a simplicial curve and a simplicial surface, respectively. Note that the geometric realization gives the induced metric on the abstract simplicial curves or surfaces.

2.3 Geometry of discrete anisotropic curve energy

2.3.1 Anisotropic curve energy and its first variation

For a discrete curve there is a natural question:

What is the unit normal, curvature and line element at the vertices ?

In this section we derive will derive the first variation formula for the anisotropic energy and extract the "curvature vector" at a vertex in order to approach to this question. However non-uniqueness of the line element at vertices gives different notions

of the discrete curvature (so-called "no free lunch" story), and we will show that various kinds of discrete curvature notions, e.g. in [19], [15], can be derived from this viewpoint.

Let $\gamma : S^1 \to \mathbb{R}_{>0}$ be a continuous function and Γ_h be a simplicial curve in $\mathbb{R}^2$, i.e., Γ_h is a geometric realization of a standard $(n-1)$-path or $(n-1)$-circle G. The set of vertices of G is denoted by V and its image is denoted by $\{p_k\}_{k=0}^{n-1}$. For each oriented edge $e_k := [p_k, p_{k+1}]$ of Γ_h we can assign an unit normal vector

$$\nu_k := R\left(\frac{p_{k+1}-p_k}{l_k}\right) := R\left(\frac{p_{k+1}-p_k}{|p_{k+1}-p_k|}\right),$$

where R is the $\pi/2$-rotation or $-\pi/2$-rotation in $\mathbb{R}^2$. It does not matter whichever we choose but we choose the same R for all k. Then the anisotropic energy of Γ_h is defined

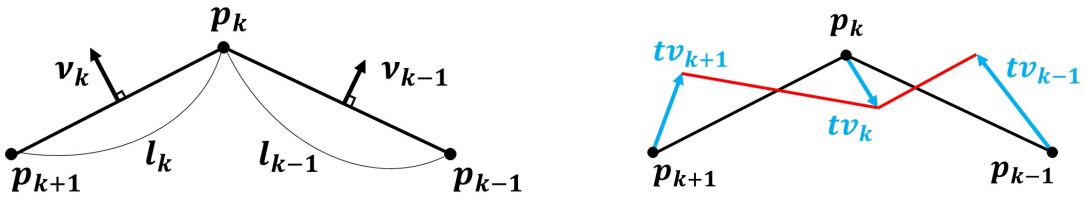

Figure 2.1: A part of a discrete curve with $-\pi/2$-rotation and its variation.

by

$$\mathscr{F}_\gamma(\Gamma_h) := \sum_k \gamma(\nu_k)|p_{k+1}-p_k| = \sum_k \gamma(\nu_k) l_k$$

By the definition of simplicial curves if we fix the orientation of the unit normal, the anisotropic energy $\mathscr{F}_\gamma$ for a discrete curve can be considered as a function $\mathscr{F}_\gamma : \mathbb{R}^{2n} \to \mathbb{R}_{>0}$.

First we derive the first variation formula, that is, we compute the directional derivative in $\mathbb{R}^{2n}$. In the following we assume that γ is of class C^1. We consider a variation

$$p_k(t) = p_k + tv_k + O(t^2), \quad k = 0, \dots, n-1$$

where ${}^t\vec{v} = ({}^tv_0, \dots, {}^tv_{n-1}) \in \mathbb{R}^{2n}$ is the "variation vector field". If p_k is a boundary point of Γ_h, then we assume $v_k = 0$.

We would like to find a vector $\nabla\mathscr{F}_\gamma \in \mathbb{R}^{2n}$ which satisfies

$$\frac{d}{dt}_{|t=0}\mathscr{F}_\gamma = \langle \vec{v}, \nabla\mathscr{F}_\gamma\rangle_{\mathbb{R}^{2n}} = \sum_k \langle v_k, \nabla_{p_k}\mathscr{F}_\gamma\rangle_{\mathbb{R}^2},$$

where we write ${}^t\nabla\mathscr{F}_\gamma = ({}^t\nabla_{p_0}\mathscr{F}_\gamma, \dots, {}^t\nabla_{p_{n-1}}\mathscr{F}_\gamma) \in \mathbb{R}^{2n}$. In this setting we have the following proposition:

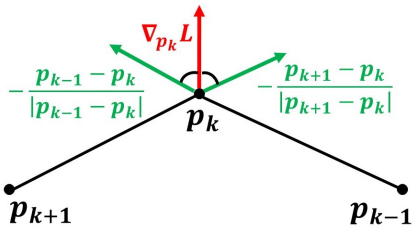

Proposition 2.3.1. Let $\gamma : S^1 \to \mathbb{R}_{>0}$ be a C^1 function and $\Gamma_h = \{p_k\}_k$ be a discrete curve. Then at each interior vertex p_k the gradient of the anisotropic energy with respect to variations of the vertices can be expressed

$$\nabla_{p_k} \mathscr{F}_\gamma = R(\xi_\gamma(\nu_k) - \xi_\gamma(\nu_{k-1})), \tag{3.1}$$

where $\xi_\gamma : S^1 \to \mathbb{R}^2$ is the Cahn-Hoffman map for γ.

Remarks . By using this formula we have

$$\delta\mathscr{F}_\gamma = \sum_k \langle R(\xi_\gamma(\nu_k) - \xi_\gamma(\nu_{k-1})), v_k\rangle = -\sum_k \left\langle \frac{1}{L_k} R(\xi_\gamma(\nu_{k-1}) - \xi_\gamma(\nu_k)), v_k \right\rangle L_k,$$

where we inserted some auxilary function $L : V_n \to \mathbb{R}_{>0}$. This kind of observation is already remarked in the paper [9]. We give some remarks for the isotropic case, i.e, $\gamma \equiv 1$ case.

(1) In this case, we have $\xi_\gamma(\nu) = \nu$ and the vector

$$\widetilde{N}_k := -\frac{1}{L_k} R(\nu_k - \nu_{k-1}) = \frac{1}{L_k}\left(\frac{p_{k+1}-p_k}{|p_{k+1}-p_k|} + \frac{p_{k-1}-p_k}{|p_{k-1}-p_k|}\right)$$

can be considered as a curvature vector on the vertex p_k because of the following reasons. First, the vector $\widetilde{N}_k$ is independent of the orientation of the unit normal. Moreover, if we assume that $X : I(\subset \mathbb{R}) \to \mathbb{R}^2$ is an arclength parametrized smooth regular curve and $\nu_X : I \to S^1$ is the (outward-pointing) unit normal, denoted by $\nu_X(s) = (\cos\theta(s), \sin\theta(s))$, the curvature κ is characterized by

$$\kappa = -\frac{d\theta}{ds}.$$

Then we can regard the norm $|\widetilde{N}_k|$ as a discretization of the above equation. From another point of view, we can regard the relation

$$\frac{1}{L_k}(T_k - T_{k-1}) = \widetilde{N}_k, \quad T_k := \frac{p_{k+1}-p_k}{|p_{k+1}-p_k|}$$

as a discrete version of the Frenet-Serret formula. As we will remark later, there are many possibilities of L_k, so we will define constant (anisotropic) curvature curves without defining the curvature notion. However, since the scaling factor L_k does not change the direction of $-\nabla_{p_k}$ Length, we take a position that the vector $-\nabla_{p_k}$ Length gives the normal direction at the vertex p_k throughout this chapter.

(2) In the length gradient case, we can give a geometric interpretation. If we fix the vertex p_{k+1} and move the vertex p_k and consider the length of the edge $e_k = [p_k, p_{k+1}]$. Then the direction which the length of the edge l_k most decreases is $(p_{k+1} - p_k)/|p_{k+1} - p_k|$. The vector $-\nabla_{p_k}$ Length is a sum of two vectors $(p_{k+1} - p_k)/|p_{k+1} - p_k|$ and $(p_{k-1} - p_k)/|p_{k-1} - p_k|$ means the steepest direction of the length function at p_k.

Before giving the proof, we derive the first variation of the unit normal.

Lemma 2.3.2. $l_k \delta\nu_k = R(v_{k+1} - v_k) - \langle R(v_{k+1} - v_k), \nu_k\rangle \nu_k$.

Remark . If we define the notation $\nabla v_k = (v_{k+1} - v_k)/l_k$, then

$$\delta\nu_k = \nabla(Rv_k) - \langle \nabla(Rv_k), \nu_k\rangle \nu_k,$$

and this can be considered as the "covariant derivative" of Rv at the edge $e_k = [p_k, p_{k+1}]$.

Proof. By using the fact

$$\delta l_k^2 = \delta|p_{k+1} - p_k|^2 = 2\langle p_{k+1} - p_k, v_{k+1} - v_k\rangle, \quad \delta l_k^2 = 2 l_k \delta l_k,$$

we have $\delta l_k = \langle -R\nu_k, v_{k+1} - v_k\rangle = \langle \nu_k, R(v_{k+1} - v_k)\rangle$ and therefore

$$\begin{aligned}\delta\nu_k &= \delta R\left(\frac{p_{k+1} - p_k}{l_k}\right) = R\left(\frac{v_{k+1} - v_k}{l_k} - \frac{p_{k+1} - p_k}{l_k^2}\delta l_k\right) \\ &= \frac{1}{l_k}(R(v_{k+1} - v_k) - \nu_k\langle \nu_k, R(v_{k+1} - v_k)\rangle)\end{aligned}$$

□

Proof of Proposition 2.3.1. By the chain rule and the Leibniz rule we have

$$\delta\mathscr{F}_\gamma := \frac{d}{dt}_{|t=0} \mathscr{F}_\gamma = \sum_k \langle D\gamma(\nu_k), \delta\nu_k\rangle l_k + \gamma(\nu_k)\delta l_k.$$

By using the previous lemma and the fact $D\gamma(\nu) \perp \nu$, we have

$$\begin{aligned}\delta\mathscr{F}_\gamma &= \sum_k \langle D\gamma(\nu_k), R(v_{k+1} - v_k)\rangle + \gamma(\nu_k)\langle \nu_k, R(v_{k+1} - v_k)\rangle \\ &= \sum_k \langle \xi_\gamma(\nu_k), R(v_{k+1} - v_k)\rangle = \sum_k \langle R(\xi_\gamma(\nu_k) - \xi_\gamma(\nu_{k-1})), v_k\rangle.\end{aligned}$$

□

Remark . We can consider the length gradient for non-manifold case, i.e.,

$$\nabla_p \,\text{Length} = -\sum_{k=1}^{m} \frac{p_k - p}{|p_k - p|}.$$

For example, when $m = 3$ (trivalent graph), ∇_p Length $= 0$ if and only if the angles of adjacent edges are $2\pi/3$ (120 degree).

2.3.2 Relation with other notions of the discrete curvature

In the lecture note by Hoffman [19], three kinds of notions of the curvature for discrete curves are defined:

(1) The curvature at vertices by using the vertex osculating circle method,

(2) The curvature at edges by using the edge osculating circle method,

(3) The curvature at vertices by using edge osculating circle for "arclength parametrized" curve.

Moreover, Hatakeyama [15] also defined the curvature for discrete curves another way. We will show that these curvature notions can be derived from our curvature vector by taking the different line elements L_k at vertices. In other words, these difference comes from the non-uniqueness of the "natural" line element at vertices.

As we have seen before, from the first variation formula

$$\delta\,\mathrm{Length} = \sum_k \langle R(\nu_k - \nu_{k-1}), v_k\rangle = -\sum_k \left\langle \frac{1}{L_k} R(\nu_{k-1} - \nu_k), v_k \right\rangle L_k,$$

we shall consider the vector

$$\widetilde{N}_k = \frac{1}{L_k} R(\nu_{k-1} - \nu_k) = \frac{1}{L_k}\left(\frac{p_{k+1} - p_k}{|p_{k+1} - p_k|} + \frac{p_{k-1} - p_k}{|p_{k-1} - p_k|}\right)$$

as the curvature vector on the vertex p_k. However, *there are many possibilities of* L_k. Therefore we call $\widetilde{N}_k$ the *discrete curvature vector with respect to* L_k. For example, the choice $2L_k = l_{k+1} + l_k = |p_{k+1} - p_k| + |p_{k-1} - p_k|$, which satisfies $\sum_k L_k = \mathrm{Length}(\Gamma_h)$, is compatible with the curve-shortening flow.

To describe the curvature notions, we have to define the angles at vertices. If we define (the absolute value of) the angle between ν_{k-1} and ν_k as θ_k, i.e.,

$$\cos\theta_k := \langle \nu_k, \nu_{k-1}\rangle = \frac{\langle p_{k+1} - p_k, p_k - p_{k-1}\rangle}{|p_{k+1} - p_k| \cdot |p_k - p_{k-1}|}.$$

In the following we assume $\cos\theta_k \neq 1$ for every k. We have to care about the signature of θ_k. Let R_θ be the θ-rotation in $\mathbb{R}^2$. We assign the signature depends on the choice of the rotation R:

$$\sigma := \begin{cases} +1 & \text{if} \quad R = R_{\pi/2}, \\ -1 & \text{if} \quad R = R_{-\pi/2}. \end{cases}$$

In this situation the signature of θ_k is determined by the equation $R_{\sigma\theta_k}(\nu_{k-1}) = \nu_k$.

Remark . For any closed curve we have $\sigma\sum_k \theta_k = 2m\pi$ for some interger m. Because if we note that

$$R_{\sigma(\theta_0 + \cdots + \theta_{n-1})}\nu_0 = \nu_n = \nu_0,$$

then we have $\sigma(\theta_0 + \cdots + \theta_{n-1}) = 2m\pi$. □

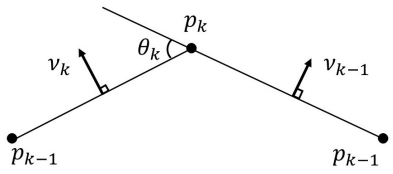

Figure 2.2: The angle at the vertex p_k ($\theta_k < 0$ in this figure).

By virtue of the fact

$$|R(\nu_{k-1} - \nu_k)| = 2\sin(|\theta_k|/2),$$

we call the value

$$\kappa(p_k) := \frac{2\sin(\theta_k/2)}{L_k}$$

the *discrete curvature at p_k with respect to L_k*.

Proposition 2.3.3 (The vertex osculating circle method [19])**.** If we choose

$$L_k = \frac{|p_{k+1} - p_{k-1}|}{2\cos(\theta_k/2)} = \frac{|p_{k+1} - p_k + p_k - p_{k-1}|}{2\cos(\theta_k/2)},$$

then the discrete curvature with respect to L_k becomes

$$\kappa(p_k) = \frac{2\sin\theta_k}{|p_{k+1} - p_{k-1}|} = \frac{2\sin\theta_k}{|p_{k+1} - p_k + p_k - p_{k-1}|}$$

and this value coincides with the curvature based on the vertex osculating circle method.

Proposition 2.3.4 (For the arclength parametrized curves [19])**.** Assume $l_k = l_{k-1} = l_0$. Then if we choose

$$L_k = l_0 \cos\frac{\theta_k}{2} = \frac{l_k + l_{k-1}}{2} \cdot \cos\frac{\theta_k}{2},$$

then the discrete curvature with respect to L_k becomes

$$\kappa(p_k) = \frac{2}{l_0}\tan\frac{\theta_k}{2}$$

and this value coincides with the curvature of arclength parametrized curve.

In the paper [15], the discrete curvature at the vertex is defined as

$$\kappa(p_k) := \frac{1}{|p_k - p_{k-1}|}\left|\frac{p_{k+1} - p_k}{|p_{k+1} - p_k|} - \frac{p_k - p_{k-1}}{|p_k - p_{k-1}|}\right| = -\frac{|\nabla_{p_k}\,\mathrm{Length}\,|}{|p_k - p_{k-1}|}.$$

Then we immediately have the following result:

Proposition 2.3.5. If we choose $L_k = l_{k-1} = |p_k - p_{k-1}|$, then the discrete curvature with respect to L_k coincides with the discrete curvature defined by Hatakeyama [15].

Before considering the edge osculating circle method, we shall modify the first variation formula from the vertex-based expression to the edge-based expression. If we put $v_k = (w_k + w_{k-1})/2$, then we have

$$\begin{aligned}\delta\,\mathrm{Length} &= \frac{1}{2}\sum_k \langle \nabla_{p_k}\,\mathrm{Length}, w_k + w_{k-1}\rangle \\ &= \frac{1}{2}\sum_k \langle \nabla_{p_k}\,\mathrm{Length} + \nabla_{p_{k+1}}\,\mathrm{Length}, w_k\rangle = -\sum_k \left\langle \frac{R(\nu_{k-1} - \nu_{k+1})}{2L'_k}, w_k \right\rangle L'_k\end{aligned}$$

where L'_k is some auxiliary function. As in the vertex case, we call the value

$$\kappa(e_k) := \frac{1}{L'_k} \cdot \sin\frac{\theta_k + \theta_{k+1}}{2}$$

the *discrete curvature at the edge* $e_k = [p_k, p_{k+1}]$ *with respect to* L'_k.

Proposition 2.3.6 (The edge osculating circle method [19])**.** If we choose

$$L'_k = l_k \cos\frac{\theta_k}{2}\cos\frac{\theta_{k+1}}{2} = |p_{k+1} - p_k|\cos\frac{\theta_k}{2}\cos\frac{\theta_{k+1}}{2},$$

then the discrete curvature with respect to L'_k becomes

$$\kappa(e_k) = \frac{\tan(\theta_k/2) + \tan(\theta_{k+1}/2)}{|p_{k+1} - p_k|}$$

and this value coincides with the curvature based on the edge osculating circle method.

Remark . To define the discrete curvature, we have to choose L_k (respectively L'_k) properly. That means if l_k, $l_{k-1} \to ds$ and $\theta_k \to 0$, then L_k (respectively L'_k) must converge to ds, i.e., L_k must be a "good" candidate for a discrete line element. We can check that L_k and L'_k satisfy this condition in the above examples.

Remark ("No free lunch" for the discrete Laplacian, cf. [41])**.** We consider these kinds of "no free lunch" story for the discrete Laplacian which will be used in the second variation formula. Let V be the vertices of a standard n-path and $X : V \to \mathbb{R}^2$ be its geometric realization (hence we have the induced metric). Then for a function $\psi : V \to \mathbb{R}^d$, the *gradient* and the *Laplacian* of ψ can be defined as

$$\nabla\psi_k := \frac{\psi_{k+1} - \psi_k}{l_k}, \quad \Delta\psi_k := \frac{1}{L_k}(\nabla\psi_k - \nabla\psi_{k-1}) = \frac{1}{L_k}\left(\frac{\psi_{k+1} - \psi_k}{l_k} - \frac{\psi_k - \psi_{k-1}}{l_{k-1}}\right),$$

where we denote $\psi_k := \psi(k)$. Note that the gradient is the "edge-based operator" but the Laplacian is the "vertex-based" operator, in addition, the discrete curvature vector $\widetilde{N}_k$ with respect to L_k can be written as Δp_k.

From another point of view, if we define the Dirichlet energy of ψ as

$$E_h(\psi) := \frac{1}{2}\sum_k |\nabla\psi_k|^2\, l_k = \frac{1}{2}\sum_k \frac{|\psi_{k+1}-\psi_k|^2}{l_k},$$

then the first variation of the energy becomes

$$\delta E_h(\psi) = \sum_k \frac{\langle \psi_{k+1}-\psi_k, \varphi_{k+1}-\varphi_k\rangle}{l_k} = \sum_k \langle \nabla\psi_{k-1}-\nabla\psi_k, \varphi_k\rangle = -\sum_k \langle \Delta\psi_k, \varphi_k\rangle L_k,$$

where we take the variation of ψ as $\psi_k(t) = \psi_k + t\varphi_k + O(t^2)$. Therefore $\delta E_h(\psi) = 0$ if and only if $\Delta\psi_k = 0$. Note that the condition $\Delta\psi_k = 0$ is independent of the choice of L_k.

As in the curvature case, the Laplacian can be changed since there is no natural "line element divisor L_k". However, with another function $\varphi : V \to \mathbb{R}$, we still have the following properties since the quanties $\Delta\psi_k L_k$ are independent of L_k:

(1) If ψ is constant, then $\Delta\psi = 0$.

(2) The condition $\Delta\psi = 0$ is independent of the choice of L_k and in this case we have the mean value property:

$$\psi_k = \frac{l_{k-1}}{l_k + l_{k-1}}\psi_{k+1} + \frac{l_k}{l_k + l_{k-1}}\psi_{k-1}.$$

(3) L^2 symmetric property:

$$\sum_k \psi_k \cdot \Delta\varphi_k \cdot L_k = \sum_k \Delta\psi_k \cdot \varphi_k \cdot L_k.$$

Note that the summation is vertex-based.

(4) Integration by parts:

$$-\sum_k \psi_k \cdot \Delta\varphi_k \cdot L_k = \sum_k \nabla\psi_k \cdot \nabla\varphi_k \cdot l_k.$$

Note that the right hand side is the edge-based summation but the left hand side is the vertex-based summation. As a corollary, the operator $-\Delta$ is positive semi-definite.

2.3.3 Parallel curves and Steiner-type formula

In this section we will derive the discrete version of the Steiner-type formula. The following type of Steiner formula is essentially appeared in some papers, for example [10]. Although they try to *extract* the curvature notion from the Steiner-type formula, we

will *derive* the Steiner-type formula by using our vertex normal and connect with the well-known curvature notion in [19].

Let $\Gamma_h = \{p_k\}_k$ be a discrete curve and take an interior vertex p_k. If we recall the length gradient

$$-\nabla_{p_k} \mathrm{Length} = R(\nu_{k-1} - \nu_k) = \frac{p_{k+1} - p_k}{|p_{k+1} - p_k|} + \frac{p_{k-1} - p_k}{|p_{k-1} - p_k|}$$

gives a candidate of the normal direction at the vertex p_k and the fact $|R(\nu_{k-1} - \nu_k)| = 2\sin(|\theta_k|/2)$, we should divide $-\nabla_{p_k} \mathrm{Length}$ by $2\sin(\theta_k/2)$ in order to get the unit normal. However this choice does not work well. In the discrete case, we should consider another factor $2\sin(\theta_k/2)\cos(\theta_k/2) = \sin\theta_k$ and put

$$N_k := -\frac{\nabla_{p_k} \mathrm{Length}}{\sin\theta_k} = \frac{R(\nu_{k-1} - \nu_k)}{\sin\theta_k} = \frac{1}{1+\cos\theta_k}(\nu_k + \nu_{k-1}),$$

if $\theta_k \neq 0$. Then we shall call the vector N_k as the *vertex normal* at the vertex p_k. Then we consider the following deformation of a discrete curve

$$p_k(t) = p_k + tN_k = p_k + t \cdot \frac{R(\nu_{k-1} - \nu_k)}{\sin\theta_k},$$

where the vertex p_k with $\theta_k \neq 0$.

Lemma 2.3.7. Assume $\theta_k, \theta_{k+1} \neq 0$. Then we have $\langle p_{k+1}(t) - p_k(t), \nu_k\rangle = 0$, therefore we call this deformation *parallel curves*.

Proof. In order to clarify the situation, we consider a more general deformation

$$N_k := -\frac{\nabla_{p_k} \mathrm{Length}}{M_k} = \frac{R(\nu_{k-1} - \nu_k)}{M_k},$$

where M_k is some auxilary function. Then we have

$$\begin{aligned}
\langle p_{k+1}(t) - p_k(t), \nu_k\rangle &= \langle (p_{k+1} - p_k) + t(N_{k+1} - N_k), \nu_k\rangle \\
&= t\left(\frac{\langle R(\nu_k - \nu_{k+1}), \nu_k\rangle}{M_{k+1}} - \frac{\langle R(\nu_{k-1} - \nu_k), \nu_k\rangle}{M_k}\right) \\
&= t\left(-\frac{\langle R\nu_{k+1}, \nu_k\rangle}{M_{k+1}} - \frac{\langle R\nu_{k-1}, \nu_k\rangle}{M_k}\right) = t\left(\frac{\sin\theta_{k+1}}{M_{k+1}} - \frac{\sin\theta_k}{M_k}\right).
\end{aligned}$$

Therefore if we choose $M_k = \sin\theta_k$, then $\langle p_{k+1}(t) - p_k(t), \nu_k\rangle = 0$. □

Theorem 2.3.8 (Discrete Steriner-type formula)**.** For parallel curves $\{p_k(t)\}_k$, we have

$$|p_{k+1}(t) - p_k(t)| = |p_{k+1} - p_k|(1 + t \cdot \kappa(e_k)),$$

where $\kappa(e_k)$ is the discrete curvature based on the edge osculating circle method [19]:

$$\kappa(e_k) = \frac{\tan(\theta_k/2) + \tan(\theta_{k+1}/2)}{|p_{k+1} - p_k|}.$$

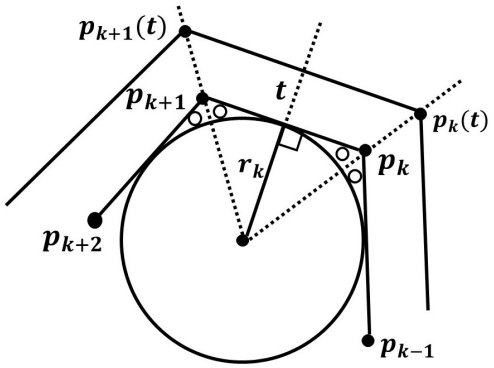

Figure 2.3: Parallel curves

Before giving the proof, we give an intuitive explanation for a special case. In the Figure 2.3, the similarity ratio of the triangles gives

$$\begin{aligned} & |p_{k+1}(t) - p_k(t)| : |p_{k+1} - p_k| = (r_k + t) : r_k \\ \iff & |p_{k+1}(t) - p_k(t)| = |p_{k+1} - p_k|(1 + t \cdot \frac{1}{r_k}) \\ \iff & |p_{k+1}(t) - p_k(t)| = |p_{k+1} - p_k|(1 + t \cdot \kappa(e_k)). \end{aligned}$$

Proof. As in the previous lemma we consider $N_k := R(\nu_{k-1} - \nu_k)/M_k$ and $p_k(t) = p_k + tN_k$. Then

$$\begin{aligned} \left\langle \frac{p_{k+1} - p_k}{|p_{k+1} - p_k|}, N_{k+1} - N_k \right\rangle &= \left\langle -R\nu_k, \frac{R(\nu_k - \nu_{k+1})}{M_{k+1}} - \frac{R(\nu_{k-1} - \nu_k)}{M_k} \right\rangle \\ &= -\left(\frac{1 - \cos\theta_{k+1}}{M_{k+1}} + \frac{1 - \cos\theta_k}{M_k} \right), \end{aligned}$$

$$\begin{aligned} |N_{k+1} - N_k|^2 &= \frac{1}{\cos^2(\theta_{k+1}/2)} + \frac{1}{\cos^2(\theta_k/2)} - 2\langle N_k, N_{k+1} \rangle \\ &= 2 + \tan^2\frac{\theta_{k+1}}{2} + \tan^2\frac{\theta_k}{2} - 2 \cdot \frac{\sin\theta_k \sin\theta_{k+1} - (1 - \cos\theta_k)(1 - \cos\theta_{k+1})}{M_k M_{k+1}}. \end{aligned}$$

If we take $M_k = \sin\theta_k$, then we have

$$\begin{aligned} \left\langle \frac{p_{k+1} - p_k}{|p_{k+1} - p_k|}, N_{k+1} - N_k \right\rangle &= -\left(\tan\frac{\theta_k}{2} + \tan\frac{\theta_{k+1}}{2} \right), \\ |N_{k+1} - N_k|^2 &= \left(\tan\frac{\theta_k}{2} + \tan\frac{\theta_{k+1}}{2} \right)^2. \end{aligned}$$

Therefore we conclude

$$\begin{aligned}
&|p_{k+1}(t) - p_k(t)|^2 \\
&= |p_{k+1} - p_k|^2 - 2t\langle p_{k+1} - p_k, N_{k+1} - N_k\rangle + t^2|N_{k+1} - N_k|^2 \\
&= |p_{k+1} - p_k|^2 + 2t|p_{k+1} - p_k|\left(\tan\frac{\theta_k}{2} + \tan\frac{\theta_{k+1}}{2}\right) + t^2\left(\tan\frac{\theta_k}{2} + \tan\frac{\theta_{k+1}}{2}\right)^2 \\
&= |p_{k+1} - p_k|^2\left(1 + t\cdot\frac{\tan(\theta_k/2) + \tan(\theta_{k+1}/2)}{|p_{k+1} - p_k|}\right)^2.
\end{aligned}$$

□

Remark . This formula itself is already appeared some papers to *extract* the discrete curvature at the vertices by using the offsets, see [5], [10]. If we take the offset of the edges, then we have the following (at least) three possiblities. By computing the length

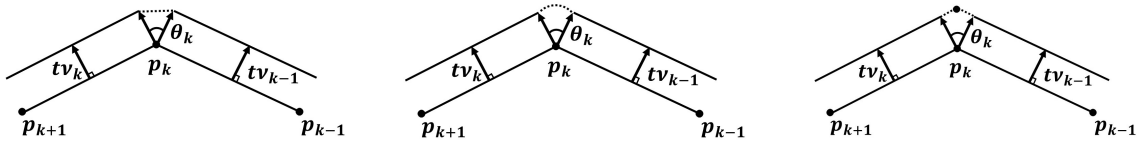

(a) $\Gamma^{(1)}_{h,t}$, connect by a segment (b) $\Gamma^{(2)}_{h,t}$, connect by an arc (c) $\Gamma^{(3)}_{h,t}$, connect by a wedge

Figure 2.4: Three possibilities to construct a new curve

of dotted curves in the figure, we can write the total length of each offsets as follows:

$$\mathrm{Length}(\Gamma^{(1)}_{h,t}) = \mathrm{Length}(\Gamma_h) + t\sum_k 2\sin\frac{\theta_k}{2}, \quad \mathrm{Length}(\Gamma^{(2)}_{h,t}) = \mathrm{Length}(\Gamma_h) + t\sum_k \theta_k,$$
$$\mathrm{Length}(\Gamma^{(3)}_{h,t}) = \mathrm{Length}(\Gamma_h) + t\sum_k 2\tan\frac{\theta_k}{2}.$$

Note that $\theta \approx 2\sin(\theta/2) \approx 2\tan(\theta/2)$ if $\theta \approx 0$. The second curve $\Gamma^{(2)}_h$ is nothing but the normal cone method (or the boundary of the Minkowski sum with the disk) known in the convex geometry. However, the only possible way which does not change the number of the vertices during the offset procedure is the third one, and by modifying the third formula gives our Steiner-type formula:

$$\begin{aligned}
\mathrm{Length}(\Gamma^{(3)}_{h,t}) &= \sum_k (l_k + 2t\tan(\theta_k/2)) \\
&= \sum_k (l_k + t(\tan(\theta_k/2) + \tan(\theta_{k+1}/2))) = \sum_k l_k(1 + t\kappa(e_k)),
\end{aligned}$$

where we put $\kappa(e_k) = (\tan(\theta_k/2) + \tan(\theta_{k+1}/2))/l_k$ (the curvature defined by the edge osculating circle).

2.3.4 Critical points of the length functional

In §2.3.2, we saw that there is no universal notion of discrete curvature. However, since our main interest is constant (mean) curvature objects, we formulate such objects by using the variational method without defining the curvature itself. In this section we focus on the length functional case and consider closed discrete curves in the following. The 2-dimensional oriented volume (i.e., the area) bounded by a closed discrete curve Γ_h is defined by

$$\mathrm{Vol}(\Gamma_h) := \frac{1}{2}\sum_k \langle p_k, \nu_k\rangle |p_{k+1} - p_k| = \frac{1}{2}\sum_k \langle p_k, Rp_{k+1}\rangle,$$

Note that the signature of the volume can be negative. Then we have the following result:

Lemma 2.3.9. For any vertex p_k of Γ_h the gradient of the volume $\nabla_{p_k}\mathrm{Vol}$ is given by

$$\nabla_{p_k}\mathrm{Vol} = \frac{1}{2}R(p_{k+1} - p_{k-1}).$$

Proof. We consider any variation ${}^t\vec{v} = ({}^tv_1, \ldots, {}^tv_n)$ and it follows from the second representation of the volume that

$$\begin{aligned}\delta\,\mathrm{Vol} &= \frac{1}{2}\sum_k \delta\langle p_k, Rp_{k+1}\rangle = \frac{1}{2}\sum_k (\langle v_k, Rp_{k+1}\rangle + \langle p_k, Rv_{k+1}\rangle)\\ &= \frac{1}{2}\sum_k (\langle v_k, Rp_{k+1}\rangle + \langle p_{k-1}, Rv_k\rangle = \frac{1}{2}\sum_k \langle R(p_{k+1} - p_{k-1}), v_k\rangle.\end{aligned}$$

□

Remark (Another "no free lunch" story)**.** We can modify the first variation formula of the volume as follows:

$$\delta\,\mathrm{Vol} = \frac{1}{2}\sum_k \langle R(p_{k+1} - p_k + p_k - p_{k-1}), v_k\rangle = \sum_k \left\langle \frac{l_k\nu_k + l_{k-1}\nu_{k-1}}{2L_k}, v_k \right\rangle L_k.$$

At a glance, it seems like a natural to choose $2L_k = l_k + l_{k-1} = \mathrm{Length}(\mathrm{star}\,(p))$ and this is also frequently used as a "vertex normal" (weighted sum of the edge normals):

$$N_k^V := \frac{l_k\nu_k + l_{k-1}\nu_{k-1}}{l_k + l_{k-1}}.$$

In addition, we have

$$-\nabla_{p_k}\mathrm{Length} = R(\nu_{k-1} - \nu_k) = \frac{\sin\theta_k}{1+\cos\theta_k}(\nu_k + \nu_{k-1}) = 2\tan\frac{\theta_k}{2}\cdot\frac{\nu_k + \nu_{k-1}}{2}.$$

by a simple calculation. Therefore, unless the curve is arclength parameterized, there are (at least) two choices of the "vertex normal" from the variational viewpoint : using the length gradient (length descent direction) or using the volume gradient (volume descent direction). This suggests that, in contrast to the smooth case, we have to choose the "prefered" vertex normal according to the energy in question. □

First, we will start from the $\gamma \equiv 1$ case.

Example 2.3.10 (Regular polygons)**.** Let us take a discrete curve $\Gamma_h^{m,n} = \{p_k\}_k$ as in the following way (including non-convex regular n-gon with radius a):

$$p_k = a \exp(2\pi\sqrt{-1}mk/n), \quad k = 0, \dots, n-1, \quad 1 \leq m \leq n-1,$$

where we assume that m and n are coprime. In particular, we sometimes call the curve $\Gamma_h^{1,n}$ as a convex regular n-gon. Note that $\Gamma_h^{n-1,n}$ is also convex but it has an opposite unit normal with $\Gamma_h^{1,n}$ (usually we assume that $\Gamma_h^{1,n}$ has the outward-pointing unit normal). Then the curve $\Gamma_h^{m,n}$ is a critical point of the functional Length $+\kappa$ Vol

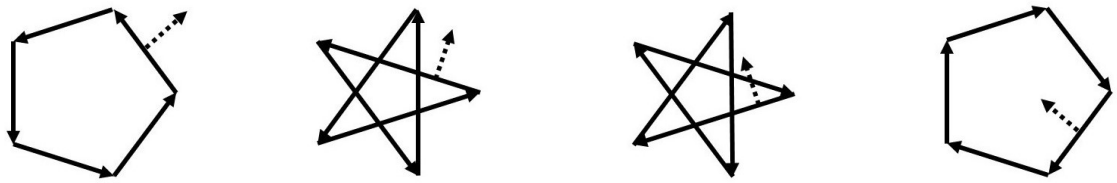

(a) $\kappa = -1/\cos(\pi/5)$ (b) $\kappa = -1/\cos(2\pi/5)$ (c) $\kappa = -1/\cos(3\pi/5)$ (d) $\kappa = -1/\cos(4\pi/5)$

Figure 2.5: Convex and non-convex regular 5-gons with radii $a = 1$.

with $\kappa = -1/(a\cos(m\pi/n))$. This value is the reciprocal of the radius of the inscribed circle of the polygon (up to the signature). We sometimes say that a convex regular n-gon with radius a (and outward-pointing unit normal) has constant curvature $\kappa_n = -1/(a\cos(\pi/n))$. Note that $\cos(\pi m/n) = -\cos(\pi(n-m)/n)$ and $\kappa_n \to -1/a$ when $n \to \infty$. We also remark that this value naturally appears in the discrete cylinder (Example 2.4.9).

We will show that these regular polygons are the only critical points for the functional Length $+\kappa$ Vol.

Theorem 2.3.11. Let $\Gamma_h = \{p_k\}_{k=0}^{n-1}$ be a closed discrete curve and take $\kappa \in \mathbb{R} \setminus \{0\}$. Then the following two conditions are equivalent:

(1) Γ_h is a critical point of the functional Length $+\kappa$ Vol.

(2) The edge length l_k and the angles θ_k are constant l_0 and θ_0 which satisfies $\kappa l_0 = 2\tan(\theta_0/2)$.

Proof. We put

$$A_k := (\nu_k - \nu_{k-1}) + \frac{\kappa}{2}(p_{k+1} - p_{k-1}), \quad k = 0, \dots, n-1.$$

Then the discrete curve Γ_h is a critical point of the functional Length $+\kappa$ Vol if and only if $A_k = 0$ for all k. By a simple calculation we have

$$\langle A_k, \nu_{k-1} \rangle = \sin\theta_k \left(\frac{\kappa l_k}{2} - \tan\frac{\theta_k}{2} \right), \tag{3.2}$$

$$\langle A_k, \nu_k \rangle = \sin\theta_k \left(\tan\frac{\theta_k}{2} - \frac{\kappa l_{k-1}}{2} \right), \tag{3.3}$$

$$\langle A_{k+1}, \nu_{k+1} \rangle = \sin\theta_{k+1} \left(\tan\frac{\theta_{k+1}}{2} - \frac{\kappa l_k}{2} \right). \tag{3.4}$$

For the necessity, that is, if we assume $A_k = 0$ for all k, then it follows from (3.2) and (3.3) that $\kappa l_k = 2\tan(\theta_k/2) = \kappa l_{k-1}$. And it also follows from (3.3), (3.4) and using $l_k = l_{k-1}$ that

$$\tan\frac{\theta_k}{2} = \frac{\kappa l_k}{2} = \frac{\kappa l_{k-1}}{2} = \tan\frac{\theta_{k-1}}{2}.$$

To prove the sufficiency, since ν_k and $p_k - p_{k-1}$ forms a basis of $\mathbb{R}^2$ and $\langle A_k, \nu_k \rangle = 0$ by using (3.2) and the assumption, all we have to prove is $\langle A_k, p_k - p_{k-1} \rangle = 0$ for all k. By using the assumption $l_k = l_{k-1} = l_0$ and $\theta_k = \theta_0$, we have

$$\begin{aligned}\left\langle A_k, \frac{p_k - p_{k-1}}{l_k} \right\rangle &= -\sin\theta_k + \frac{\kappa}{2}(l_k\cos\theta_k + l_{k-1}) \\ &= (1+\cos\theta_0)\left(\frac{\kappa l_0}{2} - \frac{\sin\theta_0}{1+\cos\theta_0} \right) = (1+\cos\theta_0)\left(\frac{\kappa l_0}{2} - \tan\frac{\theta_0}{2} \right) = 0.\end{aligned}$$

This shows $A_k = 0$ and proves the statement. □

We found that critical points of the functional Length $+\kappa$ Vol must satisfy $l_k \equiv l_0$, i.e., they must have "good coordinates (arclength parameter)". If we note that for an arclength parametrized curve we can define the curvature at vertices, the previous result can be restated as follows:

Corollary 2.3.12. Let Γ_h be an arclength parametrized discrete closed curve, i.e., $l_k \equiv l_0$, and take $\kappa \in \mathbb{R} \setminus \{0\}$. Then the following two conditions are equivalent:

(1) Γ_h is a critical point of the functional Length $+\kappa$ Vol.

(2) The discrete curvature $(2/l_0)\tan(\theta_k/2)$ is constant κ.

Corollary 2.3.13. Let $\Gamma_h = \{p_k\}$ be a critical point of the functional Length $+\kappa$ Vol. Then Γ_h must be a regular polygon (including a non-convex polygon).

Proof. Let r_k be the radius of the triangle (p_{k-1}, p_k, p_{k+1}). By using the sine law, we have $r_k = 1/(|\kappa|\cos(\theta_k/2))$ and this is independent of k by the previous result. Then all vertices of Γ_h must lie on the same circle with radius $r_0 = r_k$. By a rotation

and translation, we can put $p_k = r_0 \exp(i\varphi_k)$ with $\varphi_1 = 0$. By using the condition $\kappa l_0 = 2\tan(\theta_0/2)$, we have

$$|p_{k+1} - p_k| = l_k = l_0 \iff r_0 \cdot 2\sin\frac{\varphi_{k+1} - \varphi_k}{2} = \frac{2}{|\kappa|}\tan\frac{|\theta_0|}{2}$$
$$\iff \sin\frac{\varphi_{k+1} - \varphi_k}{2} = \sin\frac{|\theta_0|}{2} \iff \varphi_{k+1} - \varphi_k = |\theta_0|.$$

Therefore we have $\varphi_k = (k-1)|\theta_0|$ and this proves the statement. □

Remark . We will prove the instability of the non-convex regular polygons (Theorem).

2.3.5 Discrete constant anisotropic curvature curves

In this section we will define the discrete constant anisotropic (mean) curvature (CAMC) curves by using the variational principle inspired by [37]. We will derive the conservation law for the Euler-Lagrange equation and Minkowski-type formula. As an application, we will show another proof of the Chakerian-Lange theorem by using our method (Corollary 2.3.18). Finally we will give some examples of discrete CAMC curves. In connection with Chapter 1, we can give "non-uniqueness" of discrete CAMC curves.

Definition 2.3.14 (Discrete CAMC curve)**.** Let $\gamma : S^1 \to \mathbb{R}$ be a C^1 function. Then a simplicial curve Γ_h has *constant anisotropic (mean) curvature (CAMC)* if there exists a constant Λ such that

$$\nabla_p \mathscr{F}_\gamma + \Lambda \nabla_p \operatorname{Vol} = 0$$

holds for every interior vertex p. This definition is equivalent to the following equations:

$$\xi_\gamma(\nu_k) - \xi_\gamma(\nu_{k-1}) + \frac{\Lambda}{2}(p_{k+1} - p_{k-1}) = 0 \tag{3.5}$$

for any interior vertex p_k.

Remark . This definition is inspired by the definition of discrete CMC surfaces in [37]. Note that we defined the constant anisotropic curvature curve without defining the discrete anisotropic curvature. We sometimes call such a curve as *CAMC-Λ curve*.

We first remark the following fact.

Proposition 2.3.15. Let $\gamma : S^1 \to \mathbb{R}_{>0}$ be of C^2 and assume $\gamma''(\theta) + \gamma(\theta) > 0$ where we define $\gamma(\theta) := \gamma(\cos\theta, \sin\theta)$. Then any bounded curve with zero anisotropic curvature must be a segment.

Proof. When $\gamma \equiv 1$, the statement is trivial. If we assume the function γ satisfies $\gamma'' + \gamma > 0$, then the Cahn-Hoffman map $\xi_\gamma : S^1 \to W_\gamma$ becomes diffeomorphism. Therefore, the zero curvature condition $\xi_\gamma(\nu_{k-1}) = \xi_\gamma(\nu_k)$ is equivalent to $\nu_{k-1} = \nu_k$. □

Lemma 2.3.16 (Conservation law)**.** A closed discrete curve $\Gamma_h = \{p_k\}_k$ is CAMC-Λ if and only if there exists a vector $c \in \mathbb{R}^2$ such that $\xi_\gamma(\nu_k) + (\Lambda/2)(p_{k+1} + p_k) \equiv c$ for all k.

Proof. In the critical point condition (3.5), by inserting $p_k - p_k$ we have

$$\xi_\gamma(\nu_k) + \frac{\Lambda}{2}(p_{k+1} + p_k) = \xi_\gamma(\nu_{k-1}) + \frac{\Lambda}{2}(p_k + p_{k-1}) \quad \text{for all } k.$$

This implies the vector $\xi_\gamma(\nu_k) + (\Lambda/2)(p_{k+1} + p_k)$ is independent of k. □

Since the constant vector c is just a translation of the curve, it is enough to consider the case $c = 0$, then we have

$$\frac{p_{k+1} + p_k}{2} = -\frac{1}{\Lambda}\xi_\gamma(\nu_k) \quad \text{for all } k. \tag{3.6}$$

Moreover, since the Cahn-Hoffman map $\xi_\gamma : S^1 \to \mathbb{R}^2$ is a wave front (cf. [24], Proposition 5.1), every midpoint of the edge of the curve is tangent to the rescaled image of the Cahn-Hoffman map ξ_γ. Therefore discrete CAMC-Λ curves for a energy density γ must be constructed from the lines

$$\left\{ x \in \mathbb{R}^2 \mid \langle x, \nu \rangle = -\frac{1}{\Lambda}\gamma(\nu) \right\}, \quad \nu \in S^1$$

which are the tangent lines of the rescaled Cahn-Hoffman map $(-1/\Lambda)\xi_\gamma : S^1 \to \mathbb{R}^2$.

Remark . The condition in the above lemma can be considered as a conservation law for the Euler-Lagrange equation (3.5). Note that the Euler-Lagrange equation (3.5) is the vertex-based condition but the conservation law is the edge-based condition. Moreover, some calculation shows the following relation:

$$\delta(\mathscr{F}_\gamma + \Lambda \operatorname{Vol}) = \sum_k \left\langle \xi_\gamma(\nu_k) + \frac{\Lambda}{2}(p_k + p_{k+1}), R(v_k - v_{k+1}) \right\rangle.$$

From another point of view, if the curve $\{p_k\}_k$ approximates a smooth curve $p(s)$, then $p_k \approx p_{k+1} \approx p(s)$ and therefore $p(s) = -(1/\Lambda)\xi_\gamma(\nu)$. In particular $p(s) = \xi_\gamma(\nu)$ when $\Lambda = -1$. This fact is closely related to the result of F. Morgan [30], but since we did not assume the convexity for γ, the Wulff shape is replaced by the image of the Cahn-Hoffman map. □

Taking the inner product (3.6) with ν_k gives the following relation:

$$\gamma(\nu_k) = \langle \xi_\gamma(\nu_k), \nu_k \rangle = -\frac{\Lambda}{2}\langle p_{k+1} + p_k, \nu_k \rangle = -\Lambda \langle p_k, \nu_k \rangle.$$

In particular, we have the following Minkowski-type formula:

Proposition 2.3.17 (Discrete Minkowski-type formula)**.** Let $\gamma : S^1 \to \mathbb{R}$ be a C^1 function and $\Gamma_h = \{p_k\}_k$ be a closed discrete CAMC-Λ curve. Then we have the following Minkowski-type formula:

$$\sum_k (\gamma(\nu_k) + \Lambda\langle p_k, \nu_k\rangle)|p_{k+1} - p_k| = 0.$$

In connection with the convex geometry, we mention about the *discrete isoperimetric problem*, i.e., we consider the following problem:

> *For a given convex region W and number n, find the convex n-gon which have the least area containing W.*

This kind of problem is interested not only from the pure mathematics, but also from the robotics and computer aided design field, see e.g. [1]. Here we will show that our discretization method gives another proof of the following theorem:

Corollary 2.3.18 (Chakerian-Lange [8])**.** Let W be a strictly convex domain, $n \geq 3$ and $\Gamma_h = \{p_k\}_k$ be a convex n-gon of minimum area containing W. Then, the midpoints of the edges of Γ_h must lie on ∂W.

Remark . The original theorem assumed that W is just a convex region. As we will see, we have to remove the regularity assumption for the energy density function in order to overcome this restriction.

For any strictly convex domain W, it is known that there exists a convex and C^1 energy density $\gamma : S^1 \to \mathbb{R}_{>0}$ with $\partial W = \xi_\gamma(S^1)$ ([14]). We say a closed discrete curve $\Gamma_h = \{p_k\}_k$ is *circumscribed about* W_γ if for every k there exist $\lambda_k \in \mathbb{R}$ such that $(1-\lambda_k)p_k + \lambda_k p_{k+1} = \xi_\gamma(\nu_k)$. Note that we have

$$\mathscr{F}_\gamma(\Gamma_h) = 2\,\mathrm{Vol}(\Gamma_h) \iff \mathscr{F}_\gamma(\Gamma_h) - \mathrm{Vol}(\Gamma_h) = \mathrm{Vol}(\Gamma_h)$$

for any discrete curve Γ_h circumscribed about W_γ. Therefore we have the following lemma:

Lemma 2.3.19. For any discrete curve circumscribed about W_γ, the following problems are equivalent:

- Find the minimizer of the energy $\mathscr{F}_\gamma - \mathrm{Vol}$ (CAMC-(-1) curve).
- Find the minimizer of the 2-dimensional volume Vol.

In particular, the existence of the minimizer of the second problem guarantees the existence of the minimizer of the first problem.

Proof of Corollary 2.3.18. By the assumption, there exists a convex and C^1 energy density $\gamma : S^1 \to \mathbb{R}_{>0}$ with $\partial W = \xi_\gamma(S^1)$. Consider the variational problem of discrete curves for the functional $\mathscr{F}_\gamma - \mathrm{Vol}$. Then by the previous lemma, among discrete curves circumscribed about ∂W, the minimizer of the bounded area coincides with the minimizer of the energy $\mathscr{F}_\gamma - \mathrm{Vol}$. From the conservation law (Lemma 2.3.16), we have

$$\frac{p_k + p_{k+1}}{2} = \xi_\gamma(\nu_k) \quad \text{for all} \quad k,$$

for the minimizer Γ_h. This proves the statement. □

We will give some examples of discrete CAMC curves. As we will see, non-convexity of the energy density also affects the "non-uniqueness" of the discrete CAMC curves.

Example 2.3.20. We take the energy density $\gamma : S^1 \to \mathbb{R}_{>0}$ as $\gamma(\nu_1, \nu_2) = \sqrt{a^2\nu_1^2 + b^2\nu_2^2}$, where $a, b \in \mathbb{R}_{>0}$ are constant. Then the corresponding Wulff shape becomes the ellipse $(x/a)^2 + (y/b)^2 = 1$. For positive numbers $A, B > 0$, we define a map $T_{A,B} : \mathbb{R}^2 \to \mathbb{R}^2$ as $T_{A,B}(x_1, x_2) := (Ax_1, Bx_2)$. By a typical calculation, we can check the following fact:

Proposition 2.3.21 (for smooth case, see [25], Example 4.4)**.** Let $\Gamma_h = \{p_k\}_k$ be a closed discrete curve and $\Lambda \neq 0$. Then Γ_h is a critical point of the functional $\mathscr{F}_\gamma + \Lambda\,\mathrm{Vol}$ if and only if $\widetilde{\Gamma}_h := \{T_{1/a,1/b}(p_k)\}$ is a critical point of $\mathrm{Length} + \Lambda\,\mathrm{Vol}$.

Therefore, by using the previous result, every discrete CAMC curve for the density γ is "rescaled" regular polygons, i.e., if Γ_h is a regular polygon, then $T_{a,b}(\Gamma_h)$ is CAMC for γ.

The following Figure 2.6 give examples of the discrete CAMC curve ($\Lambda = -1$) for the energy density $\gamma(\nu_1, \nu_2) = \sqrt{4\nu_1^2 + \nu_2^2}$. The dotted curve represents the image of the Cahn-Hoffman map, i.e., the ellipse $x^2/4 + y^2 = 1$. In the first figure, the vertices are

$$(2, 1),\ (-2, 1),\ (-2, -1),\ (2, -1).$$

In the second figure, the vertices are

$$(2, \sqrt{2} - 1),\ (2(\sqrt{2} - 1), 1),\ (2(1 - \sqrt{2}), 1),\ (-2, \sqrt{2} - 1),$$
$$(-2, 1 - \sqrt{2}),\ (2(1 - \sqrt{2}), -1),\ (2(\sqrt{2} - 1), -1),\ (2, 1 - \sqrt{2}).$$

Note that the first and third figure have the same volume, therefore this means the minimizer for the functional $\mathscr{F}_\gamma - \mathrm{Vol}$ is not unique.

Example 2.3.22. Let us take a non-convex energy density which appeared in the Chapter 1, i.e., we put $\gamma(\nu_1, \nu_2) = \nu_1^6 + \nu_2^6$. The dotted curve represents the image of the Cahn-Hoffman map for γ. As in the smooth case, we have discrete CAMC-(-1) curves which are quite different from the Wulff shape like in the second and third figures. As we will see later, these curves are unstable (Proposition 2.3.27). □

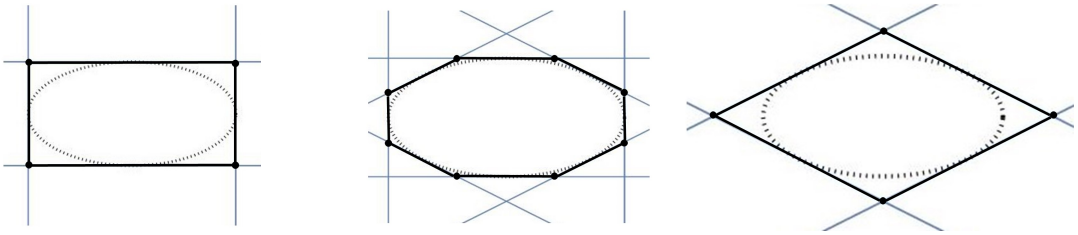

Figure 2.6: Examples of discrete CAMC-(-1) curves for $\gamma(\nu_1, \nu_2) = \sqrt{4\nu_1^2 + \nu_2^2}$.

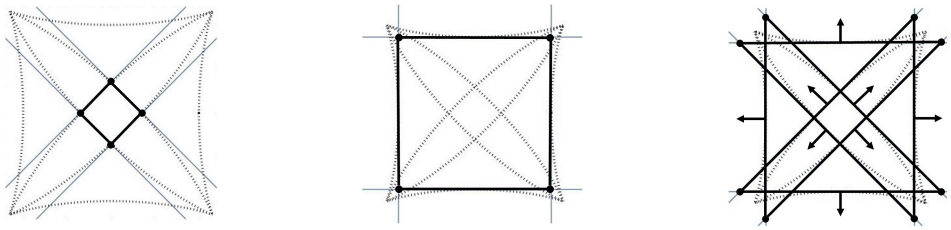

Figure 2.7: Examples of discrete CAMC-(-1) curves for $\gamma(\nu_1, \nu_2) = \nu_1^6 + \nu_2^6$.

2.3.6 Second variation of the anisotropic energy

In this section we consider the second variation of the anisotropic energy and stability of discrete CAMC curves. We will follow the argument developed in [37]. We assume that the energy density γ is of class C^2 in the following.

Let $G = (V, E)$ be a standard $(n-1)$-circle and $p : V \to \mathbb{R}^2$ be its realization and denote its image by $\Gamma_h = \{p_k\}_k$. We consider a smooth variation $p_k(t) = p_k + tv_k + O(t^2)$. Recall the first variation formula of the anisotropic energy and the 2-dimensional volume:

$$\frac{d}{dt}\mathscr{F}_\gamma = \sum_k \langle \nabla_{p_k}\mathscr{F}_\gamma, p_k' \rangle, \quad \nabla_{p_k}\mathscr{F}_\gamma = R(\xi_\gamma(\nu_k) - \xi_\gamma(\nu_k)),$$
$$\frac{d}{dt}\operatorname{Vol} = \sum_k \langle \nabla_{p_k}\operatorname{Vol}, p_k' \rangle, \quad \nabla_{p_k}\operatorname{Vol} = \frac{1}{2}R(p_{k+1} - p_{k-1}).$$

Note that if the variation is volume-preserving, then

$$0 = \delta^2 \operatorname{Vol} = \sum_k \langle \delta(\nabla_{p_k}\operatorname{Vol}), \delta p_k \rangle + \langle \nabla_{p_k}\operatorname{Vol}, \delta^2 p_k \rangle.$$

We say a variation is *admissible* (or *permissible*) if the variation is volume-preserving and fixes the boundary.

Lemma 2.3.23. Let $\Gamma_h = \{p_k\}_k$ be a discrete CAMC-Λ curve and $p_k(t) = p_k + tv_k + O(t^2)$ be an admissible variation. Then we have

$$\delta^2\mathscr{F}_\gamma := \frac{d^2}{dt^2}_{|t=0}\mathscr{F}_\gamma = \sum_k \langle \delta(\nabla_{p_k}\mathscr{F}_\gamma + \Lambda\nabla_{p_k}\operatorname{Vol}), v_k \rangle.$$

Proof. From the CAMC condition (3.5) we have

$$\begin{aligned}\delta^2\mathscr{F}_\gamma &= \sum_k \delta\langle\nabla_{p_k}\mathscr{F}_\gamma, p_k'\rangle = \sum_k \langle\delta\nabla_{p_k}\mathscr{F}_\gamma, \delta p_k\rangle + \langle\nabla_{p_k}\mathscr{F}_\gamma, \delta^2 p_k\rangle \\ &= \sum_k \langle\delta\nabla_{p_k}\mathscr{F}_\gamma, v_k\rangle + \langle -\Lambda\nabla_{p_k}\operatorname{Vol}, \delta^2 p_k\rangle \\ &= \sum_k \langle\delta\nabla_{p_k}\mathscr{F}_\gamma, v_k\rangle + \langle\Lambda\delta\nabla_{p_k}\operatorname{Vol}, \delta p_k\rangle = \sum_k \langle\delta(\nabla_{p_k}\mathscr{F}_\gamma + \Lambda\nabla_{p_k}\operatorname{Vol}), v_k\rangle\end{aligned}$$

□

Definition 2.3.24 (Stability of discrete CAMC curve)**.** Let $\gamma : S^1 \to \mathbb{R}$ be a C^2 function and $\Gamma_h = \{p_k\}_k$ be a closed discrete CAMC curve. Then Γ_h is said to be *stable* if $\delta^2\mathscr{F}_\gamma \geq 0$ for any admissible variation.

We introduce the matrix Q^γ and Q^V as follows:

$$^t\vec{v}Q^\gamma\vec{v} = \sum_k \langle\delta\nabla_{p_k}\mathscr{F}_\gamma, v_k\rangle, \quad ^t\vec{v}Q^V\vec{v} = \sum_k \langle\delta\nabla_{p_k}\operatorname{Vol}, v_k\rangle.$$

Then we can write $\delta^2\mathscr{F}_\gamma = {}^t\vec{v}(Q^\gamma + \Lambda Q^V)\vec{v}$.

Lemma 2.3.25. $^t\vec{v}Q^V\vec{v} = \sum_k \langle v_k, Rv_{k+1}\rangle$.

Proof. The proof follows from the direct computation:

$$\begin{aligned}^t\vec{v}Q^V\vec{v} &= \sum_k \langle\delta\nabla_{p_k}\operatorname{Vol}, v_k\rangle = \frac{1}{2}\sum_k \langle\delta R(p_{k+1} - p_{k-1}), v_k\rangle \\ &= \frac{1}{2}\sum_k \langle R(v_{k+1} - v_{k-1}), v_k\rangle = \sum_k \langle v_k, Rv_{k+1}\rangle.\end{aligned}$$

□

Lemma 2.3.26. $^t\vec{v}Q^\gamma\vec{v} = \sum_k \langle d\xi_\gamma(\delta\nu_k), \delta\nu_k\rangle l_k$.

Proof. If we note that $d\xi_\gamma$ is an endomorphism of the tangent space and $\delta\nu_k$ is tangent to the edge $e_k = [p_k, p_{k+1}]$, then we have

$$\begin{aligned}^t\vec{v}Q^\gamma\vec{v} &= \sum_k \langle\delta\nabla_{p_k}\mathscr{F}_\gamma, v_k\rangle = \sum_k \langle\delta R(\xi_\gamma(\nu_k) - \xi_\gamma(\nu_{k-1})), v_k\rangle \\ &= \sum_k \langle R(d\xi_\gamma(\delta\nu_k) - d\xi_\gamma(\delta\nu_{k-1})), v_k\rangle = \sum_k \langle R(d\xi_\gamma(\delta\nu_k)), v_k - v_{k+1}\rangle \\ &= \sum_k \langle d\xi_\gamma(\delta\nu_k), R(v_{k+1} - v_k)\rangle = \sum_k \langle d\xi_\gamma(\delta\nu_k), \delta\nu_k\rangle l_k\end{aligned}$$

□

Therefore we have an expression of second variation for the anisotropic energy:

$$\delta^2\mathscr{F}_\gamma = \sum_k (\langle d\xi_\gamma(\delta\nu_k), \delta\nu_k\rangle l_k + \langle v_k, Rv_{k+1}\rangle).$$

As a special case, we consider an one point variation, i.e., for a fixed vertex p_k, consider a variation vector field $v_k \in \mathbb{R}^2$ with $v_j = 0$ for $j \neq k$. As we saw in Chaper 1, the matrix $d\xi_\gamma|_\nu$ can be written as $\gamma''(\theta) + \gamma(\theta)$ when we write $\nu = (\cos\theta, \sin\theta)$ and $\gamma(\theta) = \gamma(\cos\theta, \sin\theta)$. Then the second variation formula reduces to the following form:

$$\delta^2\mathscr{F}_\gamma = \langle d\xi_\gamma(\delta\nu_k), \delta\nu_k\rangle l_k = (\gamma'' + \gamma)|_{\nu_k} \cdot |Rv_k - \langle Rv_k, \nu_k\rangle\nu_k|^2/l_k.$$

Therefore, we have the following necessary condition for the stability:

Proposition 2.3.27. Let $\gamma : S^1 \to \mathbb{R}_{>0}$ be of C^2 and Γ_h be a discrete CAMC curve. Then Γ_h is stable only if every edge of the curve is tangent to a portion of the Cahn-Hoffman map for γ which satisfies $\gamma'' + \gamma \geq 0$, i.e., the convex part of the Cahn-Hoffman map.

Example 2.3.28. The second and third curves in the Figure 2.7 are unstable since the vertical and horizontal edges are tangent to the non-convex part of the Cahn-Hoffman map (see Figure 2.8, 2.9 for the energy descent deformations under the volume-constraint condition).

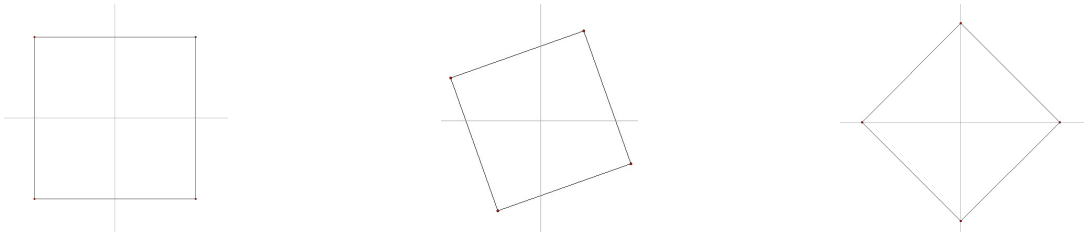

(a) energy = 8. (b) energy ≈ 5.63944664472859. (c) energy = 2.

Figure 2.8: Energy descent deformation (rotation) for unstable discrete CAMC curve.

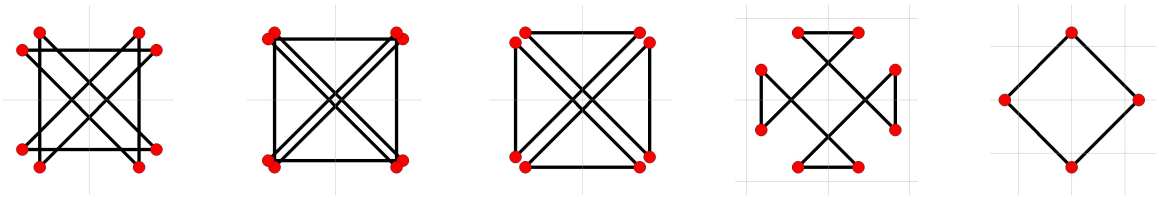

Figure 2.9: Energy descent deformation for unstable discrete CAMC curve.

In the following we will focus on the $\gamma \equiv 1$ case and denote $Q^\gamma = Q$ in this case.

Proposition 2.3.29 (Second variation formula for the length functional)**.**

$$Q = \sum_k \frac{1}{l_k}(|v_{k+1} - v_k|^2 - \langle v_{k+1} - v_k, R\nu_k\rangle^2) = \sum_k (|\nabla v_k|^2 - \langle \nabla v_k, R\nu_k\rangle^2) l_k,$$

therefore we have the following second variation formula for the length functional:

$$\delta^2 \operatorname{Length} = \sum_k (|\nabla v_k|^2 - \langle \nabla v_k, R\nu_k\rangle^2) l_k + \Lambda \langle v_k, R v_{k+1}\rangle. \tag{3.7}$$

Proof. By using Lemma 2.3.2, we have

$$\begin{aligned} Q &= \sum_k \langle \delta\nu_k, R(v_{k+1} - v_k)\rangle = \sum_k \langle R(\nabla v_k) - \langle R(\nabla v_k), \nu_k\rangle \nu_k, R(\nabla v_k)\rangle l_k \\ &= \sum_k (|\nabla v_k|^2 - \langle R(\nabla v_k), \nu_k\rangle^2) l_k = \sum_k (|\nabla v_k|^2 - \langle \nabla v_k, R\nu_k\rangle^2) l_k. \end{aligned}$$

□

In the section of the Steiner-type formula, we used the vector

$$N_k := \frac{R(\nu_{k-1} - \nu_k)}{\sin\theta_k} = \frac{1}{\sin\theta_k}\left(\frac{p_{k+1} - p_k}{l_k} - \frac{p_k - p_{k-1}}{l_{k-1}}\right)$$

as the "normal vector" at the vertex p_k. If we define the "tangent vector" T_k as $T_k = -RN_k$, then we can decompose the variation vector v_k as

$$v_k = \psi_k N_k + \eta_k T_k = \psi_k N_k - \eta_k R N_k,$$

where $\psi, \eta : V \to \mathbb{R}$ is some functions on the vertices. If $\eta_k = 0$ for all k, we sometimes call it the *normal variation*. In the following we will use this notation.

Lemma 2.3.30. The first variation formula of the volume can be written as

$$\delta \operatorname{Vol} = \frac{1}{2}\sum_k \left(\psi_k(l_k + l_{k-1}) + \eta_k(l_k - l_{k-1})\tan\frac{\theta_k}{2}\right).$$

In particular, if a curve $\{p_k\}$ satisfies $l_k \equiv l_0$, then $\sum_k \psi_k = 0$ for any volume-preserving variation.

Remark . Conversely, for such a curve, if a function $\psi : V \to \mathbb{R}$ satiefies $\sum_k \psi_k = 0$, then we can construct a volume-preserving normal variation whose variation vector is $\psi_k N_k$ (cf. [4]).

Proof. Using the first variation formula, we have

$$\begin{aligned}\delta \operatorname{Vol} &= \frac{1}{2}\sum_k \langle R(p_{k+1}-p_{k-1}), v_k\rangle = \frac{1}{2}\sum_k \langle R(p_{k+1}-p_{k-1}), \psi_k N_k + \eta_k T_k\rangle \\ &= \frac{1}{2}\sum_k \left[\psi_k l_k \frac{\langle \nu_k, R\nu_{k-1}\rangle}{\sin\theta_k} + \psi_k l_{k-1}\frac{\langle \nu_{k-1}, -R\nu_k\rangle}{\sin\theta_k} + \frac{\eta_k}{\sin\theta_k}(l_k - l_{k-1})(1-\cos\theta_k)\right] \\ &= \frac{1}{2}\sum_k \left(\psi_k(l_k + l_{k-1}) + \eta_k(l_k - l_{k-1})\tan\frac{\theta_k}{2}\right).\end{aligned}$$

□

Recall that if $\{p_k\}_k$ is a critical point of the functional Length $+\Lambda$ Vol, then we have $l_k \equiv l_0$, $\theta_k \equiv \theta_0$ and $\Lambda l_0 = 2\tan(\theta_0/2)$.

Lemma 2.3.31.

$$|v_{k+1}-v_k|^2 - \langle v_{k+1}-v_k, R\nu_k\rangle^2 = [(\psi_{k+1}-\psi_k) + \tan(\theta_0/2)(\eta_{k+1}+\eta_k)]^2.$$

Therefore we have

$$|\nabla v_k|^2 - \langle \nabla v_k, R\nu_k\rangle^2 = \left(\nabla\psi_k + \frac{\Lambda}{2}(\eta_k + \eta_{k+1})\right)^2$$

Proof. Recall that

$$\begin{aligned}\langle N_k, -RN_{k+1}\rangle &= \tan\frac{\theta_k}{2} + \tan\frac{\theta_{k+1}}{2} = 2\tan\frac{\theta_0}{2}, \\ \langle N_k, N_{k+1}\rangle &= 1 - \tan\frac{\theta_k}{2}\tan\frac{\theta_{k+1}}{2} = 1 - \tan^2\frac{\theta_0}{2}.\end{aligned}$$

If we note $|N_k| = 1/\cos(\theta_0/2)$, then

$$\begin{aligned}&|v_{k+1}-v_k|^2 \\ &= |\psi_{k+1}N_{k+1} - \psi_k N_k|^2 + 2\langle \psi_{k+1}N_{k+1} - \psi_k N_k, \eta_{k+1}T_{k+1} - \eta_k T_k\rangle + |\eta_{k+1}T_{k+1} - \eta_k T_k|^2 \\ &= \frac{\psi_{k+1}^2}{\cos^2(\theta_0/2)} - 2\psi_k\psi_{k+1}(1-\tan^2(\theta_0/2)) + \frac{\psi_k^2}{\cos^2(\theta_0/2)} - 2\langle N_k, RN_{k+1}\rangle(\psi_{k+1}\eta_k - \psi_k\eta_{k+1}) \\ &\quad + \frac{\eta_{k+1}^2}{\cos^2(\theta_0/2)} - 2\eta_k\eta_{k+1}(1-\tan^2(\theta_0/2)) + \frac{\eta_k^2}{\cos^2(\theta_0/2)} \\ &= (1+\tan^2(\theta_0/2))(\psi_{k+1}^2 + \psi_k^2 + \eta_{k+1}^2 + \eta_k^2) \\ &\quad - 2(\psi_k\psi_{k+1} + \eta_k\eta_{k+1})(1-\tan^2(\theta_0/2)) + 4\tan(\theta_0/2)(\eta_k\psi_{k+1} - \eta_{k+1}\psi_k).\end{aligned}$$

Similarly since

$$\begin{aligned}&\langle v_{k+1}-v_k, R\nu_k\rangle \\ &= \langle \psi_{k+1}N_{k+1} - \psi_k N_k + \eta_{k+1}T_{k+1} - \eta_k T_k, R\nu_k\rangle \\ &= \psi_{k+1}\frac{\langle \nu_k - \nu_{k+1}, \nu_k\rangle}{\sin\theta_{k+1}} - \psi_k\frac{\langle \nu_{k-1}-\nu_k, \nu_k\rangle}{\sin\theta_k} - \eta_{k+1}\frac{\langle \nu_{k+1}-\nu_k, R\nu_k\rangle}{\sin\theta_{k+1}} + \eta_k\frac{\langle \nu_k - \nu_{k-1}, R\nu_k\rangle}{\sin\theta_k} \\ &= (\psi_{k+1}+\psi_k)\tan\frac{\theta_0}{2} - (\eta_{k+1}-\eta_k),\end{aligned}$$

we have

$$\langle v_{k+1}-v_k, R\nu_k\rangle^2 = (\psi_{k+1}+\psi_k)^2\tan^2\frac{\theta_0}{2} - 2\tan\frac{\theta_0}{2}(\psi_{k+1}+\psi_k)(\eta_{k+1}-\eta_k) + (\eta_{k+1}-\eta_k)^2.$$

Substracting these factors we have

$$\begin{aligned}
&|v_{k+1}-v_k|^2 - \langle v_{k+1}-v_k, R\nu_k\rangle^2 \\
&= \psi_{k+1}^2+\psi_k^2+\tan^2\frac{\theta_0}{2}(\eta_{k+1}^2+\eta_k^2) - 2\psi_k\psi_{k+1}\tan^2\frac{\theta_0}{2} + 2\eta_k\eta_{k+1} \\
&\quad + 2\tan\frac{\theta_0}{2}(2\eta_k\psi_{k+1} - 2\eta_{k+1}\psi_k + \psi_{k+1}\eta_{k+1} - \psi_{k+1}\eta_k + \psi_k\eta_{k+1} - \psi_k\eta_k) \\
&\quad - 2(\psi_k\psi_{k+1}+\eta_k\eta_{k+1}) + 2\tan^2\frac{\theta_0}{2}(\psi_k\psi_{k+1}+\eta_k\eta_{k+1}) \\
&= (\psi_{k+1}-\psi_k)^2 + \tan^2\frac{\theta_0}{2}(\eta_{k+1}+\eta_k)^2 + 2\tan\frac{\theta_0}{2}(\psi_{k+1}-\psi_k)(\eta_{k+1}+\eta_k) \\
&= [(\psi_{k+1}-\psi_k) + \tan\frac{\theta_0}{2}(\eta_{k+1}+\eta_k)]^2
\end{aligned}$$

□

Lemma 2.3.32.

$$\langle v_k, Rv_{k+1}\rangle = -2\tan\frac{\theta_0}{2}(\psi_k\psi_{k+1}+\eta_k\eta_{k+1}) - (1-\tan^2\frac{\theta_0}{2})(\eta_k\psi_{k+1}-\eta_{k+1}\psi_k).$$

Proof. This is also a simple calculation:

$$\begin{aligned}
\langle v_k, Rv_{k+1}\rangle &= \langle \psi_k N_k - \eta_k RN_k, \psi_{k+1}RN_{k+1} + \eta_{k+1}N_{k+1}\rangle \\
&= (\psi_k\psi_{k+1}+\eta_k\eta_{k+1})\langle N_k, RN_{k+1}\rangle - (\eta_k\psi_{k+1}-\eta_{k+1}\psi_k)\langle N_k, N_{k+1}\rangle \\
&= -2\tan\frac{\theta_0}{2}(\psi_k\psi_{k+1}+\eta_k\eta_{k+1}) - (1-\tan^2\frac{\theta_0}{2})(\eta_k\psi_{k+1}-\eta_{k+1}\psi_k).
\end{aligned}$$

□

Theorem 2.3.33 (Second variation formula for the length functional)**.**

$$\begin{aligned}
\delta^2\,\text{Length} &= \sum_k \left[|\nabla\psi_k|^2 - \Lambda^2\psi_k\psi_{k+1} + \Lambda\tan^2\frac{\theta_0}{2}\nabla\psi_k(\eta_{k+1}+\eta_k) + \frac{\Lambda^2}{4}(\eta_{k+1}-\eta_k)^2\right] l_0 \\
&= \sum_k \left[|\nabla\psi_k|^2 - \Lambda^2\psi_k\psi_{k+1} + \tan^2\frac{\theta_0}{2}(\Lambda\nabla\psi_k(\eta_{k+1}+\eta_k) + |\nabla\eta_k|^2)\right] l_0
\end{aligned}$$

In particular, for a normal variation we have

$$\delta^2\,\text{Length} = \sum_k (|\nabla\psi_k|^2 - \Lambda^2\psi_k\psi_{k+1})l_0 = -\sum_k \psi_k(\Delta\psi_k + \Lambda^2\psi_{k+1})l_0,$$

where we use the integration by parts and take the line element at the vertex as $L_k = (l_k + l_{k-1})/2 = l_0$.

Proof. By using the previous lemmas, we have

$$\begin{aligned}
&(|\nabla v_k|^2 - \langle \nabla v_k, R\nu_k\rangle^2) l_k + \Lambda \langle v_k, R v_{k+1}\rangle \\
&= \left(|\nabla \psi_k|^2 + \Lambda \nabla \psi_k (\eta_{k+1} + \eta_k) + \frac{\Lambda^2}{4}(\eta_{k+1} + \eta_k)^2 \right) l_0 \\
&\quad - \Lambda^2 l_0 (\psi_k \psi_{k+1} + \eta_k \eta_{k+1}) - \Lambda (1 - \tan^2 \frac{\theta_0}{2})(\eta_k \psi_{k+1} - \eta_{k+1}\psi_k) \\
&= |\nabla \psi_k|^2 l_0 + \Lambda \nabla \psi_k (\eta_{k+1} + \eta_k) l_0 + \frac{\Lambda^2}{4}(\eta_{k+1} - \eta_k)^2 l_0 - \Lambda^2 \psi_k \psi_{k+1} l_0 \\
&\quad - \Lambda (1 - \tan^2 \frac{\theta_0}{2})((\psi_{k+1} - \psi_k)(\eta_{k+1} + \eta_k) - (\psi_{k+1}\eta_{k+1} - \psi_k \eta_k)) \\
&= |\nabla \psi_k|^2 l_0 + \Lambda \tan^2 \frac{\theta_0}{2} \nabla \psi_k (\eta_{k+1} + \eta_k) l_0 + \frac{\Lambda^2}{4}(\eta_{k+1} - \eta_k)^2 l_0 - \Lambda^2 \psi_k \psi_{k+1} l_0 \\
&\quad + \Lambda (1 - \tan^2 \frac{\theta_0}{2})(\psi_{k+1}\eta_{k+1} - \psi_k \eta_k).
\end{aligned}$$

Taking the summation, we have the desired result. □

2.3.7 Instability of non-convex regular polygons

It is known that embedded regular polygons are global minimizer for the discrete isoperimetric problem (see e.g. [13]). In this section we will prove the instability of the non-convex regular polygons. To prove this, we find a special variation with a help of the following discrete version of Wirtinger's inequality:

Theorem 2.3.34 (Discrete Wirtinger's inequality, [12])**.** Let $\psi_0, \dots, \psi_n$ be $(n+1)$ real numbers such that

$$\psi_0 = \psi_n, \quad \sum_{k=0}^{n-1} \psi_k = 0.$$

Then we have

$$\sum_{k=0}^{n-1} (\psi_{k+1} - \psi_k)^2 \geq 4 \sin^2 \frac{\pi}{n} \sum_{k=0}^{n-1} \psi_k^2$$

and the equality holds if and only if there exist $A, B \in \mathbb{R}$ such that

$$\psi_k = A \cos \frac{2\pi k}{n} + B \sin \frac{2\pi k}{n}.$$

We inculde the proof of this theorem for the completeness. The essential part of the proof is the analysis of the discrete Laplacian by using the circulant matrix method.

Proof of Theorem 2.3.34. By some calculation we have

$$\sum_k (\psi_{k+1} - \psi_k)^2 = \sum_k (-\psi_{k-1} + 2\psi_k - \psi_{k+1})\psi_k = \langle L\Psi, \Psi \rangle,$$

where we put

$$L = \begin{pmatrix} 2 & -1 & 0 & \cdots & 0 & -1 \\ -1 & 2 & -1 & \cdots & 0 & 0 \\ 0 & -1 & 2 & \cdots & 0 & 0 \\ \vdots & \vdots & \vdots & \ddots & \vdots & \vdots \\ -1 & 0 & 0 & \cdots & -1 & 2 \end{pmatrix}, \quad \Psi = \begin{pmatrix} \psi_0 \\ \psi_2 \\ \psi_3 \\ \vdots \\ \psi_{n-1} \end{pmatrix}.$$

The $(n \times n)$-matrix L is the circulant matrix, and the eigenvalues λ_k and eigenvectors e_k can be computed by the well known fact (cf. e.g. [11], p. 72) :

$$\lambda_k = 4\sin^2 \frac{k\pi}{n}, \quad e_k = (1, \omega^k, \ldots, \omega^{k(n-1)}) \in \mathbb{C}^n, \quad \omega = \exp(2\pi\sqrt{-1}/n).$$

In particular, L is positive semi-definite. The assumption $\sum_k \psi_k = 0$ shows that the vector Ψ is perpendicular to the vector ${}^t(1, \ldots, 1)$ which is the eigenvector of the eigenvalue $\lambda_n = 0$. Therefore for any Ψ satisfying $\sum_k \psi_k = 0$ we have

$$\sum_k (\psi_{k+1} - \psi_k)^2 = \langle L\Psi, \Psi \rangle \geq 4\sin^2 \frac{\pi}{n} \langle \Psi, \Psi \rangle$$

and the equality holds if and only if $\Psi = e_1 = e_{n-1} = {}^t(1, \omega, \ldots, \omega^{n-1})$. □

In the following, we will consider a special type of normal variation, i.e., a variation which has the form:

$$p_k(t) = p_k + t\psi_k N_k, \quad N_k = R(\nu_k - \nu_{k-1})/\sin\theta_k.$$

By the second variation formula (Theorem 2.3.33) we have

$$\delta^2 \operatorname{Length} = \sum_k (|\nabla \psi_k|^2 - \Lambda^2 \psi_k \psi_{k+1}) l_0 = \sum_k \frac{1}{l_0} \left[(\psi_{k+1} - \psi_k)^2 - 4\psi_k \psi_{k+1} \tan^2 \frac{m\pi}{n} \right]$$

for any admissible variations, where we use the relation $\Lambda l_0 = 2\tan(\theta_0/2)$ and put $\theta_0 = 2m\pi/n$ for some $m \in \mathbb{Z}$ and assume that m and n are coprime. Note that the area-preserving condition derives $\sum_k \psi_k = 0$ (Lemma 2.3.30).

Theorem 2.3.35 (Instability of non-convex regular polygons)**.** Let $n \geq 5$. By taking $\psi_k = A\cos(2\pi k/n) + B\sin(2\pi k/n)$, $(A, B) \neq (0, 0)$, we have

$$\delta^2 \operatorname{Length} = \frac{4}{l_0} \left[\sin^2 \frac{\pi}{n} - \cos \frac{2\pi}{n} \tan^2 \frac{m\pi}{n} \right] \sum_k \psi_k^2.$$

In particular, $\delta^2 \operatorname{Length} < 0$ for $2 \leq m \leq n-2$, i.e., non-convex regular polygons are unstable.

Proof. By the discrete Wirtinger's inequality we have

$$\delta^2 \,\mathrm{Length} \geq \sum_k \frac{4}{l_0}(\psi_k^2 \sin^2 \frac{\pi}{n} - \psi_k \psi_{k+1} \tan^2 \frac{m\pi}{n}).$$

In the following we use the equality condition $\psi_k = A\cos(2\pi k/n) + B\sin(2\pi k/n)$ and put $\varphi_k = -A\sin(2\pi k/n) + B\cos(2\pi k/n)$. Then we have

$$\psi_{k+1} = \psi_k \cos(2\pi/n) + \varphi_k \sin(2\pi/n), \quad \psi_k\varphi_k = \frac{1}{2}(B^2 - A^2)\sin\frac{4k\pi}{n} + AB\cos\frac{4k\pi}{n}.$$

If we note the fact $\sum_k \psi_k\varphi_k = 0$, then

$$\begin{aligned}\delta^2 \,\mathrm{Length} &= \sum_k \frac{4}{l_0}\left[\psi_k^2 \sin^2\frac{\pi}{n} - \psi_k\left(\psi_k\cos\frac{2\pi}{n} + \varphi_k \sin\frac{2\pi}{n}\right)\tan^2\frac{m\pi}{n}\right] \\ &= \frac{4}{l_0}\left[\sin^2\frac{\pi}{n} - \cos\frac{2\pi}{n}\tan^2\frac{m\pi}{n}\right]\sum_k \psi_k^2.\end{aligned}$$

If $m = 1$ or $m = n-1$, then

$$\delta^2 \,\mathrm{Length} \geq \frac{4}{l_0}\sin^2\frac{\pi}{n}\tan^2\frac{\pi}{n}\sum_k \psi_k^2 \geq 0.$$

On the other hand, for $2 \leq m \leq n-2$ and $(A,B) \neq (0,0)$ we have

$$\delta^2 \,\mathrm{Length} \leq -\frac{4\sin^2(\pi/n)(1+2\cos^2(\pi/n))}{l_0\cos(2\pi/n)}\sum_k \psi_k^2 < 0,$$

where we use the fact $\tan^2(m\pi/n) \geq \tan^2(2\pi/n)$ if $2 \leq m \leq n-2$, and $\cos(2\pi/n) > 0$ if $n \geq 5$. This proves the statement. □

2.4 Geometry of discrete anisotropic surface energy

2.4.1 Anisotropic surface energy and its first variation

Next we consider the anisotropic energy for simplicial surfaces. Let M_h be a simplicial surface and $\{\nu_T\}_{T\in M_h^{(2)}}$ be the unit normal vector fields on M_h, where $M_h^{(2)}$ is the set of 2-skeltons, i.e., the set of triangles. For a continuous function $\gamma : S^2 \to \mathbb{R}_{>0}$, we define the *anisotropic surface energy of* M_h as

$$\mathscr{F}_\gamma(M_h) := \sum_{T\in M_h^{(2)}} \gamma(\nu_T)\cdot \mathrm{Area}(T).$$

This functional can be considered as a function $\mathscr{F}_\gamma : \mathbb{R}^{3n} \to \mathbb{R}$ as in the simplicial curve case, where n is the number of vertices of M_h.

Consider a vector-valued function $v_{p_j} \in \mathbb{R}^3$ defined on the n_i interior vertices $\mathscr{V}_{int} = \{v_{p_1}, \ldots, v_{p_{n_i}}\}$ of M_h. We may extend this function to the boundary vertices of M_h as well, by assuming $v_p = 0 \in \mathbb{R}^3$ for each boundary vertex p. The vectors v_{p_j} are the variation vector field of any boundary-fixing variation of the form

$$p_j(t) = p_j + t \cdot v_{p_j} + O(t^2),$$

that is, $p_j'(0) = v_{p_j}$. We define the vector $\vec{v} \in \mathbb{R}^{3n}$ by

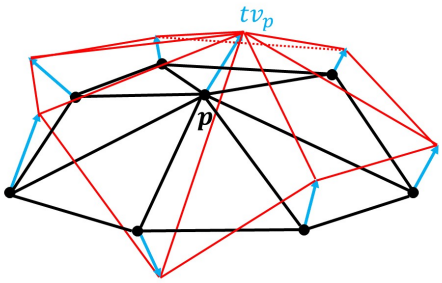

$$^t\vec{v} = (^tv_{p_1}, \ldots, ^tv_{p_n}).$$

If we modify this vector as a $(3 \times n)$-matrix $(v_{p_1}, \ldots, v_{p_n})$, each row vector can be considered as an element in $\mathscr{L}_0$, where $\mathscr{L}_0$ is the set of conforming functions on M_h which vanish on the boundary:

$$\mathscr{L}_0 := \{f : M_h \to \mathbb{R} : f \in C^0(M_h),\ f \text{ is linear on each } T \in M_h \text{ and } f|_{\partial M_h} = 0\}.$$

Now we derive the first variation formula for the anisotropic surface energy. We assume that γ is of class C^1 in the following. That means we would like to find the vectors $\nabla_{p_j}\mathscr{F}_\gamma \in \mathbb{R}^3$ which satisfies

$$\frac{d}{dt}_{t=0} \mathscr{F}_\gamma = \langle \vec{v}, \nabla \mathscr{F}_\gamma \rangle_{\mathbb{R}^{3n}} = \sum_{j=1}^{n} \langle v_{p_j}, \nabla_{p_j} \mathscr{F}_\gamma \rangle_{\mathbb{R}^3},$$

where we denote $^t\nabla \mathscr{F}_\gamma = (^t\nabla_{p_1}\mathscr{F}_\gamma, \ldots, ^t\nabla_{p_n}\mathscr{F}_\gamma) \in \mathbb{R}^{3n}$. In other words, we will calculate the directional derivative of the function $\mathscr{F}_\gamma$ in $\mathbb{R}^{3n}$.

Theorem 2.4.1. Let $\gamma : S^2 \to \mathbb{R}_{>0}$ be a C^1 function and p be an interior vertex of a simplicial surface M_h. Then at each interior vertex p the anisotropic energy gradient can be expressed in the following formula:

$$\nabla_p \mathscr{F}_\gamma = \frac{1}{2} \sum_{j=1}^{k} \xi_\gamma(\nu_j) \times (q_{j+1} - q_j) = \frac{1}{2} \sum_{j=1}^{k} (\xi_\gamma(\nu_{j-1}) - \xi_\gamma(\nu_j))) \times (q_j - p), \tag{4.1}$$

where we write star $(p) = \{T_1, \ldots, T_k\}$, $T_j = (p, q_j, q_{j+1})$, $\nu_j := \nu_{T_j}$, and $\xi_\gamma : S^2 \to \mathbb{R}^3$ is the Cahn-Hoffman map for γ.

Remarks . (1) If we take $\gamma \equiv 1$, this formula reduces to the well-known formula (so-called cotangent formula) in [34].

(2) We can define this quantity on any polyhedral surface, i.e., the quantity (4.1) is independent of the choice of the triangulation of polygons. Because the triangles lie on the same plane, they have the same unit normal. In general, we can treat the same way if the polyhedral surface contains a simply-connected subsurface lies in a plane (cf. [37], Remark 2.2).

(3) We can define the energy gradient at the edge as in the isotropic case [35], i.e., if we take an interior edge $e = q - p$ and denote the unit normal of adaject triangles $T_1 = (p, r_1, q)$ and $T_2 = (p, q, r_2)$ as ν_1, ν_2, then

$$\nabla_e \mathscr{F}_\gamma := \frac{1}{2}(\xi_\gamma(\nu_1) - \xi_\gamma(\nu_2)) \times e.$$

The proof of well-definedness is completely the same as [35], Lemma 83. From this viewpoint we can consider that the bending of a surface happens at edges instead of vertices.

Lemma 2.4.2. For a triangle $T = (p, q, r)$ we have

$$\begin{aligned}
\delta \operatorname{Area}(T) &= \frac{1}{2}[\langle \nu \times (r-q), v_p \rangle + \langle \nu \times (p-r), v_q \rangle + \langle \nu \times (q-p), v_r \rangle], \\
\delta\nu &= \frac{1}{2 \operatorname{Area}(T)} \left[(r-q) \times v_p + (p-r) \times v_q + (q-p) \times v_r - 2(\delta \operatorname{Area}(T))\nu \right],
\end{aligned}$$

where we write $\nu = \nu_T$.

Remark . Note that the first variation of the unit normal $\delta\nu = \delta\nu_T$ is tangent to the triangle T.

Proof. We put $\widetilde{\nu} = (q-p) \times (r-p)$. Then by differentiating $4 \operatorname{Area}(T)^2 = \langle \widetilde{\nu}, \widetilde{\nu} \rangle$, we have

$$\begin{aligned}
& 4 \cdot 2 \operatorname{Area}(T) \delta \operatorname{Area}(T) = 2\langle \delta[(q-p) \times (r-p)], (q-p) \times (r-p) \rangle \\
\iff & \delta \operatorname{Area}(T) = \frac{1}{2} \langle \delta[(q-p) \times (r-p)], \nu \rangle
\end{aligned}$$

Then we have

$$\begin{aligned}
\delta \operatorname{Area}(T) &= \frac{1}{2} \langle (v_q - v_p) \times (r-p) + (q-p) \times (v_r - v_p), \nu \rangle \\
&= \frac{1}{2} \langle \nu, (r-q) \times v_p + (p-r) \times v_q + (q-p) \times v_r \rangle \\
&= \frac{1}{2} [\langle \nu \times (r-q), v_p \rangle + \langle \nu \times (p-r), v_q \rangle + \langle \nu \times (q-p), v_r \rangle]
\end{aligned}$$

The second statement follows from the fact

$$\delta\nu = \frac{1}{\|\widetilde{\nu}\|}(\delta\widetilde{\nu} - 2(\delta \operatorname{Area}(T))\nu) = \frac{1}{2\operatorname{Area}(T)}(\delta\widetilde{\nu} - 2(\delta \operatorname{Area}(T))\nu).$$

□

Proof of Theorem 2.4.1. By using the lemma and the fact $D\gamma(\nu) \perp \nu$, on the triangle $T = (p, q, r)$ we have

$$\begin{aligned}
\delta(\gamma(\nu_T)\operatorname{Area}(T)) &= \langle D\gamma(\nu), \delta\nu\rangle \operatorname{Area}(T) + \gamma(\nu_T)\delta \operatorname{Area}(T) \\
&= \frac{1}{2}[\langle D\gamma(\nu), (r-q)\times v_p + (p-r)\times v_q + (q-p)\times v_r\rangle \\
&\quad + \gamma(\nu)(\langle \nu\times(r-q), v_p\rangle + \langle \nu\times(p-r), v_q\rangle + \langle \nu\times(q-p), v_r\rangle)] \\
&= \frac{1}{2}(\langle \xi_\gamma(\nu)\times(r-q), v_p\rangle + \langle \xi_\gamma(\nu)\times(p-r), v_q\rangle + \langle \xi_\gamma(\nu)\times(q-p), v_r\rangle).
\end{aligned}$$

By summing up these terms we have

$$\delta\mathscr{F}_\gamma = \sum_p \left\langle \frac{1}{2}\sum_{j=1}^{k} \xi_\gamma(\nu_j)\times(q_{j+1}-q_j), v_p \right\rangle,$$

where we write the vertices of the star (p) as $\{q_1, \ldots, q_k\}$, $q_{k+1} = q_1$, $T_j := (p, q_j, q_{j+1})$ and $\nu_j := \nu_{T_j}$. □

Remark . We can consider this formula as a special case of the smooth version of the first variation formula. On the triangle T_j, the $\pi/2$-rotation R_{T_j} in (N_{T_j}, ν_{T_j})-plane can be written as

$$R_{T_j}(x) = x \times \frac{\vec{c}_j}{|\vec{c}_j|}.$$

By using this fact, we have

$$\begin{aligned}
R_{T_j}(P_{T_j}(\xi(\nu_{T_j}))) &= R_{T_j}(\langle \xi(\nu_{T_j}), \nu_{T_j}\rangle \nu_{T_j} + \langle \xi(\nu_{T_j}), N_{T_j}\rangle N_{T_j}) \\
&= R_{T_j}(\gamma(\nu_{T_j})\nu_{T_j} + \langle D\gamma(\nu_{T_j}), N_{T_j}\rangle N_{T_j}) \\
&= \gamma(\nu_{T_j})\nu_{T_j} \times \frac{\vec{c}_j}{|\vec{c}_j|} + \langle D\gamma(\nu_{T_j}), N_{T_j}\rangle \nu_{T_j} \\
&= \frac{1}{|\vec{c}_j|}(\gamma(\nu_{T_j})\nu_{T_j}\times\vec{c}_j + \langle D\gamma(\nu_{T_j}), \vec{c}_j\times\nu_{T_j}\rangle\nu_{T_j}) \\
&= \frac{1}{|\vec{c}_j|}(\gamma(\nu_{T_j})\nu_{T_j}\times\vec{c}_j + \langle D\gamma(\nu_{T_j})\times\vec{c}_j, \nu_{T_j}\rangle\nu_{T_j}) \\
&= \frac{1}{|\vec{c}_j|}(\gamma(\nu_{T_j})\nu_{T_j}\times\vec{c}_j + D\gamma(\nu_{T_j})\times\vec{c}_j) \\
&= \frac{1}{|\vec{c}_j|}(D\gamma(\nu_{T_j}) + \gamma(\nu_{T_j})\nu_{T_j})\times\vec{c}_j = \frac{1}{|\vec{c}_j|}\xi(\nu_{T_j})\times\vec{c}_j.
\end{aligned}$$

Here we use the fact $D\gamma(\nu_{T_j}), \vec{c}_j \perp \nu_{T_j}$ (hence $D\gamma(\nu_{T_j}) \times \vec{c}_j \parallel \nu_{T_j}$). Therefore we have

$$\sum_{j=1}^{k} \langle \vec{c}_j \times \xi(\nu_{T_j}), v \rangle = \sum_{j=1}^{k} \langle -R_{T_j}(P_{T_j}(\xi(\nu_{T_j}))), v \rangle |\vec{c}_j| = \int_{\partial \mathrm{star}\,(p)} \langle -R(P(\xi)), v \rangle d\widetilde{s}$$

□

2.4.2 Discrete constant anisotropic mean curvature surfaces

The volume of oriented surface M_h is the oriented volume enclosed by the cone of the surface over the origin in $\mathbb{R}^3$

$$\mathrm{Vol}(M_h) := \frac{1}{3} \sum_{T=(p,q,r)\in M_h} \langle p, \nu_T \rangle \cdot \mathrm{Area}(T) = \frac{1}{6} \sum_{T=(p,q,r)\in M_h} \langle p, q \times r \rangle,$$

where we denote

$$\nu_T = \frac{(q-p) \times (r-p)}{\|(q-p) \times (r-p)\|}.$$

Then we have the first variation of the volume with respect to the variation vector field $\vec{v} \in \mathbb{R}^{3n}$ by

$$\frac{d}{dt}_{|t=0} \mathrm{Vol}(M_h) = \sum_p \langle v_p, \nabla_p \mathrm{Vol} \rangle,$$

where

$$\nabla_p \mathrm{Vol} = \frac{1}{6} \sum_{T=(p,q,r)\in \mathrm{star}\,(p)} q \times r.$$

Remark . Since $\partial\,\mathrm{star}\,(p)$ is a closed curve for an interior vertex p, we have

$$\sum_{T=(p,q,r)\in \mathrm{star}\,(p)} q \times r = \sum_{T=(p,q,r)\in \mathrm{star}\,(p)} (q-p) \times (r-p).$$

Therefore we can modify the first variation of the volume as follows:

$$\delta\,\mathrm{Vol} = \sum_p \left(\left\langle \frac{1}{3A_p} \sum_{T\in \mathrm{star}\,(p)} \mathrm{Area}(T)\nu_T, v_p \right\rangle \right) A_p.$$

Then we have weighted summations of the face normals which are volume descent direction:

$$N_p^V := \frac{1}{3A_p} \sum_{T\in \mathrm{star}\,(p)} \mathrm{Area}(T)\nu_T,$$

and it seems to be natural to take $3A_p = \mathrm{Area}(\mathrm{star}\,(p))$. However, since there is no natural area element at the vertices, another choice can be allowed. □

By virtue of the smooth case, we define the discrete constant anisotropic mean curvature surface as follows.

Definition 2.4.3 (Discrete CAMC surface (cf. [37], Definition 2.3))**.** Let $\gamma : S^2 \to \mathbb{R}$ be a C^1 function. Then a simplicial surface M_h has *constant anisotropic mean curvature (CAMC)* if there exists a constant Λ such that

$$\nabla_p \mathscr{F}_\gamma + 2\Lambda \nabla_p \operatorname{Vol} = 0$$

holds for all interior vertex p. If $\Lambda = 0$, we call the surface *discrete anisotropic minimal surface*. When $\gamma \equiv 1$, this reduces to the definition of the discrete CMC surfaces ([37]).

Remark . As we remarked before, if M_h is a discrete surface that contains a simply-connected discrete subsurface M_h' that lies in a plane, then it follows easily from the formula (4.1) that the discrete anisotropic minimality is independent of the choice of triangulation of the trace of M_h' as in the isotropic case (see [37], Remark 2.2).

We have the following Minkowski-type formula.

Proposition 2.4.4 (Discrete Minkowski-type formula)**.** Let $\gamma : S^2 \to \mathbb{R}$ be a C^1 function and M_h be a closed discrete CAMC-Λ surface. Then we have the following Minkowski-type formula:

$$\sum_{T=(p,q,r)} (\gamma(\nu_T) + \Lambda \langle p, \nu_T \rangle) \operatorname{Area}(T) = 0.$$

Proof. We consider the homothety $p(t) = p + tp = (1+t)p$. Then we have $\delta \mathscr{F}_\gamma(M_{h,t}) = 2\mathscr{F}_\gamma(M_h)$. On the other hand, by using the CAMC condition $\nabla_p \mathscr{F}_\gamma = -2\Lambda \nabla_p \operatorname{Vol}$ and the first variation of the volume, we have

$$\begin{aligned}
\delta \mathscr{F}_\gamma(M_{h,t}) &= \sum_p \langle \nabla_p \mathscr{F}_\gamma, p \rangle = -2\Lambda \sum_p \langle \nabla_p \operatorname{Vol}, p \rangle \\
&= -\frac{\Lambda}{3} \sum_p \sum_{\operatorname{star}(p) \ni T=(p,q,r)} \langle p, q \times r \rangle \\
&= -\Lambda \sum_{T=(p,q,r)} \langle p, q \times r \rangle = -2\Lambda \sum_{T=(p,q,r)} \langle p, \nu_T \rangle \operatorname{Area}(T).
\end{aligned}$$

Therefore we conclude

$$2\mathscr{F}_\gamma(M_h) = -2\Lambda \sum_{T=(p,q,r)} \langle p, \nu_T \rangle \operatorname{Area}(T) \iff \sum_{T=(p,q,r)} (\gamma(\nu_T) + \Lambda \langle p, \nu_T \rangle) \operatorname{Area}(T) = 0.$$

□

Remark . The following question is naturally arised from the observation in the planar curve case: can we prove the relation $(p+q+r)/3 = -(1/\Lambda)\xi_\gamma(\nu_T)$ on every triangle $T = (p, q, r)$? The answer is trivially false since we have discrete cylinders (Example 2.4.9). However, the following theorem is known in convex geometry [13].

Theorem 2.4.5 ([28], [29])**.** Of all convex polyhedra with a fixed surface area and the same number of faces, the best polyhedron with the largest volume is circumscribed about a sphere which touches each face in its barycenter.

Some calculation shows the following relation:

$$\nabla_p \mathscr{F}_\gamma + 2\Lambda \nabla_p \operatorname{Vol} = \frac{1}{2} \sum_{T=(p,q,r)\in \operatorname{star}(p)} \left(\xi_\gamma(\nu_T) + \frac{\Lambda}{3}(p+q+r) \right) \times (r-q),$$

Therefore, if every barycenter of the triangles touches to the rescaled Cahn-Hoffman map $-(1/\Lambda)\xi_\gamma$, then the surface is discrete CAMC-Λ. In particular, the regular tetrahedron, regular octahedron and regular icosahedron are discrete CMC surfaces as remarked in [35].

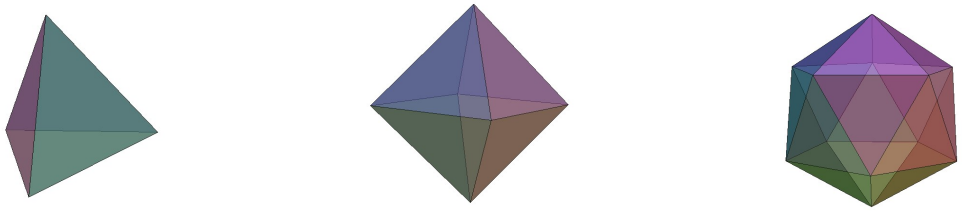

(a) Regular tetrahedron (b) Regular octahedron (c) Regular icosahedron

Figure 2.10: Discrete CMC surfaces

We also remark the following fact:

$$\gamma(\nu_T) + \Lambda \langle p, \nu_T \rangle = 0 \iff -\frac{1}{\Lambda}\xi_\gamma(\nu_T) \in \operatorname{span}\{p,\, q,\, r\}$$

for any triangle $T = (p, q, r)$. Moreover, $\gamma(\nu_T) + \Lambda\langle p, \nu_T\rangle = 0$ for every triangle $T = (p, q, r)$ if and only if the vector field $X_T := \xi_\gamma(\nu_T) + (\Lambda/3)(p + q + r)$ defines a piecewise constant vector field on the simplicial surface. For example, a discrete cylinder (Example 2.4.9) satisfies this condition with $\gamma \equiv 1$ even though the triangles of the surface does not necessarily touch to the sphere.

Another viewpoint is to consider the energy gradient on edges. As we remarked before, we can define the energy gradient on the edge $e = q - p$ as follows:

$$\nabla_e \mathscr{F}_\gamma := \frac{1}{2}(\xi_\gamma(\nu_1) - \xi_\gamma(\nu_2)) \times e, \quad \nabla_e \operatorname{Vol} = \frac{1}{6}(r_1 - r_2) \times e,$$

where we write $\operatorname{star}(e) = \{T_1, T_2\}$, $T_1 = (p, r_1, q)$, $T_2 = (p, q, r_2)$. Then we have

$$\nabla_e \mathscr{F}_\gamma - \Lambda \nabla_e \operatorname{Vol} = \frac{1}{2}\left[\left(\xi_\gamma(\nu_1) + \frac{\Lambda}{3}(p+q+r_1) \right) - \left(\xi_\gamma(\nu_2) + \frac{\Lambda}{3}(p+q+r_2) \right) \right] \times e.$$

Therefore, if we assume $\nabla_e \mathscr{F}_\gamma = \Lambda \nabla_e \operatorname{Vol}$ for every interior edge e, then

$$\omega(e) := \frac{1}{2}\left(\xi_\gamma(\nu) + \frac{\Lambda}{3}(p+q+r) \right) \times e,$$

is a well-defined discrete 1-form, where $T = (p, q, r)$ is either triangle of $\operatorname{star}(e)$.

2.4.3 Examples of discrete CAMC surfaces

Examples of discrete anisotropic minimal surfaces:

Example 2.4.6 (Discrete anisotropic Plateau-type problem)**.** For fixed points

$$q_1 = (-1, 0, -1), \quad q_2 = (0, -1, 0), \quad q_3 = (1, 0, -1), \quad q_4 = (0, 1, 0),$$

we want to find a point $p = (0, 0, h)$ which satisfies $\nabla_p \operatorname{Area} = 0$. This is one of the simplest case of the discrete Plateau-type problem. A direct calculation shows

$$\nabla_p \operatorname{Area} = \frac{2(1+2h)}{\sqrt{2h^2+2h+2}}(0, 0, 1).$$

Therefore we have $\nabla_p \operatorname{Area} = 0 \iff h = -1/2$.

Next we consider the anisotropic version of this surface. If we choose

$$\gamma : S^2 \to \mathbb{R}_{>0}, \quad \gamma(\nu_1, \nu_2, \nu_3) := \sqrt{a^2\nu_1^2 + b^2\nu_2^2 + c^2\nu_3^2},$$

then the Cahn-Hoffman map for γ is represented as

$$\xi_\gamma(\nu_1, \nu_2, \nu_3) = \frac{1}{\sqrt{a^2\nu_1^2 + b^2\nu_2^2 + c^2\nu_3^2}}(a^2\nu_1, b^2\nu_2, c^2\nu_3),$$

therefore the Wulff shape for γ is the ellipsoid $(x/a)^2 + (y/b)^2 + (z/c)^2 = 1$ and we have

$$\nabla_p \mathscr{F}_\gamma = \frac{2((a^2+b^2)h + a^2)}{\sqrt{(1+h)^2a^2 + h^2b^2 + c^2}}(0, 0, 1).$$

Therefore $\nabla_p \mathscr{F}_\gamma = 0 \iff h = -a^2/(a^2+b^2)$. We remark that if we choose $a = b = c = 1$, then $\gamma \equiv 1$ and it reduces to the previous result. These surfaces are stable since we will show that a discrete CAMC surface with only one interior vertex must be a stable (Corollary 2.4.16). Although it is difficult to find the discrete anisotropic

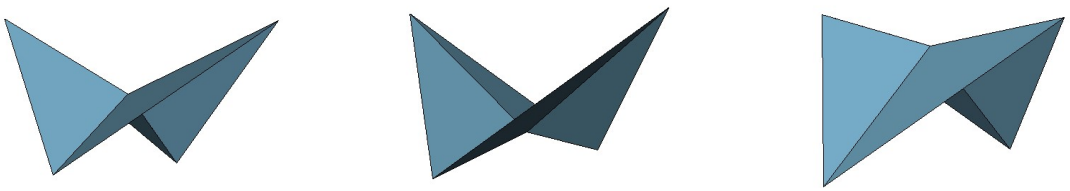

(a) $a = b = 1$ (b) $a = 2$, $b = 1$ (c) $a = 1$, $b = 2$

Figure 2.11: Discrete (stable) anisotropic minimal surfaces

minimal surfaces having more refined mesh by hand, we can visualize such surfaces numerically (gradient flow method) as in the following figures.

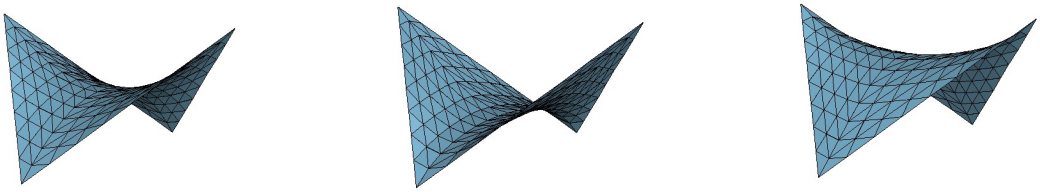

(a) $a = b = 1$ (b) $a = 2$, $b = 1$ (c) $a = 1$, $b = 2$

Figure 2.12: Discrete anisotropic minimal surfaces (numerically)

Example 2.4.7 (Square anisotropic catenoid)**.** We take $\gamma(\nu_1, \nu_2, \nu_3) = (\nu_1^8 + \nu_2^8 + \nu_3^8)^{1/8}$. For constructing Schwarz P surface (triply periodic minimal surface in $\mathbb{R}^3$), we sometimes use so-called *square catenoid* as in the Figure 2.13 (left). From the square catenoid, we can construct a square anisotopic catenoid numerically (Figure 2.13, right).

Figure 2.13: Discrete square catenoid and square anisotropic catenoid

Example 2.4.8 (Discrete timelike catenoid)**.** If we take $\gamma(\nu_1, \nu_2, \nu_3) = \sqrt{1 - 2\nu_3^2}$, $|\nu_3| < 1/\sqrt{2}$, the energy functional $\mathscr{F}_\gamma$ coincides with the area functional in the Lorentz-Minkowski space $(\mathbb{R}^3, dx_1^2 + dx_2^2 - dx_3^2)$ [17].

With this energy, we can consider a discrete version of the timelike catenoid which rotation axis is the timelike direction as in [37]. Consider the meridian curve $(x(t), 0, t)$ as

$$x(t) = r\cos\left(\frac{1}{r}at\right), \quad a = \frac{r}{\delta}\arccos\left(1 - \frac{1}{r^2}\frac{\delta^2}{1+\cos(2\pi/k)}\right)$$

Note that we have

$$\lim_{\delta\to+0}\frac{r}{\delta}\arccos\left(1 - \frac{1}{r^2}\frac{\delta^2}{1+\cos(2\pi/k)}\right) = \sqrt{\frac{2}{1+\cos(2\pi/k)}}, \quad \lim_{k\to\infty}\sqrt{\frac{2}{1+\cos(2\pi/k)}} = 1.$$

Then the discrete surface whose dihedral angle is $2\pi/k$, $k \in \mathbb{N}$, $k \geq 3$ and the profile curve $(x_j, 0, z_j)$ defined by

$$z_j := j\delta, \quad x_j := x(z_j)$$

is a discrete anisotropic minimal surface until the trapezoids are degenerate (Figure 2.14). The planar trapezoids of the surface may be triangulated arbitrarily by the previous remark.

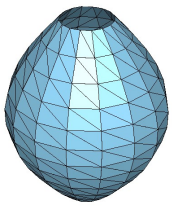

Figure 2.14: Discrete timelike catenoid (avoiding singularities)

Examples of discrete (non-zero) CAMC surfaces:

Example 2.4.9 (Discrete cylinder ([35], p. 116))**.** Let $X : \mathbb{Z}^2 \to \mathbb{R}^3$ be a map

$$X(j,l) := (a\cos(2\pi jm/k), a\sin(2\pi jm/k), el), \quad k \geq 3,\ 1 \leq m \leq k-1,\ a,\ e > 0,$$

where we assume that m and k are coprime. The image of the map X, denoted by M_h, is a "discrete cylinder". For any vertex p on the meridian line we have

$$\nabla_p \operatorname{Area} = e\sqrt{2(1-\cos(2\pi m/k))}\begin{pmatrix}1\\0\\0\end{pmatrix}, \quad \nabla_p \operatorname{Vol} = \begin{pmatrix}ae\sin(2\pi m/k)\\0\\0\end{pmatrix}.$$

Therefore if we set

$$H := H(k,e) := -\frac{1}{2a}\sqrt{\frac{2}{1+\cos(2\pi m/k)}} = -\frac{1}{2a\cos(\pi m/k)},$$

then we have $\nabla_p \operatorname{Area} + 2H\nabla_p \operatorname{Vol} = 0$ and M_h is discrete CMC surface by the definition. It is interesting that H does not depend on the value e and we saw that the value

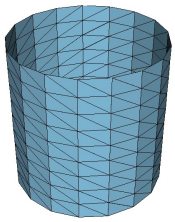

(a) $m = 1$, $k = 17$

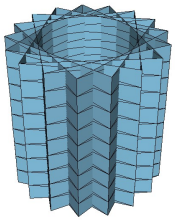

(b) $m = 5$, $k = 17$

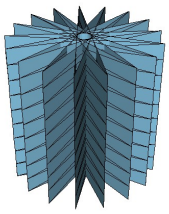

(c) $m = 9$, $k = 17$

Figure 2.15: Discrete cylinders

$-1/a\cos(\pi m/k)$ appeared as the curvature for regular k-gons. For the case $m = 1$, when $k \to \infty$ and $e \to 0$, we have a smooth cylinder with radius a and $H(k,e) \to -1/(2a)$.

Example 2.4.10 (Discrete unduloid-type surface ([35], p. 117))**.** By the similar calculation we also have a discrete unduloid-type surface. We consider the following discrete surface:

$$X(j,l) := \begin{cases}(a\cos(2\pi j/k), a\sin(2\pi j/k), el) & \text{if } l \text{ is odd},\\ (b\cos(2\pi j/k), b\sin(2\pi j/k), el) & \text{if } l \text{ is even}.\end{cases}$$

For any vertex p on the meridian curve we have

$$\nabla_p \operatorname{Area} = \frac{2(1-c)(e^2+(1+c)a(a-b))}{\sqrt{2e^2(1-c)+s^2(b-a)^2}} \begin{pmatrix} 1 \\ 0 \\ 0 \end{pmatrix}, \quad \nabla_p \operatorname{Vol} = \frac{se(2a+b)}{3} \begin{pmatrix} 1 \\ 0 \\ 0 \end{pmatrix},$$

where we put $c = \cos(2\pi/k)$ and $s = \sin(2\pi/k)$. Note that if we set $a = b$ this reduces to the discrete cylinder.

Example 2.4.11 (Visualization of generating crystals)**.** As we remarked in the preface, the anisotropic energy gives a mathematical model of small crystals. By using the energy gradient descent method, we can visualize the generation of shapes (Figure 2.16). On the other hand, although we cannot handle a non-smooth energy density by

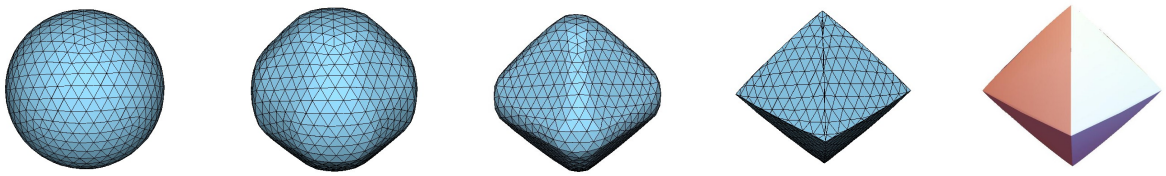

Figure 2.16: Anisotropic energy descent ($\gamma(\nu_1,\nu_2,\nu_3) = (\nu_1^{20}+\nu_2^{20}+\nu_3^{20})^{1/20}$).

out method, we can visualize such kind of objects by specifying the Cahn-Hoffman map except a measure zero set on the unit sphere (Figure 2.17).

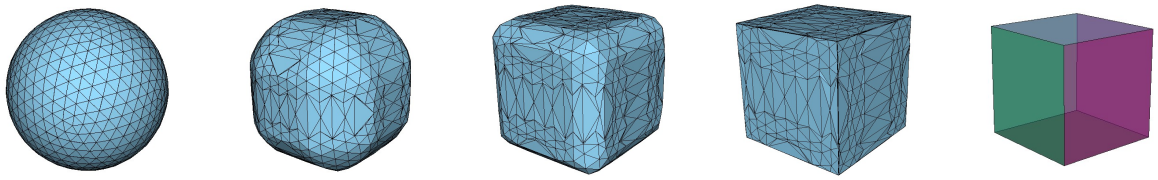

Figure 2.17: Anisotropic energy descent ($\gamma(\nu_1,\nu_2,\nu_3) = |\nu_1|+|\nu_2|+|\nu_3|$).

2.4.4 Second variation of the anisotropic energy

Next we consider the second variation of the anisotropic energy $\mathscr{F}_\gamma$ of a simplicial surface M_h. We assume that γ is of class C^2 in the following. Consider a variation of the form

$$p_j(t) = p_j + t v_{p_j} + O(t^2), \quad j = 1, \dots, n$$

with the variation vector field ${}^t v = ({}^t v_1, \dots, {}^t v_n)$. We say a variation is *admissible* (or *permissible*) if the variation is volume-preserving and fixes the boundary.

Definition 2.4.12 (Stability of discrete CAMC surface)**.** Let $\gamma : S^2 \to \mathbb{R}$ be a C^2 function and M_h be a discrete CAMC surface. Then M_h is said to be *stable* if $\delta^2 \mathscr{F}_\gamma \geq 0$ for any admissible variation.

Lemma 2.4.13 (cf. [37], Lemma 5.1)**.** For a discrete CAMC-Λ surface M_h with vertex set $\mathscr{V}$, we have

$$\delta^2\mathscr{F}_\gamma := \frac{d^2}{d^2t}_{|t=0}\mathscr{F}_\gamma = \sum_{p\in\mathscr{V}}\langle v_p, \delta(\nabla_p\mathscr{F}_\gamma + 2\Lambda\nabla_p \operatorname{Vol})\rangle.$$

for any admissible variation.

The proof is completely the same as Lemma 2.3.23.

We now decompose $\delta^2\mathscr{F}_\gamma$ into the sum of two terms

$$^t\vec{v}Q^\gamma\vec{v} := \sum_{p\in\mathscr{V}}\langle v_p, \delta(\nabla_p\mathscr{F}_\gamma)\rangle, \quad ^t\vec{v}Q^V\vec{v} := \sum_{p\in\mathscr{V}}\langle v_p, \delta(\nabla_p \operatorname{Vol})\rangle.$$

Then Q^γ and Q^V are $3n\times 3n$-matrix and

$$\delta^2\mathscr{F}_\gamma = \frac{d^2}{d^2t}_{|t=0}\mathscr{F}_\gamma = {}^t\vec{v}(Q^\gamma + 2\Lambda Q^V)\vec{v}.$$

Since

$$\begin{aligned}\langle v_p, \delta\nabla_p \operatorname{Vol}\rangle &= \frac{1}{6}\sum_{T=(p,q_j,q_{j+1})\in\operatorname{star}(p)}\langle v_p, v_{q_j}\times q_{j+1} + q_j\times v_{q_{j+1}}\rangle\\ &= \frac{1}{6}\sum_j\langle v_p, (q_{j-1}-q_{j+1})\times v_{q_j}\rangle\\ &= \frac{1}{6}\sum_j {}^t v_p[(q_{j-1}-q_{j+1})\times \boldsymbol{e}_1, (q_{j-1}-q_{j+1})\times \boldsymbol{e}_2, (q_{j-1}-q_{j+1})\times \boldsymbol{e}_3]v_{q_j},\end{aligned}$$

we have the following result:

Proposition 2.4.14 ([37], Proposition 5.2)**.** The matrix Q^V can be considered as an $n\times n$ grid with a 3×3 entry $Q^V_{p,q}$ for each pair of vertices $p, q\in\mathscr{V}_{\text{Int}}$ of M_h, so that

$$^t\vec{v}Q^V\vec{v} = \sum_{p\in\mathscr{V}}\langle v_p, \delta(\nabla_p \operatorname{Vol})\rangle$$

for the variation vector field $\vec{v}$ of any permissible variation. We have $Q^V_{p,p} = 0$ and $Q^V_{p,q} = 0$ when the vertices p and q are not adjacent, and

$$\begin{aligned}Q^V_{p,q} &= \frac{1}{6}\begin{pmatrix} 0 & r_{2,3}-r_{1,3} & r_{1,2}-r_{2,2}\\ r_{1,3}-r_{2,3} & 0 & r_{2,1}-r_{1,1}\\ r_{2,2}-r_{1,2} & r_{1,1}-r_{2,1} & 0\end{pmatrix}\\ &= \frac{1}{6}((r_1-r_2)\times \boldsymbol{e}_1, (r_1-r_2)\times \boldsymbol{e}_2, (r_1-r_2)\times \boldsymbol{e}_3)\end{aligned}$$

for adjacent unequal p and q, where (p,q,r_k) are the two triangles in $\operatorname{star}(\overline{pq})$ and $r_k = (r_{k,1}, r_{k,2}, r_{k,3})$ for $k = 1, 2$, $\{\boldsymbol{e}_1, \boldsymbol{e}_2, \boldsymbol{e}_3\}$ is the canonical basis of $\mathbb{R}^3$, and (p,q,r_2) is properly oriented and (p,q,r_1) is not.

Next we consider the matrix Q^γ. In the proof of the first variation formula (Theorem 2.4.1), we showed

$$\frac{d}{dt}\mathscr{F}_\gamma = \frac{1}{2}\sum_{T=(p,q,r)} [\langle \xi_\gamma(\nu_T)\times(r-q), v_p\rangle + \langle \xi_\gamma(\nu_T)\times(p-r), v_q\rangle + \langle \xi_\gamma(\nu_T)\times(q-p), v_r\rangle].$$

Therefore we put

$$\begin{aligned}
&{}^t\vec{v}Q^\gamma\vec{v}\\
&= \frac{1}{2}\sum_{T=(p,q,r)} [\langle d\xi_\gamma(\delta\nu_T)\times(r-q), v_p\rangle + \langle d\xi_\gamma(\delta\nu_T)\times(p-r), v_q\rangle + \langle d\xi_\gamma(\delta\nu_T)\times(q-p), v_r\rangle\\
&\quad + \langle \xi_\gamma(\nu_T)\times(v_r-v_q), v_p\rangle + \langle \xi_\gamma(\nu_T)\times(v_p-v_r), v_q\rangle + \langle \xi_\gamma(\nu_T)\times(v_q-v_p), v_r\rangle]\\
&=: \frac{1}{2}\sum_{T=(p,q,r)} (I_T + II_T).
\end{aligned}$$

A simple calculation shows that

$$II_T = -2\langle \xi_\gamma(\nu_T), v_p\times v_q + v_q\times v_r + v_r\times v_p\rangle$$

For a triangle $T=(p,q,r)$ if we put

$$A_T := (r-q)\times v_p + (p-r)\times v_q + (q-p)\times v_r = (p-r)\times(v_q-v_p) + (q-p)\times(v_r-v_p),$$

then we have

$$\begin{aligned}
\delta\nu_T &= \frac{1}{2\,\mathrm{Area}(T)}(A_T - \langle A_T, \nu_T\rangle\nu_T),\\
I_T &= \frac{1}{2\,\mathrm{Area}(T)}\langle d\xi_\gamma(A_T - \langle A_T,\nu_T\rangle\nu_T), A_T\rangle = 2\,\mathrm{Area}(T)\langle d\xi_\gamma(\delta\nu_T), \delta\nu_T\rangle.
\end{aligned}$$

The last equality follows from the facts the first variation of the unit normal $\delta\nu_T$ is tangent to the triangle and $d\xi_\gamma(\delta\nu_T)$ is perpendicular to ν_T (since $d\xi_\gamma$ is the endomorphism of the tangent space).

Proposition 2.4.15. The bilinear form ${}^t\vec{v}Q^\gamma\vec{v}$ can be represented as follows:

$${}^t\vec{v}Q^\gamma\vec{v} = \sum_{T=(p,q,r)} \frac{\langle d\xi_\gamma(A_T - \langle A_T,\nu_T\rangle\nu_T), A_T\rangle}{4\,\mathrm{Area}(T)} - \langle \xi_\gamma(\nu_T), v_p\times v_q + v_q\times v_r + v_r\times v_p\rangle,$$

where we put $A_T := (r-q)\times v_p + (p-r)\times v_q + (q-p)\times v_r$.

Although we cannot achieve to determine the explicit representation of Q^γ, we have the following facts: If we consider the matrix Q^γ as an $n\times n$ grid with a 3×3 entry $Q^\gamma_{p,q}$ for each pair of interior vertices p,q of M_h, then

(1) $Q^{\gamma}_{p,q} = 0$ when the vertices p and p are not adjacent.

(2) For the diagonal entries $Q^{\gamma}_{p,p}$ we have

$$\begin{aligned} {}^t v_p Q^{\gamma}_{p,p} v_p &= \sum_{T=(p,q,r)\in \mathrm{star}\,(p)} \frac{1}{4\,\mathrm{Area}(T)} \langle d\xi_\gamma(A_T - \langle A_T, \nu_T\rangle \nu_T), A_T\rangle \\ &= \sum_{T=(p,q,r)\in \mathrm{star}\,(p)} \frac{1}{4\,\mathrm{Area}(T)} \langle d\xi_\gamma(A_T - \langle A_T, \nu_T\rangle \nu_T), A_T - \langle A_T, \nu_T\rangle \nu_T\rangle, \end{aligned}$$

where we put $A_T = (r-q)\times v_p$.

(3) For adjacent vertices p, q if we denote the adjacent triangles $T_1 = (p, r_1, q)$ and $T_2 = (p, q, r_2)$, then

$$\begin{aligned} {}^t v_p Q^{\gamma}_{p,q} v_q = \frac{\langle d\xi_\gamma(A_1 - A_1\langle A_1, \nu_1\rangle \nu_1), A_1\rangle}{4\,\mathrm{Area}(T_1)} + \frac{\langle d\xi_\gamma(A_2 - A_2\langle A_2, \nu_2\rangle \nu_1), A_2\rangle}{4\,\mathrm{Area}(T_2)} \\ - \langle \xi_\gamma(\nu_1) - \xi_\gamma(\nu_2), v_p \times v_q\rangle, \end{aligned}$$

where we put $A_1 = (r_2 - q)\times v_p + (p - r_2)\times v_q$, $A_2 = (q - r_1)\times v_p + (r_1 - p)\times v_q$, $\nu_1 := \nu_{T_1}$ and $\nu_2 := \nu_{T_2}$.

Moreover, we still have the following stability result.

Corollary 2.4.16. Let $\gamma : S^2 \to \mathbb{R}_{>0}$ be of class C^2 and convex. If a discrete CAMC surface M_h has only one interior vertex, then it is stable.

Proof. The single interior vertex is denoted by p, and $\mathrm{star}\,(p) = M_h$. Then $Q^{\gamma} = Q^{\gamma}_{p,p}$ and $Q^{V} = Q^{V}_{p,p}$ are 3×3 matrices. By Propsition 2.4.14, $Q^V = 0$ and we have

$${}^t v_p Q^{\gamma}_{p,p} v_p = \frac{1}{4} \sum_{T=(p,q,r)\in \mathrm{star}\,(p)} \frac{1}{\mathrm{Area}(T)} \langle d\xi_\gamma(A_T - \langle A_T, \nu_T\rangle \nu_T), A_T - \langle A_T, \nu_T\rangle \nu_T\rangle.$$

for any vector $v_p \in \mathbb{R}^3$, where we put $A_T := (r-q)\times v_p$. Since the matrix $d\xi_\gamma$ is positive semidefinite on the tangent space by the assumption, we have $\delta^2 \mathscr{F}_\gamma \geq 0$ for all admissible variations. □

Remark . This is a generalization of the stability result in [37], Corollary 5.1. We also remark that the convexity condition for the energy density $\gamma : S^2 \to \mathbb{R}_{>0}$ seems to be natural requirement for the stability (cf. [31], [25], [32] for strictly convex case, [24] for convex case).

Appendix

Examples of the anisotropic energy

The following contents are contained in [39] and we will reformulate with our notation.

In the following we assume that X has a nonparametric form, i.e., $M \subset \mathbb{R}^n$ is a domain and $X(x) = (x, \varphi(x))$ for some smooth function $\varphi : M \to \mathbb{R}$. In this case, the unit normal vector field ν_X along X and the area element can be written as follows:

$$\nu_X = \frac{1}{\sqrt{1 + \|\nabla\varphi\|^2}}(\nabla\varphi, -1), \quad dA_X = \sqrt{1 + \|\nabla\varphi\|^2}dx.$$

We also assume that the image of the Cahn-Hoffman map $\widetilde{W}_\gamma$ has a nonparametric form. In this case, a local coordinate of $\widetilde{W}_\gamma$ is defined by using the projection

$$\xi_\gamma(\nu) = (y_1, \ldots, y_n, y_{n+1}) \mapsto (y_1, \ldots, y_n).$$

By using this notation, we can write the anisotropic shape operator and the anisotropic mean curvature as

$$-d\widetilde{\xi}_\gamma = -\left(\frac{\partial y_i}{\partial x_j}\right)_{i,j=1,\ldots,n}, \quad \Lambda = -\frac{1}{n}\sum_{i=1}^{n}\frac{\partial y_i}{\partial x_i}.$$

Example 2.4.17 (isotropic case)**.** If we take $\Omega = \{\nu = (\nu_1, \ldots, \nu_{n+1}) \in S^n \mid \nu_{n+1} < 0\}$ and $\gamma(\nu) \equiv 1$, then we have $\xi_\gamma(\nu) = \nu$ for $\nu \in \Omega$, $\widetilde{W}_\gamma = \Omega$ and

$$\widetilde{\xi}_\gamma = \xi_\gamma \circ \nu_X = \frac{1}{\sqrt{1 + \|\nabla\varphi\|^2}}(\nabla\varphi, -1), \quad \Lambda = -\frac{1}{n}\sum_{i=1}^{n}\frac{\partial}{\partial x_i}\left(\frac{\varphi_i}{\sqrt{1 + \|\nabla\varphi\|^2}}\right),$$

where we write $\varphi_i = \partial\varphi/\partial x_i$. Therefore X is CAMC if and only if X is a CMC hypersurface in $\mathbb{R}^{n+1}$ in the usual sense. □

Example 2.4.18 (hyperbolic case)**.** If we take $\Omega = \{\nu \in S^n \mid \nu_{n+1} < -1/\sqrt{2}\}$ and $\gamma : \Omega \to \mathbb{R}_{>0}$ to be

$$\gamma(\nu) := \sqrt{\nu_{n+1}^2 - \nu_1^2 - \cdots - \nu_n^2} = \sqrt{-1 + 2\nu_{n+1}^2}$$

Then we have

$$\xi_\gamma(\nu) = \frac{1}{\gamma(\nu)}(-\nu_1, \ldots, -\nu_n, \nu_{n+1}),$$

and the image of the Cahn-Hoffman map becomes the lower sheet of the two-sheeted hyperboloid $y_{n+1}^2 - (y_1^2 + \cdots + y_n^2) = 1$. Since

$$\int_M \gamma(\nu_X)\, dA_X = \int_M \sqrt{\frac{1 - \|\nabla\varphi\|^2}{1 + \|\nabla\varphi\|^2}} \cdot \sqrt{1 + \|\nabla\varphi\|^2}\, dx = \int_M \sqrt{1 - \|\nabla\varphi\|^2}\, dx,$$

the anisotropic surface energy coincides with the n-dimensional volume of X in the Lorentz-Minkowski space $\mathbb{R}^{n,1}$. Moreover we have

$$\widetilde{\xi}_\gamma = \xi_\gamma \circ \nu_X = \frac{1}{\sqrt{1 - \|\nabla\varphi\|^2}}(-\nabla\varphi, -1), \quad \Lambda = \frac{1}{n}\sum_{i=1}^n \frac{\partial}{\partial x_i}\left(\frac{\varphi_i}{\sqrt{1 - \|\nabla\varphi\|^2}}\right),$$

Therefore X is CAMC if and only if X is a spacelike constant mean curvature hypersurface in the Lorentz-Minkowski space $\mathbb{R}^n_1$. □

More generally we have the following result:

Theorem 2.4.19 ([17], Theorem 1)**.** Set $\Omega_1 = \{\nu = (\nu_1, \nu_2, \nu_3) \in S^2 \mid |\nu_3| > 1/\sqrt{2}\}$, $\Omega_2 = \{\nu = (\nu_1, \nu_2, \nu_3) \in S^2 \mid |\nu_3| < 1/\sqrt{2}\}$. Define a function $\gamma : S^2 \to \mathbb{R}$ as

$$\gamma(\nu_1, \nu_2, \nu_3) := \sqrt{|\nu_3^2 - \nu_1^2 - \nu_2^2|} = \sqrt{|2\nu_3^2 - 1|}.$$

Then, an immersion $X : M \to \mathbb{R}^3$ with Gauss image $\nu(M) \subset \Omega_1 \cup \Omega_2$ is anisotropic zero mean curvature if and only if the mean curvature of X is zero as an immersed surface in $\mathbb{R}^3_1$.

Example 2.4.20 (parabolic case)**.** If we take $\Omega = \{\nu \in S^n \mid \nu_{n+1} < 0\}$ and $\gamma : \Omega \to \mathbb{R}_{>0}$ to be

$$\gamma(\nu) = -\frac{1}{2}\frac{\nu_1^2 + \cdots + \nu_n^2}{\nu_{n+1}} = \frac{1}{2}\left(\nu_{n+1} - \frac{1}{\nu_{n+1}}\right)$$

Then we have

$$\xi_\gamma(\nu) = \left(-\frac{\nu_1}{\nu_{n+1}}, \ldots, -\frac{\nu_n}{\nu_{n+1}}, \frac{1 - \nu_{n+1}^2}{2\nu_{n+1}^2}\right)$$

and the image of the Cahn-Hoffman map of γ becomes the paraboloid $y_{n+1} = (1/2)(y_1^2 + \cdots + y_n^2)$. Since we have

$$\int_M \gamma(\nu_X)\, dA_X = \int_M \frac{\|\nabla\varphi\|^2}{2\sqrt{1 + \|\nabla\varphi\|^2}}\, dA_X = \frac{1}{2}\int_M \|\nabla\varphi\|^2\, dx,$$

the anisotropic surface energy coincides with the Dirichlet energy of φ. Moreover we have

$$\widetilde{\xi}_\gamma = \xi_\gamma \circ \nu_X = (\nabla\varphi, \|\nabla\varphi\|^2/2), \quad \Lambda = -\frac{1}{n}\sum_{i=1}^n \frac{\partial^2\varphi}{\partial x_i^2}, \quad H_2^\gamma = \varphi_{11}\varphi_{22} - \varphi_{12}^2.$$

Therefore X has zero anisotropic mean curvature if and only if φ is harmonic on M. Note that this geometry is called the isotropic geometry [33]. □

In the paper [39], it is remarked that the relation between the energy density and its Wulff shape by using the Legendre transformation. We will give its reformulation in our notation.

Let us consider a nonparametric case and we use the same notation as before. Let $S^n_- := \{\nu = (\nu_1, \dots, \nu_{n+1}) \in S^n \mid \nu_{n+1} < 0\}$ be the lower hemisphere of S^n, $\Omega \subset S^n_-$ be a domain and $\gamma : \Omega \to \mathbb{R}_{>0}$ be a positive-valued C^2 function. Moreover we assume that the image of the Cahn-Hoffman map ξ_γ, denoted by M_0, can be represented as a graph $M_0 = \{y \in \mathbb{R}^n \mid w = G(y)\}$ for some function G.

Let us recall the definition of the Legendre transformation. The Legendre transformation of a function $G(y) = G(y_1, \dots, y_n)$ is given by a function

$$v = G^*(p_1, \dots, p_n), \quad p_i = \frac{\partial G}{\partial y_i}, \quad G^* := -G + \sum_i y_i p_i.$$

We assume that $\det(G_{y_i y_j}) \neq 0$ to make the map $y \mapsto p$ diffeomorphism. By the definition of the anisotropic Gauss map we have $p_i = \partial G/\partial y_i = \partial \varphi/\partial x_i$. Therefore it follows from the representation of the unit normal that we have

$$G^*(p_1, \dots, p_n) = G^*(-\nu_1/\nu_{n+1}, \dots, -\nu_n/\nu_{n+1}).$$

and

$$G^*(p)dx = -\nu_{n+1} G^*(-\nu_1/\nu_{n+1}, \dots, -\nu_n/\nu_{n+1}) dA_X.$$

We will prove the coefficient of dA_X coincide with the energy density γ we gave first. If we choose the unit normal of M_0 as

$$\nu = \left(\frac{\nabla G}{\sqrt{1 + |\nabla G|^2}}, -\frac{1}{\sqrt{1 + |\nabla G|^2}} \right) = \left(\frac{\nabla \varphi}{\sqrt{1 + |\nabla \varphi|^2}}, -\frac{1}{\sqrt{1 + |\nabla \varphi|^2}} \right),$$

then the support function of M_0 becomes

$$\begin{aligned} \langle (y, G(y)), \nu \rangle_{\mathbb{R}^{n+1}} &= \frac{\langle \nabla G, y \rangle_{\mathbb{R}^n} - G}{\sqrt{1 + |\nabla \varphi|^2}} \\ &= -\nu_{n+1} G^*(p) = -\nu_{n+1} G^*(-\nu_1/\nu_{n+1}, \dots, \nu_n/\nu_{n+1}). \end{aligned}$$

On the other hand if we compute the support function of M_0 as the image of the Cahn-Hoffman map we have $\langle \xi_\gamma(\nu), \nu \rangle = \gamma(\nu)$, hence we have the desired result.

In this sense, the energy appeared in [39] (Proposition 5) can be regarded as the anisotropic energy we defined. As he mentioned there, we have the following first variation formula

$$\delta \int G^*(p)\, dx = n \int \Lambda \delta \varphi \, dx$$

for any support compact variation of φ.

Bibliography

[1] Aggarwal, A., Chang, J.S., and Yap, C.K.: Minimum area circumscribing polygons, *The Visual Computer* **1** (1985), no. 2, 112-117.

[2] Alexandrov, A. D.: A characteristic property of spheres, *Ann. Mat. Pura Appl.* **58** (1962), 303–315.

[3] Ando N.: Hartman-Wintner's theorem and its applications, *Calc. Var. Partial Differential Equations* **43** (2012), 389–402.

[4] Barbosa, J. L. and do Carmo, M.: Stability of hypersurfaces with constant mean curvature, *Math. Z.* **185** (1984), 339–353.

[5] Bauer, U., Polthier, K., and Wardetzky, M.: Uniform convergence of discrete curvatures from nets of curvature lines, *Discrete comput. geom.* **43** (2010), 798–823.

[6] Bobenko, A., and Pinkall, U.: Discrete isothermic surfaces, *J. reine angew. Math.* **30**, 4 (1996), 187–208.

[7] Brendle, S.: Embedded self-similar shrinkers of genus 0. *Ann. of Math.* **183** (2016), 715–728.

[8] Chakerian, G. D., and Lange, L. H.: Geometric Extremum Problems, *Math. Magazine* **44** (2) (1971), 57–69.

[9] Chow B., and Glickenstein, D.: Semidiscrete Geometric Flow of Polygon, *Amer. Math. Monthly* **114**, No. 4 (2007), 316–328.

[10] Crane, K., and Wardetzky, M.: A Glimpse into Discrete Differential Geometry, *Notices of American Mathematical Society* **64** (2017), 1153–1159.

[11] Davis, P. J.: Circulant Matrices, Wiley-Interscience, New York, 1979.

[12] Fan, K., Taussky, O., and Todd, J.: Discrete analogs of inequalities of Wirtinger, *Monatsh. Math.*, **59** (1955), 73–90.

[13] Florian, A.: Extremum Problems for Convex Discs and Polyhedra, in *Handbook of Convex Geometry*, North-Holland (1993), 179–221.

[14] Han, H., and Nishimura, T.: Strictly convex Wulff shapes and C^1 convex integrands, *Proc. Amer. Math. Soc.* **145** (2017), 3997–4008.

[15] Hatakeyama, Y.: Some attempts to construct geometric theories to represent and explicate physical phenomenons, PhD dissertation, Kyushu University, 2018.

[16] He, Y., Li, H., Ma, H., and Ge, J.: Compact embedded hypersurfaces with constant higher order anisotropic mean curvatures, *Indiana Univ. Math. J.* **58** (2009), 853-868.

[17] Honda, A., Koiso, M. and Tanaka, Y.: Non-convex anisotropic surface energy and zero mean curvature surfaces in the Lorentz-Minkowski space, *Journal of Math-for-Industry* **5** (2013), 73–82.

[18] Hopf, H.: Differential geometry in the large. Notes taken by Peter Lax and John W. Gray. With a preface by S. S. Chern. Second edition. With a preface by K. Voss. Lecture Notes in Mathematics **1000**. Springer-Verlag, Berlin, 1989.

[19] Hoffman, T.: Discrete Differential Geometry of Curves and Surfaces, *MI Lecture Notes* Series Vol. 18, Faculty of Mathematics, Kyushu University, 2008.

[20] Jikumaru, Y. and Koiso, M.: Non-uniqueness of closed embedded non-smooth hypersurfaces with constant anisotropic mean curvature, arXiv:1903.03958.

[21] Kälberer, F., Nieser, M., and Polthier, K.: QuadCover - Surface Parameterization using Branched Coverings, Computer Graphics Forum 26, 3 (Sept.), 375–384.

[22] Kapouleas, N.: Complete constant mean curvature surfaces in euclidean three-space, *Ann. of Math.* (2) **131** (1990), 239–330.

[23] Kapouleas, N.: Constant mean curvature surfaces constructed by fusing Wente tori, *Invent. Math.* **119** (1995), 443–518.

[24] Koiso, M.: Uniqueness of stable closed non-smooth hypersurfaces with constant anisotropic mean curvature, arXiv:1903.03951.

[25] Koiso, M. and Palmer, B.: Geometry and stability of surfaces with constant anisotropic mean curvature, *Indiana Univ. Math. J.* **54** (2005), 1817–1852.

[26] Koiso, M. and Palmer, B.: Anisotropic umbilic points and Hopf's theorem for surfaces with constant anisotropic mean curvature. *Indiana Univ. Math. J.* **59** (2010), 79–90.

[27] Lam, W. Y.: Discrete Minimal Surfaces: Critical Points of the Area Functional from Integrable Systems, *Int. Math. Res. Not.*, **2018**, Issue 6 (2018), 1808–1845.

[28] Lindelöf, L.: Propriétés générales des polyédes qui, sous une étendue superficielle donnée, renferment le plus grand volume, *Bull. Acad. Sci. St. Pétersbourg* **14**, 257–269.

[29] Minkowski, H.: Allegemeine Lehrsätze über die konvexen Polyeder, *Nachr. Ges. Wiss. Göttingen, Math. phys. KL*, 198–219.

[30] Morgan, F.: Planar Wulff shape is unique equilibrium. *Proc. Amer. Math. Soc.* **133** (2005), 809–813.

[31] Palmer, B.: Stability of the Wulff shape, *Proc. Amer. Math. Soc.* **126** (1998), 3661–3667.

[32] Palmer, B.: Stable closed equilibria for anisotropic surface energies: surfaces with edges, *Journal of Geometric Mechanics* **4** (2012), 89–97.

[33] Pottman, H., Grohs, P., and Mitra, M. J.: Laguerre minimal surfaces, isotropic geometry and linear elasticity, *Adv. Comput. Math.* **31** (2009), 391–419.

[34] Pinkall, U. and Polthier, K.: Computing Discrete Minimal Surfaces and Their Conjugates, *Experim. Math.*, **2**(1) (1993), 15–36.

[35] Polthier, K.: Polyhedral surfaces with constant mean curvature, TU-Berlin, Habilitationsschrift, 2002.

[36] Poelke, K., and Polthier, K.: Boundary-aware Hodge decompositions for piecewise constant vector fields, *Computer-Aided Design*, **78** (2016), 126–136.

[37] Polthier, K. and Rossman, W.: Discrete constant mean curvature surfaces and their index, *J. reine angew. Math.*, **549** (2002), 47–77.

[38] Razafindrazaka, F. H., Yevtushenko, P., Poelke, P., Polthier, K., and Goubergrits, L.: Hodge Decomposition of Wall Shear Stress Vector Fields characterizing Biological Flows, *R. Soc. Open Sci.* **6** (2019), No. 2, February, 181970, 14pp.

[39] Reilly, R. C.: The relative differential geometry of nonparametric hypersurfaces, *Duke Math. J.* **43** (1976), 705–721.

[40] Taylor, J. E.: Crystalline variational problems, *Bull. Amer. Math. Soc.* **84** (1978), 568–588.

[41] Wardetzky, M., Mathur, S., Kälberer, F., and Grinspun, E.: Discrete Laplace operators: No free lunch, Eurographics Symposium on Geometry Processing (2007), Alexander Belyaev, Michael Garlad (Editors).

[42] Wente, H. C.: Counterexample to a conjecture of H. Hopf. *Pacific J. Math.* **121** (1986), 193–243.

[43] Winterbottom, W. L.: Equilibrium shape of a small particle in contact with a foreign substrate. *Acta Metallurgica* **15** (1967), 303–310.

[44] Wulff, G.: Zur Frage der Geschwindigkeit des Wachsthums und der Auflösung der Krystallflächen. *Zeitschrift für Krystallographie und Mineralogie* **34** (1901), 449–530.